LANDSCAPE- AND REGIONAL-SCALE QUANTIFICATION OF NITROUS OXIDE EMISSION FROM A SUBHUMID TRANSITIONAL GRASSLAND-FOREST REGION

A Thesis

Submitted to the College of Graduate Studies and Research

in Partial Fulfillment of the Requirements for the

Degree of Doctor of Philosophy

in the Department of Soil Science

University of Saskatchewan

Saskatoon

By

Marife D. Corre

Winter 1997

UNIVERSITY OF SASKATCHEWAN

College of Graduate Studies and Research

SUMMARY OF DISSERATATION

Submitted in partial fulfillment

of the requirements for the

DEGREE OF DOCTOR OF PHILOSOPHY

by

Marife D. Corre

Department of Soil Science

University of Saskatchewan

Winter 1997

Examining Committee:

Dr. L.W. Martz	Dean/Associate Dean/Dean's Designate, Chair College of Graduate Studies and Research
Dr. D. Anderson	Chair of Advisory Committee Department of Soil Science
Dr. D. Pennock	Co-supervisor, Department of Soil Science
Dr. C. van Kessel	Co-supervisor, Department of Soil Science
Dr. E. de Jong	Department of Soil Science
Dr. C. Maulé	Department of Agricultural and Bioresource Engineering

External Examiner:

Dr. A. R. Mosier
Soil Plant Nutrient Research
U.S. Department of Agriculture - ARS
Ft. Collins, CO, U.S.A. 80522

LANDSCAPE- AND REGIONAL-SCALE QUANTIFICATION OF NITROUS OXIDE EMISSION FROM A SUBHUMID TRANSITIONAL GRASSLAND-FOREST REGION

This study was conducted to obtain landscape- and regional-scale estimates of N_2O emissions for a representative part of the Black soil zone of Saskatchewan. A 4318-km^2 study region was stratified based on soil texture and land use. At the regional scale, soil texture was the proxy variable used to represent the differences in soil moisture regimes and soil fertility, whereas land use was the surrogate variable used to reflect the differences in N and C cycling. Soil landscapes were selected to cover the range of soil texture and land use characteristics in the study region. At the landscape level, shoulder and footslope complexes were used as the spatial sampling units to cover the range of topographical and soil characteristics within the landscape. At the landform complex level, soil moisture (as assessed by volumetric moisture content and water-filled pore space) was the most important factor controlling N_2O emission. At the landscape scale, soil moisture was, in turn, influenced by topography, and on the seasonal scale it was affected by climatic factor(s) (e.g., precipitation). The annual N_2O emissions were calculated as the sum of the spring and the summer to fall fluxes. The spring emission was estimated by interpolating the N_2O fluxes measured on discrete sampling days, whereas the summer to fall emission was estimated by establishing regression models that related N_2O fluxes to water-filled pore space. Regional estimates of N_2O emissions were obtained using the GIS database of soil texture and land use types. The average annual fluxes for fertilized cropped, fallow, pasture, and forest areas, weighted by their areal extent in the different textural areas of the study region, were 2.01, 0.12, 0.04, and 0.02 kg N_2O-N ha^{-1} yr^{-1}, respectively. The weighted-average annual fluxes for the medium- to fine-textured and sandy-textured areas were 1.31 and 0.04 kg N_2O-N ha^{-1} yr^{-1}, respectively. Assuming that the proportions of the area covered by the different land use and soil

texture categories in this study region are typical for the Black soil zone, the weighted-average annual flux for this soil zone is 0.90 kg N_2O-N ha^{-1} yr^{-1}. For the total area of 7844 x 10^3 ha of the Black soil zone in Saskatchewan, a total flux of about 7 x 10^6 kg N_2O-N yr^{-1} was calculated.

BIOGRAPHICAL

February, 1967	Born in Bohol, Philippines
April, 1987	B. Sc. in Agriculture (major in Soil Science), Visayas State College of Agriculture, Philippines
September, 1992	M. Sc. in Soil Science, State University of Gent, Belgium

HONOURS

University Graduate Scholarship, Univ. of Saskatchewan, Sep 94 - Apr 97

University Graduate Assistantship, Univ. of Saskatchewan, Nov 92 - Aug 94

Belgian Government Development Cooperation Scholarship, Sep 90 - Sep 92

Excellent Student Scholarship, Visayas State Coll. of Agriculture, Jun 83 - Apr 87

PUBLICATIONS

Refereed:

Corre, M. D., C. van Kessel, and D. J. Pennock. 1996. Landscape and seasonal patterns of nitrous oxide emissions in a semiarid region. Soil Sci. Soc. Am. J. 60:1806-1815.

Corre, M. D., C. van Kessel, D. J. Pennock, and M. P. Solohub. 1995. Ambient nitrous oxide emissions from different landform complexes as affected by simulated rainfall. Comm. Soil Sci. Plant Anal. 26:2279-2293.

Vermoesen, A., M. D. Corre, and O. Van Cleemput. 1992. Nitrous oxide emission during nitrification. pp. 33-34. *In*: E. Francois, K. Pithan, and N. Bartiaux-

In presenting this thesis in partial fulfillment of the requirements for a Postgraduate degree from the University of Saskatchewan, I agree that the libraries of this University may make it freely available for inspection. I further agree that permission for copying this thesis in any manner, in whole or in part, for scholarly purposes may be granted by the professors who supervised my thesis work, or in their absence, by the Head of the Department or the Dean of the College in which my thesis work was done. It is understood that any copying or publication or use of this thesis or parts thereof for financial gain shall not be allowed without my written permission. It is also understood that due recognition shall be given to me and to the University of Saskatchewan in any scholarly use which may be made of any material in my thesis.

Requests for permission to copy or to make other use of material in this thesis in whole or part should be addressed to:

Head of the Department of Soil Science
University of Saskatchewan
51 Campus Drive
Saskatoon, Saskatchewan, Canada
S7N 5A8

ABSTRACT

This study was conducted to obtain landscape- and regional-scale estimates of N_2O emissions for a representative part of the Black soil zone of Saskatchewan. A 4318-km^2 study region was stratified based on soil texture and land use. At the regional scale, soil texture was the proxy variable used to represent the differences in soil moisture regimes and soil fertility, whereas land use was the surrogate variable used to reflect the differences in N and C cycling. Soil landscapes were selected to cover the range of soil texture and land use characteristics in the study region. At the landscape level, shoulder and footslope complexes were used as the spatial sampling units to cover the range of topographical and soil characteristics within the landscape. At the landform complex level, soil moisture (as assessed by volumetric moisture content and water-filled pore space) was the most important factor controlling N_2O emission. At the landscape scale, soil moisture was, in turn, influenced by topography, and on the seasonal scale it was affected by climatic factor(s) (e.g., precipitation). The annual N_2O emissions were calculated as the sum of the spring and the summer to fall fluxes. The spring emission was estimated by interpolating the N_2O fluxes measured on discrete sampling days, whereas the summer to fall emission was estimated by establishing regression models that related N_2O fluxes to water-filled pore space. Regional estimates of N_2O emissions were obtained using the GIS database of soil texture and land use types. The average annual fluxes for fertilized cropped, fallow, pasture, and forest areas, weighted by their areal extent in the different textural areas of the study region, were 2.01, 0.12, 0.04, and 0.02 kg N_2O-N ha^{-1} yr^{-1}, respectively. The weighted-average annual fluxes for the medium- to fine-textured and sandy-textured areas were 1.31 and 0.04 kg N_2O-N ha^{-1} yr^{-1}, respectively. For the study region, the weighted-average annual flux was 0.90 kg N_2O-N ha^{-1} yr^{-1}.

ACKNOWLEDGMENTS

I am extremely grateful and indebted to my supervisors, Dr. D.J. Pennock and Dr. C. van Kessel, for their guidance, support, and enthusiasm throughout my Ph.D. endeavor. My appreciation is also extended to the members of the advisory committee, Dr. D.W. Anderson (committee chair), Dr. E. de Jong, and Dr. C. Maulé for their interest and advice during the course of my study, and Dr. A.R. Mosier for acting as the external examiner for my dissertation defence.

The study was made possible through the financial support of the Agriculture and Agri-Food Canada Greenhouse Gas and Climate Change Initiatives, and the graduate scholarship provided by the University of Saskatchewan.

Special thanks to K. Elliott, C. Wong, R. Anderson, Q. Chen, G. Parry, and all the summer students of the Soil Genesis and Stable Isotopes Laboratories. I also thank Dr. F. Walley, and all the graduate students, faculty, and staff of the Department of Soil Science for the informative discussions and for the friendly working environment. The cooperation provided by the farm owners of the study sites and the Conservation Learning Center, especially Pat Flaten, is also greatly appreciated.

My sincere gratitude is extended to Dr. O. Van Cleemput and Dr. G. Stoops for their assistance and continued encouragement since the time I was applying for Ph.D. study and through all these years.

Thanks to all my friends (Argañosa, Kingwell, Pope, and Tabil families, Beth and Villa; to name only a few) who have made my stay in Saskatoon a memorable one. I am also grateful to a Friend who pushed hard on me the idea of proceeding for Ph.D. My heartfelt gratitude goes to my parents, Francisco and Sotera, for their unfailing love and confidence in me, and to my sister, brothers (Quinlog, Antipas, and Corre families) and Ed Veldkamp for their support and inspiration.

DEDICATION

To HIM who made all things possible in my life . . .

"Unless the LORD builds the house,

the builders labor in vain"

- Psalm 127:1 -

TABLE OF CONTENTS

LIST OF TABLES

LIST OF FIGURES

LIST OF ABBREVIATIONS

DNRA	Dissimilatory nitrate-reduction to ammonium
ANR	Assimilatory nitrate reduction
WFPS	water-filled pore space
DNDC	DeNitrification-Decomposition model
NGAS	N_2 and N_2O from nitrification and denitrification model
CASA	Carnegie-Ames-Stanford Biosphere model
GIS	Geographic information system(s)
LANDSAT TM	Land satellite thematic mapper
DEM	Digital elevation model
EDA	Exploratory data analysis
CV	Coefficient of variation
MDCD	Minimum detectable concentration difference
W	Kendall coefficient of concordance
VSMB	Versatile soil moisture budget
GCP	Ground control points
DN	Digital numbers
ERDAS	Earth resources data analysis systems
SPANS	Spatial analysis systems

1. INTRODUCTION

Nitrous oxide (N_2O) is a trace gas that has received considerable attention because of its importance in atmospheric chemistry and its influence in controlling the global heat budget. Interest in quantifying N_2O flux rates from various ecosystems has accelerated recently for two reasons: the increase in atmospheric N_2O concentration, and the imbalance in its global budget. Concentration of N_2O in the global atmosphere has been rising over the last 20 years at the rate of 0.2 to 0.3 % yr^{-1} (Weiss, 1981; Brasseur and Hitchman, 1988; Khalil and Rasmussen, 1992) to the 310 parts per billion volumetric (ppb_v) present in today's atmosphere (Elkins and Rossen, 1989). Ice core data that indicate a concentration of around 280 ppb_v in the pre-industrial period (Pearman et al., 1986) suggest that this rise reflects a long-term trend (IPCC, 1990). This rate of increase represents a 3.5 Tg N_2O-N yr^{-1} atmospheric accumulation, beyond the present photodissociation rate of 10.5 Tg N_2O-Nyr^{-1} in the stratosphere. The atmospheric accumulation and stratospheric photodissociation of N_2O add up to 14 Tg N_2O-N yr^{-1} as the total sink (McElroy and Wofsy, 1986).

Analyses of the global N_2O budget (e.g., Keller et al., 1986; McElroy and Wofsy, 1986; Watson et al., 1990; Robertson, 1993) indicated an imbalance in the estimates of the global sources and sinks. The estimates of the global sources are about 30 % lower than the estimates of the global sinks. Of the total global sources, about 70 % of emitted N_2O is derived from the soil (Bouwman, 1990; Houghton et al., 1992). Inverse modeling of the global atmosphere using observed interhemispheric N_2O ratios (Prinn et al., 1990) suggests that about one-half of the present atmospheric

accumulation rate ought to be coming from sources in tropical regions and about one-half from temperate regions. Examination of the global budget showed that identified tropical sources are about three times greater than identified temperate sources, suggesting that the sources in temperate region are possibly more poorly known than those of the tropical region (Robertson, 1993). Hence, there is a need for sufficiently detailed investigations that would provide a mechanistic understanding of N_2O emission at a large scale. Groffman (1991) discussed ecological approaches of quantifying N_2O emission through consideration of the gradients of its controlling factors at the landscape and regional scales. Studies on N_2O emission that employed these ecological approaches (e.g., Matson and Vitousek, 1990; Matson et al., 1991; Mosier et al., 1996) illustrated how information from soil science, geomorphology, and ecosystem ecology provided the framework for extrapolating N_2O fluxes to a large scale.

In areas of semiarid to subhumid cold continental climate (e.g., Prairie Provinces of Canada), where emissions are considered less important than in areas of tropical and humid temperate climate, data on N_2O emissions are particularly scanty. Such data may nonetheless be significant in defining global atmospheric balances. In the Prairie Provinces of Canada, N_2O emissions from undisturbed natural ecosystems are not known. Moreover, earlier studies on N gas losses conducted in agricultural soils mainly focused on denitrification. Denitrification is only one of the processes contributing to N_2O production, and hence denitrification losses cannot simply be related to N_2O evolution.

The major difficulty in the development of annual estimates of N_2O emissions at the landscape and regional scales is the high degree of spatial and temporal variability. Many recent review papers (e.g., Schimel et al., 1988; Matson et al., 1989; Groffman, 1991; Robertson, 1993; Schimel and Potter, 1995) have addressed

investigation strategies for dealing with the characteristically high variability of N_2O emission. Improved assessment of N_2O emission requires techniques for reducing random variation within experimental units, and knowledge of the factors that result in systematic variation among landscapes and across seasons. Placing the investigation scheme in the context of the large-scale factors that regulate N_2O emission is the key to subsequent spatial and temporal extrapolation of fluxes.

The primary objectives of this research were (1) to determine the soil and environmental factors that regulate N_2O emission, and the spatial and temporal patterns of N_2O emission in different landscapes, and (2) to obtain landscape- and regional-scale estimates of N_2O emissions in the Black soil region.

2. LITERATURE REVIEW

2.1 Effects of N_2O Emission

Nitrous oxide has the capacity to absorb the infrared portion of the electromagnetic spectrum, and contributes approximately 5 % of the global warming potential in the assessment of the greenhouse effect (Rodhe, 1990). On a molar basis, N_2O is 206 times more potent than CO_2 in absorbing the infrared radiation. When evaluating the effects of N_2O on climate over a 20-yr time frame, it has 270 times higher global warming potential than CO_2 (Duxbury et al., 1993).

Nitrous oxide has also been implicated as the major natural regulator of stratospheric O_3 (Crutzen and Ehhalt, 1977), which effectively controls the earth's ultraviolet-B (UV_B) radiation balance. Hahn and Crutzen (1981) elucidated the oxidation of N_2O to nitric oxide (NO) via photolytically produced atomic oxygen in the upper stratosphere (> 25 km) through the following series of reactions:

$$O_3 + h\nu \longrightarrow O + O_2$$

$$O + N_2O \longrightarrow 2NO$$

$$NO + O_3 \longrightarrow NO_2 + O_2$$

Under steady-state (pre-industrial) conditions, this set of reactions balances the formation of O_3 in the stratosphere. Because these reactions represent the only major sink for N_2O, N_2O has an atmospheric residence time of about 150 yr. This contrasts with a lifetime for CH_4 of about 10 yr, implying that the effects of the present loading rate (0.25 % yr^{-1}) will be long-lasting (Robertson, 1993).

Certain aquatic systems and anaerobic soils have large potentials for reducing N_2O to N_2. However, slow rates of dissolution of atmospheric N_2O and its slow transport in wet and/or flooded soils prevent these systems from being a significant regulator of atmospheric N_2O (Ryden, 1981; Duxbury and McConnaughey, 1986). Thus, the only known significant sink for N_2O is photolysis in the stratosphere (Watson et al., 1990).

2.2 N_2O-producing Processes in Soils

It is clear that soil generally acts as a source of N_2O (Mosier et al., 1981; Seiler and Conrad, 1981). There are five processes that contribute to N_2O formation in soils: chemo-denitrification, dissimilatory NO_3^--reduction to NH_4^+, assimilatory NO_3^--reduction, nitrification, and denitrification. Studies have shown, however, that nitrification and denitrification are generally the most important N_2O-producing processes in the soil environment (Hutchinson and Davidson, 1993). Nitrification accounted for over 60 % of the N_2O produced in undisturbed, semiarid shortgrass steppe and shrub-steppe ecosystems (Parton et al., 1988b; Mummey et al., 1994). Martikainen (1985) also reported a 20 % contribution of nitrification to emitted N_2O in a strongly acid forest soil fertilized with urea. However, the N_2O yield from nitrification is typically less than 1 %, and therefore N_2O is often considered as largely produced by denitrification (Hutchinson and Davidson, 1993; Ambus and Christensen, 1994).

2.2.1 Chemo-denitrification

This process is a collective term for a set of reactions that describe the abiotic production of N_2O. The most important of these reactions is the production of N_2O by NO_2^- or nitrous acid (HNO_2) in acid soils (Nelson, 1982), especially those high in

organic matter content (Blackmer and Cerrato, 1986). Smith and Chalk (1980) indicated that a Van Slyke-type reaction may be partially responsible for this process:

$$NH_2\text{-}R\text{-}NH_2 + 2HNO_2 \rightleftharpoons OH\text{-}R\text{-}OH + N_2O + N_2 + H_2O$$

Other abiological processes for N_2O production include decomposition of hydroxylamine (NH_2OH) and reaction of NO_2^- with phenolic constituents of soil organic matter (Nelson, 1982).

2.2.2 Dissimilatory NO_3^--reduction to NH_4^+, and assimilatory NO_3^--reduction

Dissimilatory NO_3^- reduction to NH_4^+ (DNRA) is a process in which microorganisms make energy available for cell growth and maintenance (Harris, 1982). This is expected to be significant primarily in anaerobic habitats, since O_2 inhibits the activity of the enzyme involved and also represses the enzyme synthesis (Mosier et al., 1983). This process is mediated by the same environmental factors as denitrification, and it is not yet known why one or the other dominates in a specific habitat. However, Tiedje et al. (1982) hypothesized that DNRA is favored when NO_3^- (e^- acceptor) supply is limiting, and denitrification is favored when carbon (e^- donor) supply is limiting. In addition, in systems where anaerobic conditions are maintained for long periods, such as in sediments and rice paddy soils, the reduction of NO_3^- to NH_4^+ is significant and is often the major fate of NO_3^- (Tiedje et al., 1981). In environments where O_2 status is more transient, as in most soils, denitrification should dominate. Whereas denitrification results in a loss of N from the system, DNRA generally conserves N.

Assimilatory NO_3^- reduction (ANR) is a process of N incorporation into cell biomass. With this difference in purpose (compared to DNRA), it is expected that the quantities of NO_3^- reduced and the environments in which each process occurs are different (Tiedje et al., 1981). Assimilatory NO_3^- reduction is expected only in the

absence of NH_4^+ and organic N, and is thought to be a relatively minor fate of NO_3^-. Though not regulated by O_2, ANR would be expected only in aerobic habitats, since the repression of the enzyme involved by NH_3 is generally high in anaerobic habitats due to the absence of nitrification (Mosier et al., 1983).

The DNRA and ANR reductive reaction sequences are similar insofar as the same intermediate, NO_2^-, is involved. Nitrous oxide leakage possibly exists to augment detoxification of microorganisms by NO_2^- through additionally using NO_2^- as alternate electron sink (Mosier et al., 1981). Only a few studies have dealt with N_2O production by DNRA and ANR processes due partly to the fact that these processes appear to have little environmental significance, and these studies can also be complicated by the many bacteria and fungi, which possess more than one type of NO_2^--reducing enzyme.

2.2.3 Nitrification

There is abundant evidence that N_2O is usually included among the products of chemoautotrophic nitrification (Fig. 2.1). Ritchie and Nicholas (1972) first reported the reduction of NO_2^- to N_2O by dissimilatory NO_2^- reductase synthesized by *Nitrosomonas europaea* in pure culture. Several years later Bremner and Blackmer (1978) recognized that nitrifying microorganisms were responsible for the production of a fraction of the soil-emitted N_2O formerly attributed entirely to denitrification. Recent evidence suggests that production of N_2O by autotrophic NH_4^+ oxidizers in soil results from a reductive process in which the organisms use NO_2^- as an electron acceptor, especially when O_2 is limiting (Poth and Focht, 1985). This mechanism not only allows the organisms to conserve limited O_2 for the oxidation of NH_4^+, but also avoids the potential for accumulation of toxic levels of NO_2^-.

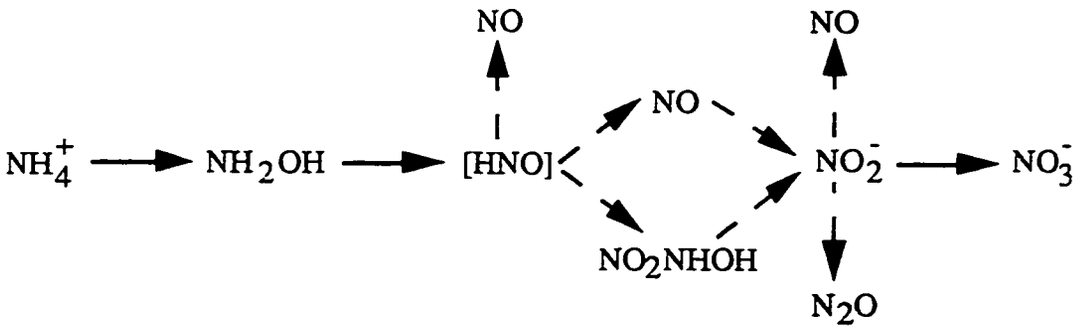

Fig. 2.1. Pathway of chemoautotrophic nitrification. Dashed lines and bracket indicate incompletely known processes and intermediates (From Firestone and Davidson, 1989).

2.2.4 Denitrification

Denitrification is defined as the dissimilatory reduction of oxides of N to produce N_2O and N_2 by a taxonomically diverse and physiologically different bacterial groups. These organisms are facultative aerobic bacteria that synthesize a series of reductases to utilize successively more reduced N oxides as electron acceptors in the absence of O_2 (Knowles, 1982). The generally recognized reductive sequence is:

NO_3^- -----> NO_2^- -----> NO -----> N_2O -----> N_2

Nitrous oxide is an obligatory intermediate to N_2. Hence, denitrification also represents the only biological process for the consumption of N_2O (Firestone, 1982). Denitrifiers are so widely distributed in nature that any restriction of the denitrifying activity in a given habitat can only be assumed to result not from lack of enzyme, but rather from limited substrate availability or the environmental conditions that regulate the process (Firestone and Davidson, 1989).

2.3 Measurement Methods for N_2O Emissions

There are three main techniques developed to measure surface-atmosphere N_2O exchange: micrometeorological methods (Mosier and Hutchinson, 1981; Smith et al., 1994), the diffusion theory approach (Burton and Beauchamp, 1994), and chamber-based methods (Denmead, 1979; Hutchinson and Mosier, 1981; Ambus et al., 1993). The micrometeorological approach is costly and not applicable when research objectives require quantitative measures of trace gas exchange at spatial scales below the resolution possible with micrometeorological techniques. Applications of diffusion theory are also subject to considerable and unknown uncertainties when trace gas sources or sinks are not uniformly distributed in the soil or located too close to the surface for gradients to be measured, or when non-diffusive transport is involved. In the above situations, chamber techniques are often applicable (Livingston and Hutchinson, 1995).

There are two primary types of chambers: steady-state (Denmead, 1979), and non-steady-state systems (Hutchinson and Mosier, 1981; Ambus et al., 1993). The terms 'dynamic' or 'open' are sometimes used synonymously to describe steady-state systems, and 'static' or 'closed' are often applied to non-steady-state systems. In open chambers, a constant N_2O concentration gradient controlling molecular diffusion across the soil-atmosphere interface is maintained. In closed chambers, the trace gas concentration gradient is diminishing in response to continual increase in concentration within the chamber air (Denmead and Raupach, 1993). Closed chambers are useful in quantifying low exchange rates, whereas open chambers are preferred for monitoring N_2O exchange rates at fixed locations over extended or repeated time periods. Hutchinson and Mosier (1979) found that a substantial proportion of the fluxes

measured by closed chambers were below the detection limits reported for open chambers.

There are two types of closed chambers: vented (Matthias et al., 1980; Hutchinson and Mosier, 1981) and sealed chambers (Ambus et al., 1993; Ambus and Christensen, 1995). Gas transport across the soil-atmosphere interface occurs through molecular diffusion and mass flow. Transport by mass flow occurs in response to a difference in pressure between soil air and the overlying atmosphere and pressure fluctuations due to surface wind turbulence (reviewed in detail by Livingston and Hutchinson, 1995). Vented chambers are designed to communicate atmospheric pressure changes and fluctuations to the enclosed air volume. Air exchange through the vent due to molecular diffusion is assumed negligible over relatively short deployment periods (Hutchinson and Mosier, 1981). In sealed chambers, mass flow is suppressed, and molecular diffusion is the main agent of N_2O exchange. The elimination of the pumping action imposed by changes in ambient pressure and by wind turbulence would reduce N_2O emission until the concentration gradient in the soil atmosphere readjusts to a higher level capable of again driving a flux equal to the rate of production (Kimball and Lemon, 1972; Kimball, 1983). When permeability is low, as is characteristic of moist fine-textured soils, molecular diffusion dominates gas transport. In well-drained, porous soils or litter layers, the relative importance of mass flow increases (Livingston and Hutchinson, 1995). It is important that the chamber type, dimension, and deployment period are carefully selected so that feedback of the chamber air to the subsurface concentration gradient is minimized over the measurement period (Matthias et al., 1978; Hutchinson and Mosier, 1981).

If the chamber dimension, deployment period, and sampling protocol are suitably matched to the N_2O exchange rate and site characteristics, a linear model may be adopted, which assumes a constant exchange rate over the period of observation. If

the net rate of exchange is not constant over the measurement period, a non-linear model must be employed (Hutchinson and Livingston, 1993). Matthias et al. (1978) and Hutchinson and Mosier (1981) proposed separate non-linear models, each based on the theory of molecular diffusion in soils. The iterative approach required by the flux estimation model of Matthias et al. (1978) is more difficult to apply than that of Hutchinson and Mosier (1981). The model of Hutchinson and Mosier (1981) has been successfully applied in several N_2O emission studies (Mosier and Hutchinson, 1981; Mosier et al., 1982; Folorunso and Rolston, 1984; Hutchinson and Brams, 1992). However, as pointed out by Livingston and Hutchinson (1995), the greatest challenge in the use of chambers pertains to how best to represent N_2O flux rates over spatial and temporal domains beyond those measured. Inappropriate sampling design and data analyses, or the interpretation of data beyond the time and space domains for which they were designed, can lead to misrepresentation of the true exchange rates for the area and period of interest.

2.4 Variability of N_2O Emissions

One of the major impediments to the development of regional budgets for N_2O emission is the substantial spatial and temporal variability in N_2O fluxes. Numerous ground-based studies have examined N_2O fluxes from a variety of ecosystems; these studies have revealed great variability with time at a given site, within an ecosystem of a particular type (e.g., temperate sagebrush steppe), and between ecosystems of different types (e.g., temperate sagebrush steppe vs. temperate shortgrass steppe) (Parton et al., 1988b; Matson et al., 1991; Mummey et al., 1994; Goodroad and Keeney, 1984).

Nitrous oxide is produced mainly by nitrification and denitrification (Hutchinson and Davidson, 1993); these processes are variable because they are controlled by factors that vary in space and in time. Robertson et al. (1988) found

considerable variation at a scale of 0.9 m, whereas Parkin et al. (1987) demonstrated substantial variation even at <0.1-m scale. This spatial variability was caused by the random pattern of anaerobic microsites of high denitrification activity, referred to as "hotspots". In a study conducted in a sandy soil, hotspots persisted from days to weeks, and their persistence was mainly driven by C respiration (organic hotspots) and not by soil physical factors giving a local inhibition of O_2 diffusion (structural hotspots) (Christensen et al., 1990b). An increase in soil respiration was observed before an increase in denitrification, indicating that there must be a great increase in O_2 consumption before the denitrification hotspot is formed. Dissimilar patterns of CO_2 and N_2O fluxes were observed from a clay soil, and structural hotspots were suspected to cause the anaerobic microsites (Ambus and Christensen, 1994). Structural hotspots are more likely to occur in fine-textured soils rather than in coarse-textured soils.

In a general sense, however, N_2O fluxes across a geographic region vary in response to major and repetitive differences in the soil environment (Matson et al., 1989; Groffman, 1991; Robertson, 1993; Parkin, 1993). For example, at a micro-to-plot scale, control is exerted by availability of soil water, labile C, and inorganic N. These factors are, in turn, influenced by soil type and plant community type at the landscape scale. The distribution of soil types and plant community is interrelated, and their variation in a region is again largely controlled by geomorphology, land use, and climate. In this case, ecosystem properties can be thought of as continua on scales from local to regional. This concept has been supported clearly by the results of studies in geostatistical analysis of spatial variability of N_2O emission. Ambus and Christensen (1994) reported that the autocorrelation observed at 1-m scale was influenced by the dispersion of anaerobic microsites, while autocorrelation beyond 7-m scale was due to soil moisture variability governed by topography. Similarly, Robertson et al. (1988) found that denitrification rates had high degree of spatial

dependence within 1 to 40 m, and that most of the variation for these rates could be attributed to spatial autocorrelation at >1-m scale. The spatial characteristics of the measured denitrification rates were partly associated with topography.

Matson et al. (1989) and Parkin (1993) believe that measuring and understanding the spatial and temporal variability of N_2O emission is a better approach, rather than trying to average out this variability by randomly selecting samples with the assumption of their representativeness in a given area. Any attempt to account for variability would require an overwhelming number of sample locations, many with daunting logistical problems. On the other hand, characterizing the spatial and temporal variability is profitable in several ways. First, it provides information on the spatial distribution and temporal timing of N_2O fluxes, which could reveal much about the controlling variables. Understanding the controls of N_2O emission would, in turn, lead to improved investigation methods. Secondly, the information on the spatial and temporal variability of N_2O emission provide the basis for extrapolating fluxes from local to regional scale. Reliable estimates of regional N_2O fluxes require knowledge of the factors that result in systematic variation across the region. Without a mechanistic understanding of the factors governing the flux rates, the choice of predictor variables becomes empirical and extrapolation becomes problematic (Schimel et al., 1988).

2.5 Controls on the Spatial and Temporal Patterns of N_2O Emissions

The factors controlling N_2O emission can be best related to the factors regulating the main processes responsible for its production (i.e., nitrification and denitrification). Davidson (1991) presented a conceptual "hole-in-the-pipe" model to show that three levels of regulations are determinant to N gas flux: (1) factors which control nitrification and denitrification processes dictating N fluxes, (2) factors which

control the partitioning of N gases , and (3) factors which control the diffusion of trace gas across the aqueous-gas interface. The first level of regulation considers the factors that determine the availability of substrates (i.e., NH_4^+, NO_3^-, NO_2^-, and C) for N_2O production via nitrification and denitrification. The second level of regulation relates to the relative availabilities of electron donors (usually organic C) and electron acceptors (O_2 and N oxides) that affect the N_2O:N_2 ratio from denitrification (Firestone et al., 1980) . Similarly, [NH_4^+], pO_2, and acidity affect activities of nitrifying bacteria (Firestone and Davidson, 1989).

The third level of regulation reflects the physical conditions in the soil that affect the transport processes of N_2O and its possible consumption prior to its escape from the soil to the atmosphere. Biogenic N_2O moves from the aqueous solution to the gaseous phase of the soil and then must diffuse through gas-filled pores before being emitted to the atmosphere. The probability of consumption of N_2O increases as impediments to its transport increase. The exchange of gas between the soil surface and the adjacent atmosphere can occur by means of two mechanisms: diffusion and advection (reviewed in detail by Livingston and Hutchinson, 1995). Diffusive gas transport depends primarily on the total volume and tortuosity of continuous air-filled pore space. Advective gas transport is affected by gaseous permeability which, in turn, is dependent on total porosity, pore-size distribution, and tortuosity (Hillel, 1982). Soil water and texture dramatically affect gas transport in soils (Focht, 1992). Wetting a soil reduces its air-filled porosity and increases the tortuosity, thus rapidly precluding convective gas transport and greatly reducing diffusive gas transport. In fine-textured soils, wetting reduces the continuity between pore spaces at a far greater rate than the fraction of air-filled pore space is reduced, so gas transport is diminished long before air-filled porosity is eliminated. In coarse-textured soils, the continuity between pore

spaces is maintained over a large range of soil water content and gas transport is less affected by reductions in air-filled porosity. Quite a different form of movement of gases in the soil is the transfer of dissolved gases. The solubility of gas species in water can also result in different concentration gradients at air-water interfaces, and thus to differences in the rate of molecular diffusion. Precipitation and percolating water also affect gas transport by physically displacing the air in soil pore spaces, by transporting dissolved atmospheric gases into the soil, and by vertically or laterally transporting soil gases in solution (Livingston and Hutchinson, 1995).

2.5.1 Microsite-to-field scale and daily-time scale

Studies conducted in the field have shown that soil O_2 status is the most important factor controlling N_2O emission. It is relatively well understood that the absence of O_2 or reduced O_2 availability is required for both the synthesis and activity of the enzymes involved in N_2O production (Linn and Doran, 1984). As O_2 supply gradually diminishes, availability of N and C becomes increasingly important (Burton and Beauchamp, 1985; Davidson and Swank, 1986, Vermes and Myrold, 1992; Van Kessel et al., 1993). Mosier and Hutchinson (1981) observed that high substrate concentration was not sufficient to cause high N_2O flux, but limited O_2 status was necessary. Of the N_2O-producing processes, denitrification dominates in very wet soils, while nitrification dominates at more moderate soil moisture (Linn and Doran, 1984).

2.5.1.1 Soil O_2 status

Several soil properties influence the O_2 status in the soil. The most important parameter is soil water which functions to promote N_2O production by reducing O_2 diffusion and by promoting the diffusion of mineral N and soluble C (Vermes and

Myrold, 1992). Soil moisture also affects other edaphic parameters that relate to microbial activity. Davidson and Swank (1986) found significant correlation between water-filled pore space (WFPS) and available C, and nitrification and mineralization potentials, which suggests that soil moisture not only promotes denitrification by affecting O_2 diffusion but also by directly stimulating microbial activity. In a forest ecosystem, WFPS, temperature and base saturation accounted for 43 % of the variation of N_2O emission (Davidson and Swank, 1986). In a cropped field, soil water alone explained 28 % of the variation of N_2O emission (Mosier and Hutchinson, 1981).

2.5.1.2 Soil N and C availability

Despite the increasing understanding of cellular level controls on N_2O production, applying this knowledge to explain and predict *in situ* activity remains challenging. For example, is it well established in laboratory studies that NH_4^+ availability is an important controller of nitrification, as is NO_3^- for denitrification, but there is a lack of an universally applicable assay for soil N availability. An assay based on net nitrification correlated well with N_2O emission in temperate forest soils (Robertson and Tiedje 1984; Bowden et al., 1990). On the other hand, a net mineralization assay correlated with N_2O flux in tropical forest soils (Bowden et al., 1992), but not in nearby pastures (Matson and Vitousek, 1987). All these correlations and others tend to be site-specific or study-specific (Davidson and Swank, 1986; Vermes and Myrold, 1992). Failure to find a common measure for N availability probably arises from several confounding factors: (1) the N availability assay appropriate for one ecosystem may not be applicable in another because of their differences in the processes involving N, and (2) other process-limiting factors that interact with N availability (e.g., the supply of O_2 or organic C) are probably more important at some sites than others.

Unlike nitrification, denitrification in soil is more directly dependent on the availability of organic compounds which act as electron donors and sources for cellular material (Robertson, 1989). The presence of ample C substrate can also cause rapid O_2 consumption and possible depletion of O_2 in soil microenvironments, indirectly enhancing N_2O production (Christensen et al., 1990b). It is generally concluded that, when availability of electron acceptors (NO_3^-) is high relative to the availability of electron donors (organic C), the dominant N product of denitrification is N_2O; when the converse is true, N_2 is the dominant N product (Bowman and Focht, 1974; Firestone et al., 1980). However, this relationship cannot be the sole determinant factor of product proportion for *in situ* activity in a heterogeneous soil because changes in other factors (e.g., soil water, pH) may also affect the end products.

2.5.1.3 Diurnal and day-to-day variation

In some cases a clear diurnal pattern in N_2O emission has been observed, which was suggested to be related to the effect of diurnal pattern in temperatures on the production of N_2O by soil microorganisms (Ryden et al., 1978; Denmead et al., 1979). In contrast, Blackmer et al. (1982) reported that the diurnal pattern of N_2O emissions is caused largely by changes in the solubility of N_2O in soil water induced by diurnal changes in soil temperature. Hence, the amplitudes of N_2O diurnal patterns are determined largely by the amount of soil water. Mosier (1989) showed a commonly encountered diurnal variability in N_2O emission that is not predictable as a function of soil temperature. This situation occurred under conditions of favorable soil water for N_2O production. When water was added, elevated N_2O fluxes occurred for hours to days, returning to relatively low levels where soil temperatures controlled the diurnal variation. Moreover, neither the amplitudes nor the times of minima and maxima in the N_2O diurnal pattern were predicted solely from soil temperature (Blackmer et al.,

1982). They concluded that there is no short time during a 24-h period that is satisfactory for assessing N_2O evolution. Diurnal variation is also expected to be overshadowed by the seasonal variation which would be more important in estimating N_2O losses (Goodroad and Keeney, 1984).

To quantify annual N_2O emissions using chamber-based methods, the day-to-day variation in activity must be considered. This day-to-day variability is probably caused largely by the wetting and drying cycles in the soil. Numerous studies have demonstrated increased N_2O fluxes following precipitation and irrigation events (Ryden and Lund, 1980; Rolston et al., 1982; Sexstone et al., 1985; Davidson and Swank, 1986; Van Kessel et al., 1993). When dry soil is wetted, both organic C and inorganic N become rapidly available due to the turnover of microbial biomass that died from desiccation and starvation in dry soil (Bottner, 1985). Increase in soil respiration following wetting also reduces the partial pressure of O_2 within the soil. Nitrifying and denitrifying bacteria can become active within minutes of wetting a very dry soil (Davidson et al., 1990). This day-to-day variation in N_2O emission activity illustrates that a simple interpolation of measured fluxes between discrete sampling days does not give a good estimate of annual flux. Frequent sampling must be undertaken in order to account for the temporal temperature cycles and the temporal fluctuations in soil water in response to precipitation.

2.5.2 Landscape and seasonal scale

2.5.2.1 Landscape-scale pattern of N_2O emissions

Approaches in investigating N_2O emissions at the landscape scale have used stratification methods that consider either mainly topography (Davidson and Swank, 1986; Robertson et al., 1988; Parton et al., 1988b; Parsons et al., 1991; Elliott and de

Jong, 1992; Pennock et al., 1992; Van Kessel et al., 1993; Groffman et al., 1993a; Ambus and Christensen, 1995; Mosier et al., 1996), or topography-related variables (Groffman and Tiedje, 1989a; Matson et al., 1991). For the first group of studies mentioned above, the rationale for using topography as the variable in stratifying a landscape was based on previous findings that topography controls differences in soils and water distribution, which influences patterns of plant production and levels of organic matter in the landscape. Thus topography should also influence N_2O emission. On the other hand, the drainage class, which was used by Groffman and Tiedje (1989a) in further stratifying catenas of different soil texture, is influenced by topography. Matson et al. (1991) stratified a sagebrush steppe landscape based on vegetation types. In this area, however, differences in vegetation types are controlled by precipitation accumulation and redistribution which, in turn, are influenced by topography. Variation in topography interacts with strong winds and precipitation to cause a complex of shrub communities that are related to landscape position (Burke et al., 1989).

In the semiarid to subhumid agricultural landscapes of Saskatchewan, the different landform elements identified in the landscape have distinct rates of denitrification with a spatial pattern that remained consistent throughout the season: higher denitrification rates on the footslopes than on the shoulders (Pennock et al., 1992; Elliott and de Jong, 1992; Van Kessel et al., 1993). Denitrification rates, soil water, and soil respiration exhibit a similar spatial pattern, with soil water and soil respiration highly correlated to denitrification rates. No spatial relation was observed between denitrification rates and NO_3^- levels. This was attributed to the loss of natural variation in mineral N as a result of fertilization. The factors controlling the spatial

pattern of denitrification on these landscapes were influenced by more fundamental hydrologic and pedologic processes.

In the temperate forest landscapes of Michigan, Robertson et al. (1988) observed that denitrification rates were distinctly patterned, with high activities in the swales or lowland area. Moisture availability was strongly patterned and moderately correlated with denitrification. Moreover, Groffman and Tiedje (1989a) observed a strong relationship between denitrification and drainage in three catenas of different texture. Within each catena, the poorly-drained soils had higher rates of activity than the somewhat poorly and well-drained soils. The poorly-drained soils were consistently wetter, and had higher NO_3^-, organic C and N levels than the well-drained soils. The increased fertility in the poorly-drained soils relative to the well-drained soils is probably the long-term product of interaction of moisture, plant productivity and litter quality factors. In a North Carolina forest ecosystem, denitrification was strongly affected by soil moisture, which in turn was determined by precipitation events and slope position; rates were lower on the midslope than the toeslope landscape positions (Davidson and Swank, 1986).

In an uncultivated sod landscape of Kentucky, Parsons et al. (1991) observed higher denitrification rates on the bottom slope than on the top slope. On the bottom slope, denitrification rates were also highly correlated with WFPS and soil respiration. Similarly, on a coastal grassland area of Denmark, consistently higher N_2O emissions were observed on the bottom slope than on the mid- and top-slopes (Ambus and Christensen, 1995). On the other hand, in a tall grass prairie landscape of Kansas, Groffman et al. (1993a) did not observe a consistent topography-related pattern of denitrification activity. Analysis of soil patterns in this area has shown that loess deposition created areas of deep, fine-textured soils in the summit positions. These soils had denitrification rates as high as those deep, fertile soils farther down the slope.

In this landscape, topography was not the main controller of denitrification because it was not the only geomorphic factor controlling soil distribution.

In a shortgrass steppe landscape of Colorado, Parton et al. (1988b) and Mosier et al. (1991; 1996) found that N_2O emissions were higher on the swale than on the midslope. The difference in N_2O evolution was mainly attributed to differences in water availability between these two slope positions. In a sagebrush steppe landscape of Wyoming, where stratification was based on differences in vegetation types occupying different slope positions, the N_2O emissions of the soil with the footslope-vegetation were higher than those soils with the backslope- and shoulder-vegetations (Matson et al., 1991). In this landscape, the effects of differences in vegetation types and of topography on N_2O emission are inter-related. The different vegetation types have different patterns of nitrogen cycling that are controlled principally by soil moisture availability that is, in turn, controlled by landscape topography.

2.5.2.2 Seasonal-scale pattern of N_2O emissions

In semiarid to subhumid agricultural landscapes, denitrification rates were high in the beginning of the growing season and virtually ceased by the onset of frost in fall (Elliott and de Jong, 1992, and Van Kessel et al., 1993). The high activity during the early growing season was attributed to the effects of N fertilization and the occurrence of high and frequent rainfall. The decrease in activity towards fall was mainly due to the decrease in soil water content, as a result of crop usage and low rainfall.

In temperate forest landscapes, rates of denitrification and/or N_2O flux were high in spring and in fall (Goodroad and Keeney, 1984; Groffman and Tiedje, 1989a; Bowden et al., 1990; Ambus and Christensen, 1995). The spring and fall pulses of activity appear to have been driven by high contents of soil water and by lack of competition for mineral N among nitrifiers/denitrifiers and vegetation at these time, and

probably also by high content of available C as a result of freezing and thawing common during these periods. The seasonal pattern was also closely tied to the activity of the mainly deciduous forest trees. The end of the spring pulse of denitrification coincided with tree "leaf break", and the onset of fall pulse of denitrification was coincident with leaf senescence and litterfall (Groffman and Tiedje, 1989a). Groffman et al. (1993b) studied the early spring N dynamics in a temperate forest landscape. They found that microbial biomass was the key regulator of the fate of added ^{15}N. In the well-drained summit position, the largest movement of N was into the microbial biomass and total soil N. As a result of this strong immobilization, there was little nitrification and denitrification of added ^{15}N. In the poorly-drained toeslope position, there was no apparent movement of ^{15}N into microbial biomass. As consequence, availability of $^{15}NH_4^+$ and rates of nitrification were high. Accumulation of NO_3^- in this landscape position, along with high moisture content, fostered high denitrification N losses.

Rates of denitrification and/or N_2O flux were observed to be high in spring and low in fall and summer in a shortgrass steppe landscape (Mosier et al., 1991), sod landscape (Parsons et al., 1991), and tallgrass prairie landscape (Groffman et al., 1993a). Groffman et al. (1993a) observed that similar to denitrification rates, soil water and mineral N also decreased from spring into summer and fall. Matson et al. (1991) reported that net N mineralization, net nitrification, and NO_3^- concentrations were high early in spring and dropped by late June in a sagebrush steppe landscape of Wyoming. Ammonium, on the other hand, remained elevated throughout the summer. However, the temporal variation in N_2O flux rates could not be explained on the basis of variation in soil N pools alone. In a shrub-steppe landscape of Washington, Mummey et al. (1994) indicated that N_2O flux from this ecosystem was regulated by

interactions between soil water content, and N-mineralization and N-immobilization. Low soil moisture content and intense competition among microorganisms and plants for available N probably resulted in low N_2O flux rates during most of the summer months. Similar results were obtained from a shortgrass steppe landscape of Colorado, where seasonal variations in N_2O flux were related to variations in mineral N dynamics; high rates of N_2O flux occurred during high rates of inorganic N turnover (Parton et al., 1988b).

Another factor that influences seasonal variation of N_2O emission is temperature. In winter, snow cover insulates the soil and may prevent freezing of the subsoil; when soils are not frozen microbial N_2O production may continue albeit at a reduced rate. Furthermore, N_2O solubility generally increases as the solution temperature decreases (Weiss and Price, 1980); this implies that during fall and winter the N_2O emitted from the soil could be lower than the actual N_2O produced in the soil because part of the N_2O produced stayed in the soil solution (Davidson and Swank, 1986; Burton and Beauchamp, 1994). Burton and Beauchamp (1994) examined the profile of N_2O concentrations over an extended period in a soil subject to freezing. They observed accumulations of N_2O during the winter in the soil beneath the frozen layer. The surface flux events in the early spring were attributed, in part, to the changes in N_2O solubility associated with the warming of the soil, and also to thawing of the frozen layer that would permit release of N_2O trapped below it.

2.5.3 Regional-scale regulators of N_2O emissions

Groffman (1991) presented an approach of quantifying ecological controls of N_2O emission at the regional scale. At the regional scale, landscapes are chosen as experimental units to systematically cover the range of conditions within the region.

The distribution of soil types and plant communities, which are factors considered at the landscape scale, is largely controlled by glacial geology, land use patterns, and climate at the regional scale. The glacial geology (i.e., distribution of glacial landforms and parent sediments) in a region strongly influences soil texture (Pastor et al., 1982), which in turns influences water availability, plant community, and N cycling dynamics in the landscape (Schimel et al., 1985a, 1985b). In studies conducted for regional-scale quantification of N_2O emission, soil texture and land use were factors used in stratifying the region. Climatic factors such as precipitation and temperatures were also used as the driving variables in predictive models for extrapolating fluxes from daily to seasonal and annual estimates.

In the tallgrass prairie region (Groffman et al., 1993a), the stratification by land use types included unburned, burned, burned/grazed, and cultivated sites. Denitrification was consistently higher in unburned sites than in burned and burned/grazed sites and was lowest in the cultivated site. This result was expected since the unburned sites had the highest soil water and NO_3^- levels among the native prairie sites. Denitrification was low in the cultivated site, despite high levels of NO_3^-. However, this site was consistently drier than the native prairie sites and had markedly lower levels of total organic C, microbial biomass C, activities of the enzymes active in nitrification and denitrification. These results suggest that changes in soil moisture and the C cycle associated with cultivation may reduce the inherent potential for biogenic N gas emissions from some agricultural ecosystems.

Conversion of forests and grasslands to croplands accelerates the mineralization of C and N, at least during the first few years, and N_2O emissions are expected to increase. Mosier et al. (1991) observed higher N_2O emissions from cropland than from native grassland after eight years of cultivation without N fertilization. Globally, land use conversion is important now only in tropical areas. Most of the conversion of

forests and grasslands in the northern hemisphere occurred 50 to 200 years ago (Hammond, 1990). In the temperate zone, agricultural soils show high N_2O emissions as a result of N fertilization (Eichner, 1990; Mosier 1994). Ambus and Christensen (1995) observed the highest N_2O emission on a fertilized agricultural site followed by coastal grassland, forest, riparian grassland, and abandoned farmland sites. Among native land use types, Goodroad and Keeney (1984) observed N_2O emission activity in the following decreasing order: drained marsh > coniferous forest > wet meadow > deciduous forest > prairie > undrained marsh. Drained organic soils undergo accelerated decomposition and mineralization. The aforementioned studies showed that different land use types differ in N_2O emission activity because of their differences in the N and C cycling.

McKenney et al. (1980) investigated the N_2O emission activity in two agricultural soils of different texture. At the same level of N fertilizer, N_2O emissions in the clay-textured soil were two orders of magnitude higher than in the sandy-textured soil, even though the latter had a longer history of fertilization. In the Michigan forested region, Groffman and Tiedje (1989a) investigated denitrification in three catenas of different texture with each catena subdivided into different drainage classes. At each drainage class, denitrification rates were lowest in the sandy soil, intermediate in the loam soil, and highest in the clay loam soil. The direct effect of soil texture on N_2O emission is through its influence on WFPS, which in turn affects the microbial production of N_2O and the gas transport. Its indirect effect can be linked to its influence on plant community composition and N cycling. In the northern temperate forest region, studies have shown that soil texture exerts a strong influence on soil moisture dynamics, which affect plant community composition, which in turn influences plant canopy chemistry and litter quality, and ultimately soil N cycling (Pastor et al., 1984; McClaugherty et al., 1985). The fine-textured soils hold more

water and support vegetation of higher litter quality (lower lignin:N ratio) than the coarse-textured soil. Sites with high litter quality have more dynamic soil N cycles, with high rates of mineralization, nitrification (Pastor et al., 1984), and denitrification (Groffman and Tiedje, 1989a).

2.6 Modeling N_2O Emissions

A number of different approaches have been used to develop models on denitrification and N_2O production. In general these models can be categorized into three types: 1) biochemically based models, 2) simplified process models, and 3) soil structural models. The biochemically based models were designed primarily to address instantaneous N_2O production as a function of the diffusion of nitrogen substrate and O_2 within soil microsites (Focht, 1974; McConnaughey and Bouldin, 1985; Leffelaar and Wessel, 1988). Menton or double Monod kinetics are appropriately applied at such scales. Li et al. (1992) developed a biochemically based model, the DeNitrification-Decomposition (DNDC) model, which simulates at the large scale what are conventionally thought of as soil microsite, electron donor-acceptor processes.

The simplified process models, on the other hand, generally represent N_2O emission without simulated microbial dynamics and gas transport, but include information concerning the spatial and temporal variability of large-scale controls such as soil temperature, moisture, texture, and organic matter availability (Parton et al., 1988a; Parton et al., 1996; Potter et al., 1996). Simplified models are designed to run the type of data collected in field experiments. Most field experiments do not measure the data required to run many of the complex biochemically based models (e.g., microbial dynamics and biomass, detailed time series of NO_3^- and NH_4^+, gas diffusion rates, and other soil physical parameters), which would be needed to test,

validate, or parameterize numerous reaction terms in biochemically based models. Groffman (1991) argues that explicit representation of microbial processes is progressively lost when moving from smallest to largest scale, but can be replaced by relating the activity to large-scale controlling factors investigated through a hierarchical approach.

The soil structural models have been used to simulate soil denitrification. These models represent soil physical processes like diffusion of gases and solutes into soil aggregates and explicitly represent the distribution of soil aggregates. The models assume that denitrification primarily occurs in anaerobic soil aggregates and that diffusion of O_2, N_2O, and NO_3^- into and out of soil aggregates needs to be represented (Arah and Smith, 1989; Smith, 1990; Arah, 1990).

2.6.1 Biochemically based model

The DNDC model was designed to simulate agroecosystem-level N_2O and N_2 fluxes with explicit consideration of enzyme kinetic and microbial biomass dynamics. The thermal-hydraulic submodel uses soil texture, daily air temperature and precipitation events to calculate soil temperature and moisture profiles and soil water fluxes through time. Soil temperature and moisture are the two key factors controlling the temporal variation of the rates of decomposition and denitrification. The decomposition submodel includes microbial oxidation reactions, including nitrification, and the effect of management practices on such processes. The N_2O emission from the nitrification process is modeled as a function of soil temperature and NH_4^+ concentration. The denitrification submodel is rainfall event-driven and relatively explicit in the manner it deals with microbial growth controls, substrate and enzyme kinetics, and nitrogen species reduction reactions (Li et al., 1992). Schimel and Potter

(1995) pointed out that the greatest challenge in the use of such models arise from the inadequacy of databases describing the process controls. The biochemically based expressions require specification of numerous reaction terms, including those for microbial growth rates, reaction rate constants, and diffusion coefficients.

2.6.2 Simplified process model

In the Century model, Parton et al. (1988a) used a largely empirical formulation in which N_2O production was estimated from soil moisture, soil temperature and soil NO_3^- concentration. In this model, the relationships between N_2O production and environmental variables were developed from an extensive database of grasslands, including both field and laboratory studies. However, this model did not simulate the underlying enzyme kinetic and microbial growth processes. An important assumption in the Century model is that microbial biomass levels are always sufficient to achieve maximal rates of N_2O production permitted by prevailing temperature, moisture and NO_3^- concentrations. The data requirements are average monthly or weekly climate attributes (temperature and precipitation), soil texture, and management characterization. The central issue implied herein is whether changes in soil moisture and heat conditions that occur at the daily time step can be captured adequately in a temporally aggregated parameter for longer (monthly) time step ecosystem studies.

Parton et al. (1996) presented a general model for N_2 and N_2O production from nitrification and denitrification (NGAS), which is designed to be incorporated into nitrogen cycling models and used to simulate regional and global trace gas production as a function of climates, soil properties, and management practices. The NGAS model uses a daily time step and is a hybrid between the detailed process oriented models (Li et al., 1992) and the simplistic nutrient cycling models (Parton et al., 1988b). The

NGAS model was developed and tested using both laboratory and field data from a number of studies. The N_2O produced from nitrification (N_{N2O}) is calculated by the following function:

$$N_{N2O} = N_{H2O}\, N_{pH}\, N_t\, (K_{mx} \text{ (N turnover)} + N_{mx}\, N_{NH4} \text{ (excess } NH_4\text{)})$$

where N_{H2O} is the effect of water-filled pore space (which changes as a function of soil texture), N_{pH} is the effect of soil pH, and N_t is the effect of soil temperature. The N turnover coefficient (K_{mx}) is a function of soil texture, soil N fertility, N fertilizer additions, and soil management practices. The N_{mx} is the maximum nitrification N_2O gas flux (30 g N ha^{-1} d^{-1}) with excess soil NH_4^+, which also varies as a function of soil texture. The N_2 and N_2O produced from denitrification (D_t) is modeled as follows:

$$D_t = \min (F_d(NO_3), F_d(CO_2))\, F_d(WFPS)$$

where $F_d(NO_3)$ is the maximum total N gas flux for a given soil NO_3^- level (assuming high respiration rates), $F_d(CO_2)$ is the maximum total N gas flux for a given soil respiration rate (assuming high NO_3^- levels), and $F_d(WPFS)$ is the effect of water-filled pore space on the denitrification rate. The ratio of N_2:N_2O ($R_{N2/N2O}$) gas flux during denitrification is extremely variable, and is represented as follows:

$$R_{N2/N2O} = \min (F_r(NO_3), F_r(CO_2))\, F_r(WFPS)$$

$$D_{N2O} = D/(1.0 + R_{N2/N2O})$$

$$D_{N2} = D/(1.0 + 1.0/R_{N2/N2O})$$

where $F_r(NO_3)$ is the effect of soil NO_3^- on the ratio, $F_r(CO_2)$ is the effect of soil respiration on the ratio, and $F_r(WFPS)$ is the effect of water-filled pore space on the ratio.

Potter et al. (1996) reported a global-level ecosystem model that integrates global satellite, climate, vegetation, and soil data sets. Nitrous oxide emissions were estimated by using an expanded version of the Carnegie-Ames-Stanford (CASA) Biosphere model. The CASA model is a process formulation of coupled ecosystem production and soil carbon-nitrogen fluxes that is driven by gridded global data sets for climate, radiation, and remotely sensed vegetation index. In this extended version of the CASA model, the authors developed algorithms to implement the first two levels of regulation on N gas production from the "hole-in-the-pipe" conceptual model of Davidson (1991) (section 2.5). The N_2O production from natural soils (the model will still have to be tested for nitrogen fertilizer amendments) was simulated by calculating climate and soil indices as controls on the spatial and temporal distribution of C and N fluxes among various litter and soil pools. The trace gas emissions are based directly on predicted rates of N mineralization (representing the first level of regulation) and on index of water-filled pore space (I_W; representing the second level of regulation). Potential production of total nitrogen trace gases (N_T), $NO + N_2O + N_2$, at the soil surface is treated as a fixed percentage of gross mineralized nitrogen (MIN_T) at any given time step. As a first estimate for N_T, a value of 2 % times monthly MIN_T is set. This estimation was guided by the data from the review of more than 100 field experiments by Eichner (1990). The ratio of $NO:N_2O:N_2$ production from MIN_T is derived from soil moisture effects on gaseous N emissions. Both NO and N_2O are produced at intermediate levels of I_W. At higher I_W levels, where reducing conditions develop, relatively more N_2O is produced. Under very wet soil conditions, only N_2 is produced. Conclusive validation of the CASA model is hampered by mismatched temporal and spatial scales of predicted and measured emission fluxes and their controllers. The results from the model, however, strongly advocate the concept that patterns of soil texture capture important variations in N gas fluxes over large areas.

2.7 Spatial Extrapolation

The simplest and most commonly used approach for spatial extrapolation of fluxes is 'measure and multiply' (Schimel and Potter, 1995). In this approach, the measurements are made in a range of surface types (vegetation, soil , or ecosystem) and fluxes are multiplied by areas. Hence, a total flux over all surface types is computed as:

$$F = \Sigma (A_i \, . \, F_i)$$

where F is the total flux, A_i is the area of surface type i, and F_i is the annual flux from surface type i. The mapped surface type is used as a surrogate for the actual independent variables, and no explicit use is made of correlations with forcing functions (i.e., relationships between flux rate and a series of independent variables). A variant on this approach is the use of GIS technology where multiple effects of mapped variables are overlain (i.e., soil types or texture classes overlain by land use types), and fluxes are associated with each discrete cell or unit.

Matson and Vitousek (1990) have used the 'measure and multiply' approach in their estimate of tropical N_2O flux. Matson et al. (1991) also used this approach in estimating N_2O flux from sagebrush ecosystems, using different vegetation types as the mapped variable. The areal coverage of the different vegetation types was determined from thematic mapper data analysis of Reiners et al. (1989). A similar approach was cited by Groffman (1991) in estimating the regional denitrification losses from temperate forest of Michigan. Estimates for denitrification losses for the region were produced using a GIS database containing soils and land use information. Soil information was digitized from the soil association map of Michigan, and land use classes were derived from Landsat thematic mapper imagery.

2.7.1 Land use characterization by remote sensing

The basic principle involved in remote sensing methods is that in different wavelengths of the electromagnetic spectrum, each type of objects reflects or emits a certain intensity of light which is a characteristics of its physical or compositional attributes (Gupta, 1991). Using this information from one or more wavelength ranges, it is possible to distinguish different types of objects and map their distribution. The curves showing the intensity of light emitted by the different objects at different wavelengths, called spectral response curves, constitute the important basic information required in image analysis. Figure 2.2 shows a generalized spectral response curves of water, vegetation, and soil.

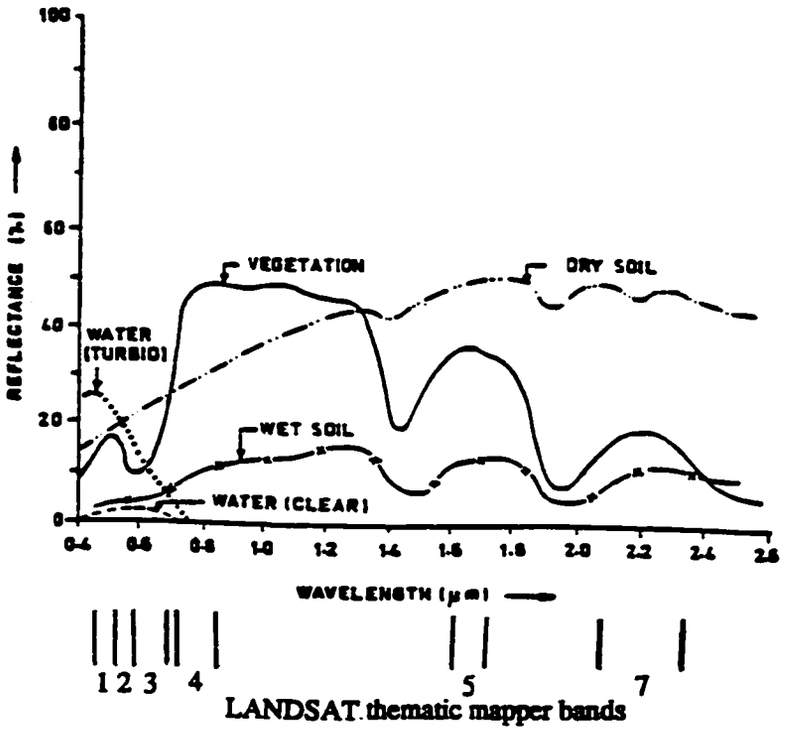

Fig. 2.2. Typical spectral reflectance curves for vegetation, soil, and water (From Gupta, 1991).

The deep clear water body exhibits low reflectance overall. The turbid shallow water has high reflectance at the low wavelengths, due to multiple scattering of

radiation by the suspended silt, and due to bottom reflectance. The basic peculiarity of the spectral reflectivity of soil is the increase of its spectral brightness at the high wavelengths. Soil spectral curves vary in dependence on the soil characteristics such as texture and organic matter content (Spiridonov et al., 1981; Henderson et al., 1992). The spectral reflectance of vegetation is governed by pigment, size and health of the leaves. In the visible region the leaf spectra is governed by leaf pigment, while in the near infrared region the spectral reflectance depends on the type of foliage and cell structure. Reflectance in the near infrared region has also a direct relationship with the leaf area index (Arai, 1992). Cropped area shows high reflectance whereas the forested area shows low reflectance due to shadows and wood that contribute to the spectral response (Townshend, 1984).

LANDSAT thematic mapper (TM) data consist of seven bands: bands 1 (blue-green, 0.45-0.52 μm), 2 (green, 0.52-0.60 μm), 3 (red, 0.63-0.69 μm), 4 (near infrared, 0.76-0.90 μm), 5 (middle infrared, 1.55-1.75 μm), 6 (thermal infrared, 10.40-12.50 μm), and 7 (middle infrared, 2.08-2.35 μm). Fung and LeDrew (1987) mentioned that multispectral data acquired from most remote sensors exhibit high interband correlations or involve a certain degree of redundancy. Choosing the band combinations for a specific purpose is decided from the statistics of a scene, taking full account of any correlations that exist between different bands (Sheffield, 1985). It is critical that the user should merge multispectral data sets that are complementary rather than duplicative.

Trolier and Philipson (1986) reported that TM bands 3, 4 and 5 were superior to other TM spectral bands for defining hydrologic related land use and land cover characteristics. From their results, it was clear that there was a fair amount of redundant information in the seven TM bands. Interpretations of the TM bands 1 to 3 were nearly identical. They suggested that band 3 would be best among the visible

bands because it is less affected by atmospheric scattering, and offered positive identification of some land use types where bands 1 and 2 did not. In band 3, strong chlorophyll absorption and high reflectance for soils were also observed (Salomonson et al., 1980). This band is useful for discriminating vegetated and fallow areas. Interpretation of band 4 showed strong absorption for water and high reflectance for vegetation. Band 5 was useful for identifying cropland, wetlands, water bodies, and grassland. The composite image of TM bands 3, 4, and 5 was the most useful single image for separating cropland, forested area, and wetland based on tonality, and field shape and boundary (Trolier and Philipson, 1986). During the mid-growing season, when there was a great deal of similarity between young crop and pasture, their identification was aided by associated field features (i.e., shape and boundary of the fields). Sheffield (1985) also ranked bands 3, 4, and 5 combination as one of the top five out of thirty five triplet band combinations of TM data used for interpretation in a number of scenes in the U.S. with different ground cover characteristics.

Remote sensing techniques provide spatially extensive data sets of land use characteristics, which can serve as a factor in stratifying a study area into spatial units with different trace gas emission activity. Data derived from remote sensing can be integrated with GIS database of soil characteristics (e.g., soil texture), which can also be used as the stratification factor(s). The landscape- and regional-scale estimates of trace gas fluxes can be obtained by linking these large-area data sets with the quantitative relationships established between fluxes and temporal predictive variables.

3. SOIL-LANDFORM ASSOCIATIONS AT THE RESEARCH SITES: IMPLICATIONS FOR A SPATIAL SAMPLING SCHEME FOR NITROUS OXIDE EMISSION QUANTIFICATION

3.1 Introduction

Existing conceptual approaches for quantifying N_2O emissions at the landscape scale have emphasized the need to determine the basic spatial unit in the landscape, which serves as an integrative variable of the factors that control N_2O emission at this scale (e.g., soil type, plant community type; Groffman, 1991). Studies of N_2O emissions at the landscape scale have used stratification methods that consider either mainly topography or topography-related variables (e.g., drainage). The rationale for using topography as the variable in stratifying a landscape is based on previous findings that topography controls differences in soils and water distribution, which influence patterns of plant production and levels of organic matter in the landscape. Thus topography should also influence N_2O emission.

Pennock et al. (1987) developed a method of quantitatively classifying a soil landscape into functionally different units (i.e., landform complexes) based on slope variables, which relate to the differences in soils and hillslope hydrology in the landscape. These landform complexes had also proved to reflect the differences in rates of soil physical and biochemical processes in the landscape (Elliott and de Jong, 1992; Pennock et al., 1992; Van Kessel et al., 1993; Pennock et al., 1994). In order to obtain a landscape-based estimate of N_2O emission, it is important to establish a basic spatial sampling unit in the landscape from which determination of fluxes and

comparison of fluxes among sites are to be based. The objective of this part of the study is to establish a spatial sampling unit for quantifying N_2O emissions at the landscape scale.

3.2 Materials and Methods

3.2.1 Research design

The selection of sampling sites was governed by the present understanding of the regional controls on N_2O emission. Both field-based research (Groffman and Tiedje, 1989a; Mosier et al., 1996) and existing models of N_2O emission (Parton et al., 1996; Potter et al., 1996) suggest that the texture of the parent sediments and land use exert a strong, indirect control on N_2O emissions at the regional scale. The site selection within the delineated study region was stratified by texture and land use to reflect these differences. The study region (63 km x 74 km) was located in the Black soil zone with its center near St. Louis, Saskatchewan, Canada (105° 45' W, 53° 1' N). It was stratified into three textural types: glacio-lacustrine clays, glacio-lacustrine silts and very fine sands, and glacio-fluvial sands. The study sites selected in the glacio-lacustrine clay and silt areas are classified as Blaine Lake (silty clay loam) or Hamlin (fine sandy loam)-Blaine Lake Association map units, and the study sites selected in the glacio-fluvial sand area are classified as Meota (fine to coarse loamy sand) or Hamlin-Meota Association. The clay contents of the associations are: 15 to 35 % (Blaine Lake Association), 12 to 16 % (Hamlin Association), and 5 to 11 % (Meota Association) (Acton and Ellis, 1978). Hereafter, the aforementioned study sites selected in the three textural areas will be referred to as clay loam, fine sandy loam, and sandy areas, respectively.

In the clay loam area, a long-term (broken prior to 1920) cultivated site and a pasture site (converted from forest to grass in early 1970s) were selected in 1993. In

the cultivated site, two adjacent fields were selected in 1993 for the N_2O emission measurements: fallow and cropped fields (section 5.2.1). The soil characteristics reported here were those sampled at the cropped site, as both the fallow and the cropped sites are considered similar, being located in similar landscape and having the same cropping history. In the pasture site, the upper portion of the landscape was dominated mainly by smooth bromegrass (*Bromus inermis* Leyss.) whereas the lower portion of the landscape was still uncleared and occupied by aspen (*Populus tremuloides* Michx.). This type of land use, where the sloughs are still forested, is typical in the clay loam and fine sandy loam areas. In the fine sandy loam area, a long-term (broken prior to 1920) cropped site was selected in 1994. In the sandy landscape, cropped, pasture (seeded to alfalfa; *Medicago sativa* L.), and forest (with continuous aspen cover) sites were selected in 1994.

3.2.2 Sampling design and soil characteristics analyses

All sites were characterized as having a hummocky surface form with a complex sequence of slopes extending from rounded depressions to conical knolls. The slopes were generally 4-6 %. The sites were sampled using a square or rectangular grid sampling design (Table 3.1). The sampling points within the grid were separated by a 15 m spacing (e.g., Figs. 3.1 and 3.2). At each site, the topography of the sampling grid was surveyed using a laser theodolite (Sokkisha Electronic Total Station, Set 5; Sokkisha Co., Ltd., Tokyo, Japan). The topographical surveys of each site were used to derive a Digital Elevation Model (DEM) of the elevation surface. A series of slope morphological and positional attributes were calculated for each 5 m by 5 m cell of the DEM, and these attributes were used to classify each cell into one of the seven landform elements - slope segments with a defined range of slope curvature and gradient

Table 3.1. Location of the sites in the selected study region within the Black soil zone.

Texture	Land use	UTM† Coordinates (m)	Sampling grid
Clay loam	Cropped	448700 E., 5875100 N.	10 x 10
	Pasture‡	448790 E., 5874110 N.	9 x 10
Fine sandy loam	Cropped	447980 E., 5875200 N.	7 x 7
Sandy	Cropped	444500 E., 5869700 N.	7 x 7
	Pasture	443700 E., 5869800 N.	7 x 7
	Forest	445300 E., 5869900 N.	6 x 7

† All sites are in UTM zone 13.

‡ The upper level and shoulder complexes are occupied by bromegrass, and the footslope and level-depressional complexes are dominated by aspen.

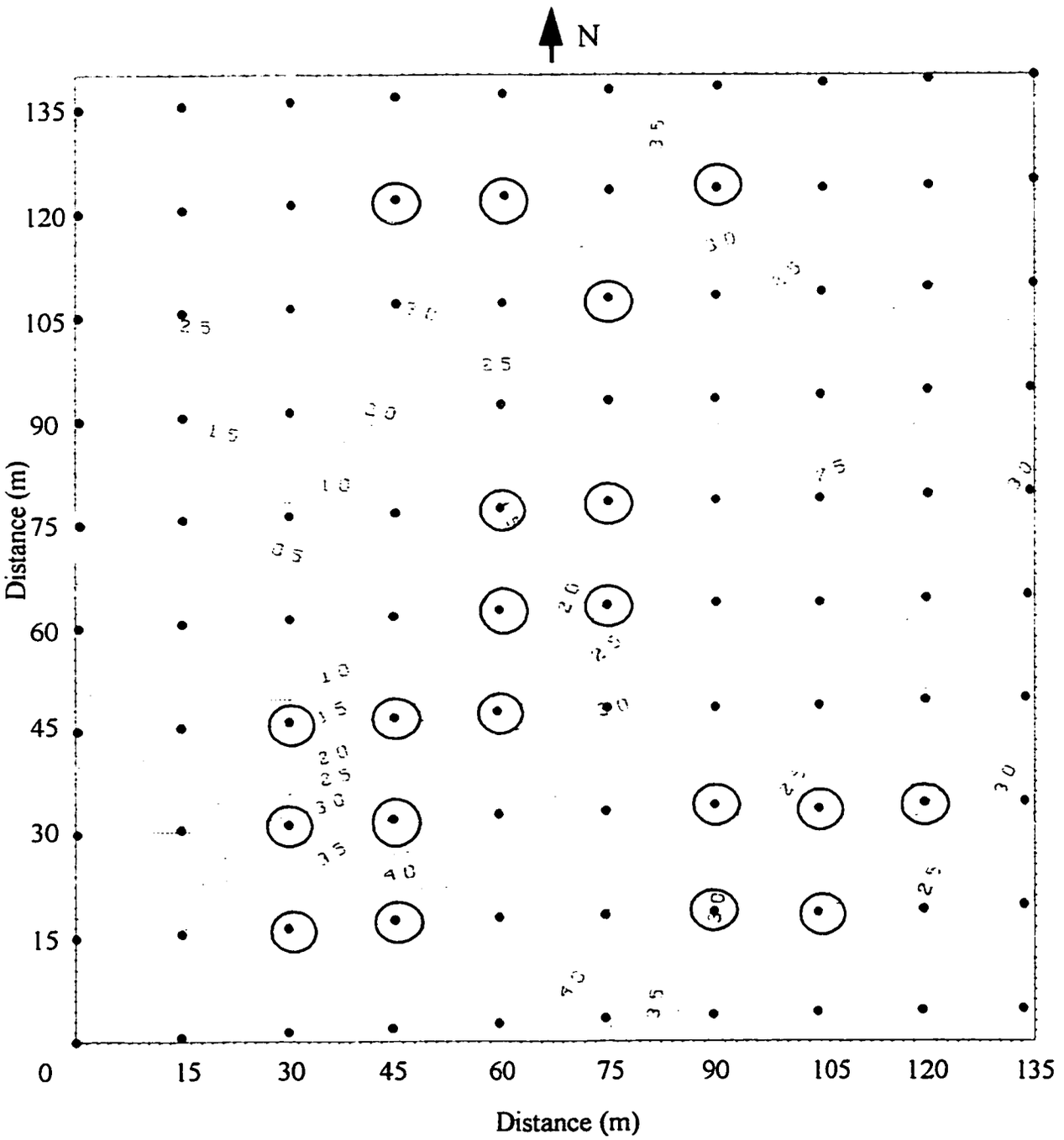

Fig. 3.1. Topographic map and sampling grid in the clay loam, cropped site.

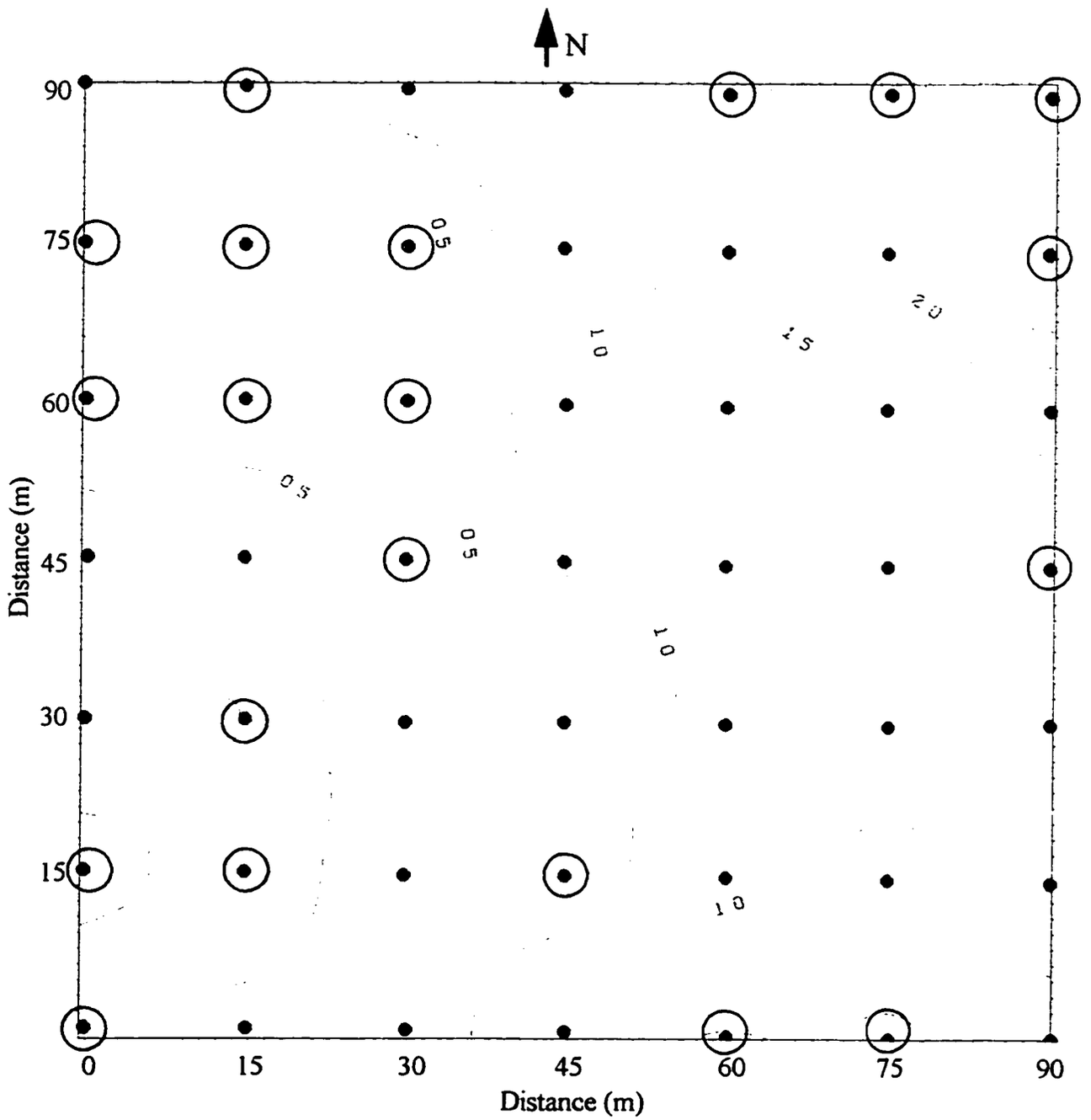

Fig. 3.2. Topographic map and sampling grid in the sandy, fertilized oat site.

(Pennock et al., 1987). These landform elements can then be combined into larger spatial units, termed landform element complexes (Pennock et al. 1994), using a spatial filtering algorithm. The latter process also incorporates information on the catchment area that contributes flow to each cell in the DEM. The four landform element complexes developed in Pennock et al. (1994) were used to stratify the landscapes into meaningful spatial units: upper levels (those with no significant plan and profile curvature and catchment areas less than 250 m^2), shoulders (those with convex profile curvatures and limited catchment area), low-catchment area footslopes (those with concave profile curvatures and catchment areas less than 250 m^2), and high-catchment area footslopes and level depressional complexes (those with either concave profile curvatures or no significant profile curvatures but with catchment areas greater than 250 m^2).

At each site, the soil at each sampling point was sampled for determination of bulk density, total N, and total organic C at 0 to 15-cm depth. The bulk density was determined using a soil core method. Total soil N was determined by total combustion at 1200 °C (RoboPrep; Europa Scientific, Crewe, England). Total C was determined on finely ground soil samples using a LECO CR-12 Carbon Determinator (LECO Corp., St. Joseph, MO). The amount of inorganic C in the samples was negligible, and thus values for total C are synonymous with total organic C. Measurement of the thickness of the A horizon and classification of the soil profile were also carried out for each sampling point. For the A horizon thickness and soil profile classification, in the cultivated sites, the sampling was carried out using a truck-mounted hydraulic drill, whereas in the forest and pasture sites soil pits were dug.

The distributions of the bulk density, A horizon thickness, total N, and total organic C are summarized using median and interquartile range measures. The distribution of the soil parameters in some individual landform complexes exhibited

skewness values over 2.0, and this, coupled with the small sample sizes in some landform complexes, precluded the use of standard parametric statistical measures. Differences among landform complexes within a given site and among sites were assessed using Kruskal-Wallis H test and its multiple comparison extension at an α level of at least 0.10.

3.3 Results and Discussions

3.3.1 Soil-landform relationship

Tables 3.2 to 3.7 show the association between soil distribution and landform at the study sites. The shoulder complexes typically experience high rates of runoff and soil loss (especially in the cultivated landscapes) and are dominated by Regosolic, Calcareous, and Orthic Black Chernozems. In the shoulder complex of the pasture site in the sandy area, some Gleysols were observed particularly on the convergent (concave plan curvature) shoulder (Table 3.6). In the upper level complex, where water generally moves vertically into the profile, Orthic Black Chernozems dominate (Table 3.2 to 3.5). The low-catchment footslopes are dominated by Orthic Black Chernozems with minor occurrence of Gleyed Black Chernozems and Gleysols. In the high-catchment footslope and level depressional complexes, the proportion of Gleysols versus Orthic Black Chernozems is higher than that in the low-catchment footslopes.

The difference in the characteristics of Gleysols occurring between the sandy area and the clay loam and fine sandy loam areas (Fig. 3.3) is related to their differences in parent materials. The minimal amount of clay in the glacio-fluvial sandy area (sandy sites) precludes the development of the Btg horizon in Gleysols, whereas Btg horizon development occurs in Gleysols in the glacio-lacustrine clay and silt areas (clay loam and fine sandy loam sites). This signifies that in Gleysolic soils in the sandy sites, water will drain freely and anaerobic or reduced O_2 condition from horizonation

Table 3.2. Distribution of soils in the landform complexes at the clay loam, cropped site.

Landform complexes	Proportion in the landscape	Regosolic	Chernozemic				Gleysolic		
		Orthic Regosol	Rego Black	Calcareous Black	Orthic Black	Gleyed Black	Orthic Humic	Humic Luvic	Orthic Luvic
	%								
Upper Level	19	0	0	0	19	0	0	0	0
Shoulder	36	5	0	0	31	0	0	0	0
Low-catchment footslope	11	0	0	0	7	2	0	2	0
High-catchment footslope	34	0	0	0	25	0	7	2	0

Table 3.3. Distribution of soils in the landform complexes at the clay loam, pasture site.

Landform complexes	Proportion in the landscape	Regosolic	Chernozemic				Gleysolic		
		Orthic Regosol	Rego Black	Calcareous Black	Orthic Black	Gleyed Black	Orthic Humic	Humic Luvic	Orthic Luvic
	%								
Upper Level	25	0	0	0	25	0	0	0	0
Shoulder	30	0	0	0	30	0	0	0	0
Low-catchment footslope	23	0	0	4	19	0	0	0	0
High-catchment footslope	22	0	0	0	7	0	4	7	4

Table 3.4. Distribution of soils in the landform complexes at the fine sandy loam cropped site.

Landform complexes	Proportion in the landscape	Regosolic	Chernozemic				Gleysolic		
		Orthic Regosol	Rego Black	Calcareous Black	Orthic Black	Gleyed Black	Orthic Humic	Humic Luvic	Orthic Luvic
	%								
Upper Level	2	0	0	0	2	0	0	0	0
Shoulder	49	0	2	4	43	0	0	0	0
Low-catchment footslope	33	0	0	0	25	0	8	0	0
High-catchment footslope	16	0	0	0	4	0	12	0	0

Table 3.5. Distribution of soils in the landform complexes at the sandy, cropped site.

Landform complexes	Proportion in the landscape	Regosolic	Chernozemic				Gleysolic		
		Orthic Regosol	Rego Black	Calcareous Black	Orthic Black	Gleyed Black	Orthic Humic	Humic Luvic	Orthic Luvic
	%								
Upper Level	13	0	0	0	13	0	0	0	0
Shoulder	27	0	0	0	27	0	0	0	0
Low-catchment footslope	13	0	0	0	10	3	0	0	0
High-catchment footslope	47	0	0	0	29	12	6	0	0

Table 3.6. Distribution of soils in the landform complexes at the sandy, pasture site.

Landform complexes	Proportion in the landscape	Regosolic	Chernozemic				Gleysolic		
		Orthic Regosol	Rego Black	Calcareous Black	Orthic Black	Gleyed Black	Orthic Humic	Humic Luvic	Orthic Luvic
	%								
Upper Level	0	0	0	0	0	0	0	0	0
Shoulder	30	0	2	0	12	4	12	0	0
Low-catchment footslope	36	0	0	0	24	0	12	0	0
High-catchment footslope	34	0	0	0	17	0	17	0	0

Table 3.7. Distribution of soils in the landform complexes at the sandy, forest site.

Landform complexes	Proportion in the landscape	Regosolic	Chernozemic				Gleysolic		
		Orthic Regosol	Rego Black	Calcareous Black	Orthic Black	Gleyed Black	Orthic Humic	Humic Luvic	Orthic Luvic
	%								
Upper Level	0	0	0	0	0	0	0	0	0
Shoulder	45	7	0	0	38	0	0	0	0
Low-catchment footslope	38	0	0	0	38	0	0	0	0
High-catchment footslope	17	0	0	0	10	5	2	0	0

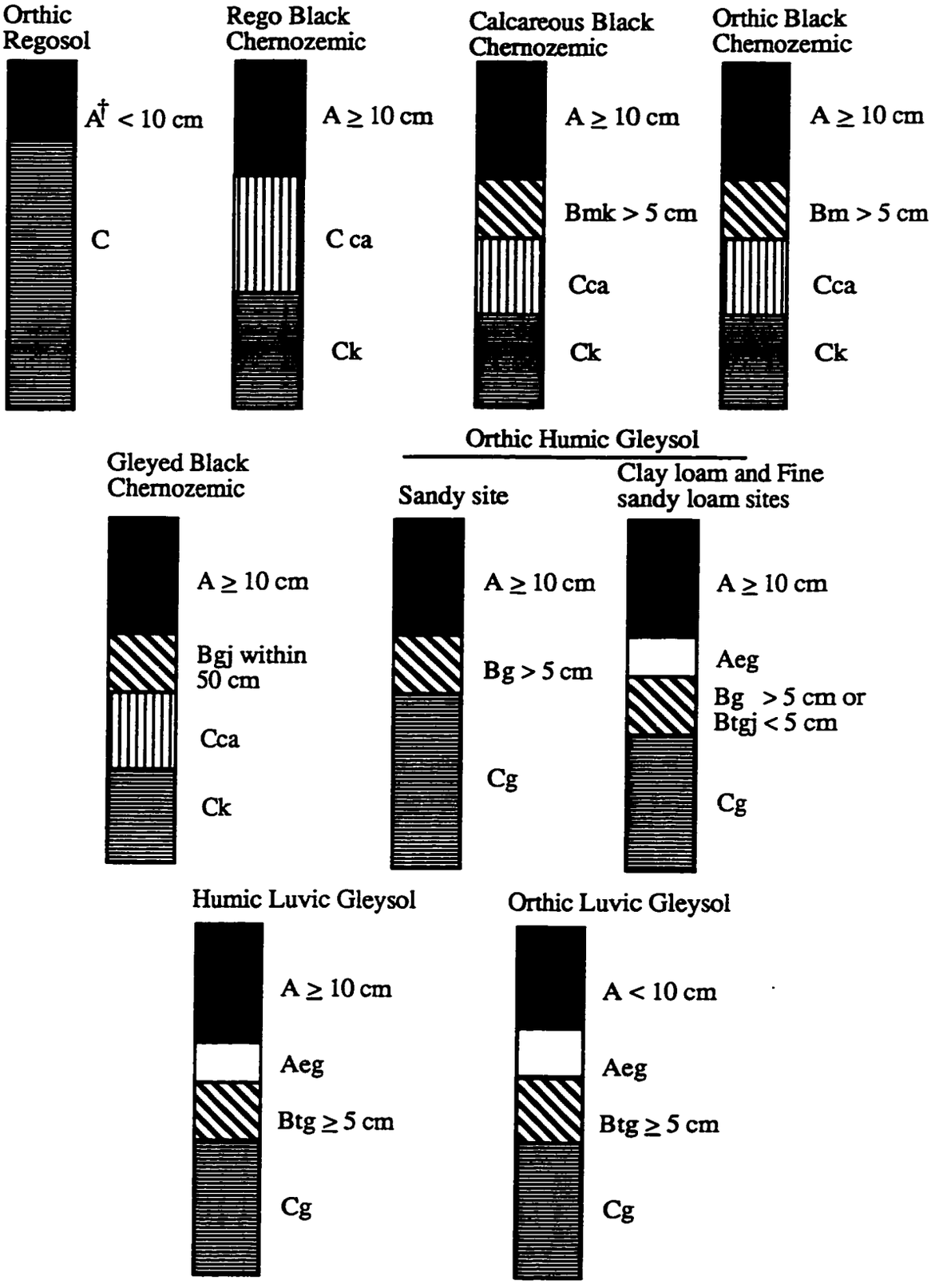

† A horizon could also be Ah, Ahe, or Ap.

Fig. 3.3. General representation of the soils observed in the study sites.

effects is less intensive. On the other hand, in Gleysolic soils in the clay loam and fine sandy loam sites, the Btg horizon will slow down the water movement within the profile, lengthening the duration of anaerobic or reduced O_2 condition.

In general, the soil-landform association showed a progression from the driest soils (Orthic Regosols) to the wettest soils (Gleysols) on the shoulder and upper level complexes to the footslope and level depressional complexes. These soil-slope associations occur because of the influence of hillslope morphology on surface and subsurface water movement (reviewed in Pennock et al., 1987). The clear association between landform and soil type observed in the study sites reflects the action and interaction of hydrological and geomorphic processes. The hydrological pattern results from differential water movement and concentration within hillslopes in response to changes in slope morphology and hydraulic conductivity of parent sediments (Pennock and Acton, 1989).

3.3.2 Soil physical and biochemical characteristics

The bulk density at 0 to 15-cm depth did not show any major differences among the different landform complexes within a site, except in the pasture site in the clay loam area (Table 3.8). At this site, the bulk densities in the footslopes are lower than those in the shoulders. This was attributed to the presence of LFH horizon ($\leq$ 3 cm) of the soils on the footslopes, which are occupied by aspen. The LFH horizon is absent in the soils on the shoulders, which are utilized for bromegrass. There was a clear difference in bulk densities among sites; the forest (with an LFH horizon ranging from 3 to 8-cm thick) and pasture sites in the sandy area and the pasture site in the clay loam area had lower values than any of the cropped sites (Table 3.12). This result is

Table 3.8. Median and interquartile range (in brackets) for bulk density (g cm^{-3} at 0-15 cm) in different textural groups and land use types in the study region stratified by landform element complexes.

Texture	Land use	Upper level	Shoulder	Low-catchment footslope	High-catchment footslope
Clay loam	Cropped	1.25 a†	1.34 a	1.24 a	1.34 a
		(0.14)	(0.19)	(0.30)	(0.17)
	Pasture	1.18 ab	1.22 a	1.05 b	0.99 b
		(0.21)	(0.11)	(0.31)	(0.33)
Fine sandy loam	Cropped	insufficient sample	1.34 a	1.24 a	1.34 a
			(0.12)	(0.10)	(0.20)
Sandy	Cropped	1.39 a	1.48 a	1.38 a	1.38 a
		(0.25)	(0.11)	(0.23)	(0.18)
	Pasture	no sample	1.25 a	1.20 a	1.15 a
			(0.25)	(0.21)	(0.28)
	Forest	no sample	1.00 a	0.97 a	0.92 a
			(0.17)	(0.13)	(0.19)

† Medians with the same letter within a given row are not significantly different (Kruskal-Wallis H test, $\alpha = 0.10$).

consistent with the observation of Pennock et al. (1994) where bulk densities tend to increase with years of cultivation.

Differences in thickness of the A horizon among landform complexes within a site were observed in the pasture site in the clay loam area and in the cropped sites in the clay loam and fine sandy loam areas. At these sites, the footslopes had thicker A horizons than the shoulder and upper level complexes (Table 3.9). In the cropped sites, these differences probably reflect a long-term deposition of soils from the upper to the lower landscape positions associated with cultivation-induced erosion. In the pasture site in the clay loam area, the thicker A horizon in the moist, aspen-dominated footslopes than in the dry, bromegrass-grown shoulders probably reflects the interaction of soil moisture dynamics and plant community composition, which influences organic matter accumulation in the soil. The A horizon thickness also differs among sites; the clay and fine sandy loam sites had thicker A horizon than the sandy sites (Table 3.12). This could be again related to the soil moisture and vegetation quality interaction; fine-textured soils can hold more water and support vegetation of high quality (lower lignin:N ratio) than the coarse-textured soils (Pastor et al., 1984; McClaugherty et al., 1985), which may result in higher soil organic matter accumulation in the former than in the latter.

The total soil N and total organic C differ only among landform complexes in the pasture site in the clay loam area; higher values were observed in the footslopes than in the upper level and shoulder complexes (Tables 3.10 and 3.11). This pattern is similar to that observed for A horizon thickness, and further indicates the long-term interaction of soil moisture, plant composition and litter quality, and microbial activity, which resulted in higher levels of total N and total organic C in the moist, lower landscape positions than on the dry, upper landscape positions. The total N also differs among sites, with generally higher levels in the clay loam and fine sandy loam sites

Table 3.9. Median and interquartile range (in brackets) for thickness of A horizon (cm) in different textural groups and land use types in the study region stratified by landform element complexes.

Texture	Land use	Upper level	Shoulder	Low-catchment footslope	High-catchment footslope
Clay loam	Cropped	21 b†	22 b	25 ab	31 a
		(18)	(7)	(11)	(20)
	Pasture	16 b	14 b	20 ab	25 a
		(9)	(8)	(11)	(5)
Fine sandy loam	Cropped	insufficient sample	12 c	22 b	52 a
			(9)	(13)	(23)
Sandy	Cropped	17 a	16 a	21 a	20 a
		(8)	(6)	(18)	(10)
	Pasture	no sample	18 a	19 a	20 a
			(9)	(12)	(9)
	Forest	no sample	20 a	16 a	16 a
			(9)	(8)	(11)

† Medians with the same letter within a given row are not significantly different (Kruskal-Wallis H test, $\alpha = 0.10$).

Table 3.10. Median and interquartile range (in brackets) for total soil N (Mg ha^{-1} at 0-15 cm) in different textural groups and land use types in the study region stratified by landform element complexes.

Texture	Land use	Upper level	Shoulder	Low-catchment footslope	High-catchment footslope
Clay loam	Cropped	5.5 a†	5.8 a	6.1 a	6.0 a
		(1.4)	(2.6)	(2.8)	(2.4)
	Pasture	6.4 b	6.0 b	6.7 ab	7.8 a
		(3.0)	(1.8)	(2.5)	(2.3)
Fine sandy loam	Cropped	insufficient sample	7.9 a	5.5 a	6.5 a
			(4.2)	(3.5)	(2.0)
Sandy	Cropped	2.2 a	2.7 a	insufficient sample	2.2 a
		(0.5)	(1.0)		(1.3)
	Pasture	no sample	6.2 a	4.4 a	5.8 a
			(3.4)	(6.8)	(8.0)
	Forest	no sample	2.7 a	2.4 a	2.6 a
			(1.0)	(0.8)	(0.7)

† Medians with the same letter within a given row are not significantly different (Kruskal-Wallis H test, $\alpha = 0.10$).

Table 3.11. Median and interquartile range (in brackets) for total organic C (Mg ha^{-1} at 0-15 cm) in different textural groups and land use types in the study region stratified by landform element complexes.

Texture	Land use	Upper level	Shoulder	Low-catchment footslope	High-catchment footslope
Clay loam	Cropped	69.9 a†	66.5 a	71.2 a	73.6 a
		(19.1)	(27.9)	(35.8)	(28.0)
	Pasture	80.5 b	76.9 b	88.7 ab	99.4 a
		(30.5)	(20.4)	(37.2)	(39.6)
Fine sandy loam	Cropped	insufficient sample	68.5 a	58.2 a	74.6 a
			(33.5)	(25.0)	(25.5)
Sandy	Cropped	33.4 a	28.2 a	34.0 a	23.7 a
		(14.6)	(12.0)	(25.1)	(10.8)
	Pasture	no sample	51.2 a	42.5 a	36.7 a
			(23.9)	(37.0)	(69.2)
	Forest	no sample	40.6 a	40.1 a	40.9 a
			(9.3)	(5.1)	(8.2)

† Medians with the same letter within a given row are not significantly different (Kruskal-Wallis H test, $\alpha = 0.10$).

Table 3.12. Median and interquartile range (in brackets) for soil characteristics in different textural groups and land use types in the study region.

Texture	Land use	Bulk density ($g\ cm^{-3}$)	A hor. thickness (cm)	Total N ($Mg\ ha^{-1}$)	Total organic C ($Mg\ ha^{-1}$)
Clay loam	Cropped	1.33 a†	24 a	5.8 ab	70.0 b
		(0.17)	(13)	(2.1)	(25.6)
	Pasture	1.05 b	19 ab	6.7 a	82.9 a
		(0.18)	(9)	(2.0)	(25.7)
Fine sandy loam	Cropped	1.40 a	20 ab	6.7 a	62.3 b
		(0.13)	(21)	(3.4)	(28.3)
Sandy	Cropped	1.44 a	18 b	2.3 b	28.6 d
		(0.19)	(8)	(1.2)	(14.2)
	Pasture	1.15 ab	17 b	4.6 ab	45.0 c
		(0.37)	(10)	(6.7)	(33.7)
	Forest	0.98 b	17 b	2.6 b	40.5 c
		(0.16)	(8)	(0.8)	(7.2)

† Medians with the same letter within a given column are not significantly different (Kruskal-Wallis H test, $\alpha = 0.01$).

than in the sandy sites (Table 3.12). In the sandy area, the slightly higher total N in the pasture site (planted to alfalfa) than in the cropped and forest sites was probably due to the high N content of organic matter from alfalfa residues. The C/N ratios, if calculated by landform complexes, were also lowest in the sandy, pasture site. The total organic C in the clay loam and fine sandy loam sites was also higher than in the sandy sites (Table 3.12). The influence of higher clay contents on soil organic C storage has been widely examined, and is related to both the chemical stabilization of organic matter by clay colloidal material and the increased moisture holding capacity, and therefore increased productivity of higher clay soils (Schimel et al., 1994). Within the same texture, the cultivated sites have lower total organic C than the uncultivated sites. This is consistent with the findings of Pennock et al. (1994) where progressive loss of soil organic C was observed with years of cultivation.

3.4 Implications for N_2O Emission Studies at the Landscape Scale

A clear relationship exists at the study sites between soil distribution and quantitatively defined landform segments. The distinct, replicable association between landform and soil type indicates the occurrence of distinctive pedogenic regimes, which are influenced by the hydrological pattern of the hillslope, and allowed the development of the general conceptual model of soil formation in these landscapes (Pennock et al., 1994). As discussed by Parkin (1993), there are three primary factors controlling variability of microbial processes in the landscape: soil type, surface topography, and water distribution. Soil type provides an integrative indication of factors such as texture, top soil depth, organic matter content, and nutrient status. Surface topography is a surrogate variable used to reflect conditions such as top soil depth and drainage. Both of these factors may serve to provide indications concerning water distribution at the landscape level. Hence, the landform complex-soil association observed at the

study sites provides a basic spatial unit for assessing microbial processes, e.g., N_2O emission, at the landscape scale. The differences in soil physical and biochemical characteristics that were observed among the sites also warrant the importance of stratifying a region based on texture of parent sediments and land use types. The approach used in this study, i.e., scaling-up from the individual grid cell level to broader landform groupings, provides one mechanism for generalizing from individual field observations to landscape and regional scales of the study.

For the assessment of N_2O emissions at each study site, the landform complexes were further generalized into two major groups: upper level and shoulder complexes and footslope and level-depressional complexes. In the succeeding chapters, these two major groups of landforms are simply referred to as shoulder and footslope complexes. The reasons for these groupings are:

1. Overall two major soil-landform assemblages can be generalized from this study; the upper level and shoulder complexes are dominated by Orthic Regosols and thinner variants (Rego and Calcareous Black) of the Chernozemic Order, whereas the footslope and level-depressional complexes were generally occupied by thick Orthic Black to Gleyed Black Chernozems and Gleysols.
2. In terms of soil moisture status, the upper landscape positions (upper level and shoulder complexes) would be likely subjected to drier condition than the lower landscape positions (footslopes and level-depressional complexes). Topography induces water redistribution through its effect on drainage, surface and subsurface water flow, and lateral flow of shallow groundwater that re-emerges in localized depressions.
3. In terms of sample allocation, the upper level, low-catchment footslope, or high-catchment footslope and level-depressional complexes did not occupy large enough areas in some study sites to provide a sufficient number of sampling points.

4. SEALED CHAMBER METHOD OF MEASURING NITROUS OXIDE EMISSION: LINEAR VS. DIFFUSION-BASED FLUX MODELS

4.1 Introduction

The sealed chamber is one of the many types of non-steady-state chambers used to measure gas exchange across the soil-atmosphere boundary. Non-steady-state chambers are so-called because the gradient of a trace gas in underlying soil continually adjusts to the changing concentrations in the chamber headspace (Livingston and Hutchinson, 1995). The chamber method, also termed the soil cover method, has been proven as the most useful approach for direct field measurement of N_2O emission (Hutchinson and Mosier, 1981; Goodroad and Keeney, 1984; Ambus and Christensen, 1995). Researchers agree that the method is efficient, and reduces the potential error associated with the disturbance at the study site that might alter its N_2O emission activity.

A major, but frequently overlooked, source of bias in individual chamber-based estimates of trace gas exchange is the use of inappropriate procedures for computing flux from the concentration data. Numerous models can be defined to relate the exchange rate of a trace gas to its time-dependent concentration in the atmosphere of the enclosed chamber. A linear model is often used to approximate the relation between observed concentrations and time under the assumption that for short deployment periods, the rate of change is nearly constant. The validity of assuming a linear model to describe the exchange process depends on the conditions that vary with each chamber deployment. In some conditions, such as during the measurement of small exchange rates, limits imposed by sampling logistics and analytical precision often

preclude shortening the sampling period enough to avoid significant nonlinearity. Application of a linear model to nonlinear data may seriously underestimate the unperturbed flux (Hutchinson and Livingston, 1993). An alternative to the linear model is the exponential model based partly on diffusion theory. Diffusion theory accounts for the feedback effects of the chamber on the exchange process, and predicts the decreasing rate of change in headspace concentration with time (Matthias et al., 1978; Hutchinson and Mosier, 1981).

The objective of this component of the study was to compare the N_2O fluxes estimated from linear regression and from the exponential model established by Hutchinson and Mosier (1981). Application of an inappropriate model may represent a potentially serious source of measurement bias that may influence not only summary statistics for the study, but also larger scale budgets based on the data.

4.2 Materials and Methods

The data set of N_2O emissions measured periodically from 30 June 1994 to 19 May 1995 at the clay loam, cropped site (fertilized wheat) and the sandy, cropped site (fertilized oat) were used. The clay loam site represented areas with high potential for N_2O production and where the exchange process is slow. The sandy site represented areas with low potential for N_2O production and where the exchange process is fast. At each site, two spatial sampling units were used: shoulder and footslope complexes (as discussed in section 3.4). On each landform complex, ten sampling points were selected from a grid sampling design with 15-m spacing (Figs. 3.1 and 3.2). The N_2O emissions were measured using a sealed chamber method (Fig. 5.1, section 5.2.3). The sites, gas sampling method, and N_2O concentration analysis are described in detail in sections 5.2.1 to 5.2.3. Estimates of N_2O fluxes were calculated using the exponential model developed by Hutchinson and Mosier (1981), which was based on

diffusive gas exchange. Their model is applicable when the change in concentration (C) is measured for two successive periods of equal length ($t_2 = 2t_1$) :

$$N_2O \text{ flux} = \frac{V (C_1 - C_0)^2}{A\, t_1 (2C_1 - C_2 - C_0)} \ln \frac{(C_1 - C_0)}{(C_2 - C_1)}$$

$$\text{for } \frac{(C_1 - C_0)}{(C_2 - C_1)} > 1 \qquad [1]$$

In Eq. [1], V (L) is the chamber volume, A (m^2) is the covered soil area, and C_0, C_1, and C_2 are the N_2O concentrations ($\mu L\ N_2O\ L^{-1}$) at t_0, t_1, and t_2, respectively. The initial N_2O concentration of each chamber (C_0 at t_0) was assumed equal to the ambient air samples collected at each site on each sampling day. The gas samples from the chamber were taken after 2 hours (t_1) and 4 hours (t_2) of trapping. Fluxes estimated from this model were compared with the fluxes calculated from linear regression. For each chamber and on each sampling day, linear regression equations were established between time of trapping (t_0, t_2, and t_2) and the corresponding N_2O concentrations (C_0, C_1, and C_2). The linear fitting was forced through the value of C_0 at t_0. The N_2O fluxes ($\mu L\ N_2O\ m^{-2}\ h^{-1}$) calculated from these models were converted into $\mu g\ N_2O\text{-}N\ m^{-2}\ d^{-1}$ using the gas equation, PV = nRT (P - standard pressure, V - volume of N_2O, n - moles of N_2O, R - gas constant, and T - temperature). The daily mean air temperature measured in the field was used in the gas equation.

The basis for comparing the data from Eq. [1] and linear regression was taken from Anthony et al. (1995). It was assumed that soil-atmosphere N_2O exchange is driven primarily by diffusion, which should generate N_2O accumulation curves like the type 1 and type 4 curves in Fig. 4.1 for production and consumption situations, respectively. The remaining four curve types should be observed only when the changes in concentration during each 2-h period are small compared with the measurement variability inherent in the data (i.e., the random variability associated with collection, handling, and analysis of the samples). Alternatively, their occurrence could

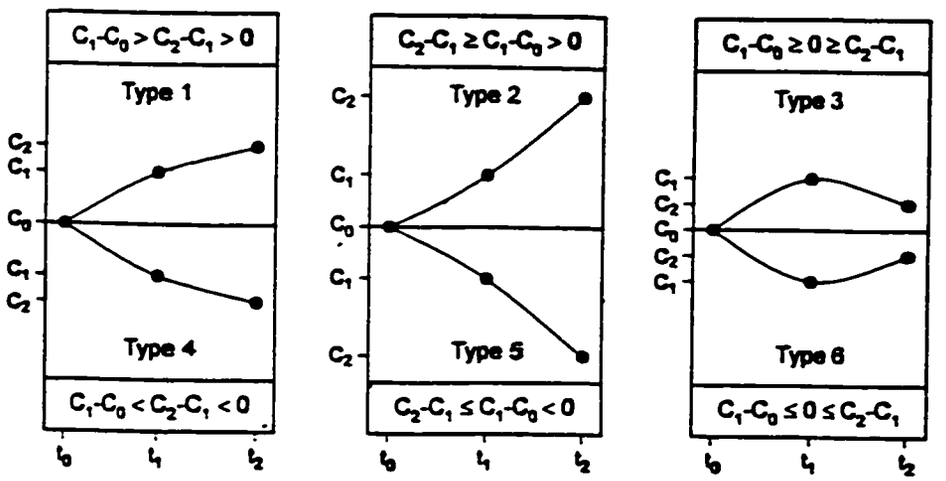

Fig. 4.1. Six possible curve shapes for N_2O accumulation in a non-steady-state chamber during two successive equal periods beginning with chamber deployment (From Anthony et al., 1995).

suggest that production and consumption was not constant during the deployment period or that diffusion was not the mechanism governing gas transport.

The availability of only three observations for each chamber deployment precluded using a nonlinear regression approach to partition measurement variability (for this approach see Hutchinson and Livingston (1993)). An arbitrary estimate of this parameter was adopted, similar to the approach used by Anthony et al. (1995). The "minimum detectable concentration difference (MDCD)" in the present study was defined on a daily basis as twice the mean absolute difference between successive replicate analyses of the ambient air sample that was routinely performed following every twentieth gas sample injection. At each curve type, the results are presented for the entire data set and for the chamber deployments at which N_2O concentrations at t_1 and t_2 both exceeded the MDCD. Comparison of the N_2O flux estimates obtained between the two models was carried out using the Mann-Whitney U test, which is a nonparametric test equivalent to t-test for non-normal data sets. Evaluation of the

significance of each linear regression slope was performed using a simple *t*-test at α = 0.05.

4.3 Results and Discussion

Data for the 380 chamber deployments in the clay loam site are summarized in Table 4.1. The median values, being more resistant than the mean values to the influence of outliers, were used to represent the central tendency for each curve type that characterized the whole data gathered during the 30 June 1994 to 19 May 1995 sampling period. On the footslope complex, for the 74 type 1 cases with changes in concentration greater than the MDCD, Eq. [1] yielded flux estimates that averaged 164 % greater than linear regression ($P = 0.08$). For the 58 type 1 cases on the shoulder complex, Eq. [1] showed flux estimates that averaged 258 % higher than linear regression ($P = 0.01$). Considering all cases categorized under type 1 curve, Eq. [1] yielded flux estimates greater than linear regression that averaged to 174 % and 301 % on the footslope and shoulder complexes, respectively.

At the sandy site (Table 4.2), the 46 type 1 cases on the footslope complex with changes in concentration greater than the MDCD showed estimates of N_2O fluxes that averaged 147 % higher using Eq. [1] than linear regression ($P = 0.02$). On the shoulder complexes, Eq. [1] yielded fluxes that averaged 212 % higher than linear regression ($P = 0.03$). For all cases categorized under type 1 curve, similar magnitude of differences in flux estimates between the two models were also observed (140 % and 209 % on the footslope and shoulder complexes, respectively). Although the absence of statistical estimates of measurement variability in Eq. [1] limits interpretation if the calculated fluxes are different from zero, examination of the frequency distributions of flux estimates from both models showed that in all sampling days Eq. [1] yielded

Table 4.1. **The clay loam, fertilized wheat site during the 30 June 1994 to 19 May 1995 sampling period: total number of cases with each of the N_2O accumulation curve types defined in Fig. 1, number of cases of each type for which changes in concentration at t_1 and t_2 exceeded the minimum detectable concentration difference (MDCD), median N_2O fluxes for each group computed from Eq. [1] and linear regression (LR), and the number of linear regression flux estimates that were significantly different from zero ($P \leq 0.05$).**

		All cases				Cases ≥ MDCD			
Landform complexes	Curve type	No. of cases	Median N_2O flux ($\mu g\ N\ m^{-2}\ d^{-1}$)		No. of cases $P \leq 0.05$	No. of cases	Median N_2O flux ($\mu g\ N\ m^{-2}\ d^{-1}$)		No. of cases $P \leq 0.05$
			Eq. [1]	LR			Eq. [1]	LR	
Footslope	1	76	1857	908	23	74	1857	908	23
	2	45	271	265	22	36	763	783	19
	3	34	undefined†	64	0	14	undefined	101	0
	4	0	-	-	-	0	-	-	-
	5	4	-21	-32	0	0	-	-	-
	6	34	undefined	28	0	0	-	-	-
	Total	190				124			
Shoulder	1	67	747	196	8	58	1044	240	9
	2	69	83	214	21	50	225	341	12
	3	28	undefined	51	0	12	undefined	101	0
	4	1	-179	-25	0	0	-	-	-
	5	0	-	-	-	0	-	-	-
	6	25	undefined	-12	0	0	-	-	-
	Total	190				120			

† For curve types 3 and 6, the logarithmic term in Eq. [1] is undefined.

Table 4.2. **The sandy, fertilized oat site during the 30 June 1994 to 19 May 1995 sampling period: total number of cases with each of the N_2O accumulation curve types defined in Fig. 1, number of cases of each type for which changes in concentration at t_1 and t_2 exceeded the minimum detectable concentration difference (MDCD), median N_2O fluxes for each group computed from Eq. [1] and linear regression (LR), and the number of linear regression flux estimates that were significantly different from zero ($P \leq 0.05$).**

Landform complexes	Curve type	All cases: No. of cases	All cases: Median N_2O flux ($\mu g\ N\ m^{-2}\ d^{-1}$) Eq. [1]	All cases: Median N_2O flux ($\mu g\ N\ m^{-2}\ d^{-1}$) LR	All cases: No. of cases $P \leq 0.05$	Cases ≥ MDCD: No. of cases	Cases ≥ MDCD: Median N_2O flux ($\mu g\ N\ m^{-2}\ d^{-1}$) Eq. [1]	Cases ≥ MDCD: Median N_2O flux ($\mu g\ N\ m^{-2}\ d^{-1}$) LR	Cases ≥ MDCD: No. of cases $P \leq 0.05$
Footslope	1	56	308	129	18	46	442	202	15
	2	49	40	89	12	12	499	398	7
	3	19	undefined†	-10	0	2	undefined	103	0
	4	0	-	-	-	0	-	-	-
	5	4	-17	-34	0	0	-	-	-
	6	62	undefined	17	0	0	-	-	-
	Total	190				60			
Shoulder	1	24	234	89	10	16	330	234	7
	2	53	27	67	13	18	299	290	8
	3	50	undefined	38	0	5	undefined	120	0
	4	5	-50	-23	0	0	-	-	-
	5	5	-7	-23	0	0	-	-	-
	6	53	undefined	13	0	0	-	-	-
	Total	190				39			

† For curve types 3 and 6, the logarithmic term in Eq. [1] is undefined.

higher means, medians, and ranges than the linear regression model for cases belonging to curve type 1.

The results in the two sites indicated that the type 1 cases, which have qualified the diffusion-based assumption of Eq. [1], included most of the data with the greatest influence on the magnitude of N_2O emission. Curve type 1 had 54 % and 63 % of all the cases that exceeded MDCD in the clay loam and sandy sites, respectively. Tables 4.1 and 4.2 also showed that data for curve types 3 through 6 supported the contention that their calculated N_2O fluxes were only within the magnitude of the inherent variability of N_2O emission measurement. For example, for the 126 cases in the clay loam site and 198 cases in the sandy site for curves 3 to 6, none of the linear regression flux estimates were significantly different from zero, and their mean absolute fluxes were only about 12 and 3 $\mu g\ N_2O\text{-}N\ m^{-2}\ d^{-1}$ in the clay loam and sandy sites, respectively. Of those number of cases, only 26 cases (11 %) in the clay loam site and 7 cases (7 %) in the sandy site exceeded the MDCD, which belong to curve type 3. These type 3 cases represent conditions where the build-up of N_2O concentration in the chambers was so small or only within the magnitude of the inherent measurement variability that the fluxes could not be calculated using Eq. [1] and that the slope from linear regressions were not significantly different from zero. The type 2 cases represent situations where the flux was large compared with measurement variability, but so nearly linear that even relatively small errors sometimes caused the change in concentration from t_1 to t_2 to be higher than from t_0 to t_1, which violates the assumption of which Eq. [1] is based. Considering the cases that exceeded MDCD, cases belonging to Type 2 constitute 35 % and 30 % in the clay loam and sandy sites, respectively, and their flux estimates obtained from Eq. [1] and linear regression did not significantly differ ($P > 0.20$).

Equation [1] appears to be more applicable for estimating daily N_2O fluxes from the data gathered in this study, as its diffusive-based assumptions included most

of the data with greatest influence on the magnitude of N_2O emission. If the rate of change in N_2O concentration in the headspace of the sealed chamber is not constant with time or exhibits a nonlinear behavior, employing a linear model to describe the exchange process may substantially underestimate the flux. A downward bias would be introduced in the summary statistics, as well as the landscape- and regional-scale budgets based on those estimates.

5. LANDSCAPE-SCALE PATTERNS AND SEASONAL FLUCTUATIONS OF NITROUS OXIDE EMISSION

5.1 Introduction

Studies of N_2O emission from different ecosystems are abundant, but few studies have addressed the problem of scaling up point-in-time and -in-space measurements to annual fluxes for large areas. The inherently high spatial and temporal variation of N_2O emission have hindered attempts to establish long-term or large-scale predictive relationships with its controlling variables. A relatively recent approach to dealing with the high variability of N_2O emission activity is by increasing the scale of investigation in both time (seasonal rather than daily) and space (landscape scale rather than field scale) (Groffman, 1991). At the regional scale, landscapes are considered as the experimental units, and in turn at the landscape scale, meaningful sampling units ("field" units) are selected to characterize the range of conditions within the landscape.

At a field scale, soil water accounted 28 % of the variation of N_2O emission from a cropped field (Mosier and Hutchinson, 1981), while WFPS did not correlate with N_2O emission from forest ecosystem in North Carolina (Davidson and Swank, 1986). However, in a landscape-scale study, Groffman and Tiedje (1989b) were able to explain 86 % of the annual denitrification losses from forest ecosystem in Michigan by incorporating into their model variables that regulate denitrification only indirectly (i.e., soil texture and soil drainage). Recent studies in Saskatchewan, Canada have evaluated the landscape-scale patterns of denitrification and how these patterns interact with soil water, N, and C dynamics in the landscape (Elliott and de Jong, 1992;

Pennock et al., 1992; Van Kessel et al., 1993). Data from these studies suggest the presence of distinct controls on denitrification in this region, and that evaluation of the spatial and seasonal patterns of these controls could be used to scale up N_2O emissions to annual fluxes at the landscape and regional scales.

For this component of the study, it is hypothesized that geomorphology and land use should be strong controllers of N_2O emission at the landscape and regional scales. It is likely, for example, that soil texture will influence N_2O emission because of interactions between texture and soil moisture for a given landscape and climatic zone. Since land use is often strongly related to nitrogen availability (Groffman, 1991), differences in land use should also exhibit differences in N_2O emission. Hence, the region was stratified based on texture of parent sediments and land use, and N_2O emission was investigated in soil landscapes chosen as representative units of the region. The objectives were (i) to determine the landscape-scale patterns and seasonal fluctuations of N_2O emission, and (ii) to demonstrate the relationship between large-scale (distal) controllers and microbial (proximal) factors of N_2O emission. Such data should prove useful in evaluating or validating models for quantifying N_2O emissions at the landscape and regional scales, in developing management strategies to reduce emissions, and in improving investigation methods for similar studies conducted at a large scale.

5.2 Materials and Methods

5.2.1 Site description and landscape-scale sampling scheme

The selection of representative landscapes within the study region and the derivation of the spatial sampling unit within a landscape was discussed previously in section 3. There were three landscapes selected based on texture of parent sediments: clay loam, fine sandy loam, and sandy areas (section 3.2.1). In the clay loam area, a

pasture, fallow, and cropped sites were selected. The fallow site was summer fallowed from July 1993 until April 1994; it was grown to unfertilized canola (*Brassica rapa* L.) during the early part of the 1993 growing season. The cropped site was seeded to unfertilized canola and fertilized wheat (*Triticum aestivum* L.) in 1993 and 1994, respectively. The inclusion of an unfertilized field in the beginning of the study was intended to provide base line information of its N_2O emission activity for comparison to fertilized fields. In 1994, fertilizers were applied at 28 kg N ha^{-1} as anhydrous ammonia at seeding (May 11) and 57 kg N ha^{-1} as liquid urea at seedling stage (June 10). In the fine sandy loam area, N_2O emissions were measured beginning on 18 May 1994 in a site seeded to fertilized canola. Anhydrous ammonia was applied (62 kg N ha^{-1}) at seeding (15 June 1994). In the sandy area, N_2O emissions were measured beginning on 30 June 1994 in cropped, pasture, and forest sites. The cropped site was seeded to oat (*Avena sativa* L.) and fertilized with 45 kg N ha^{-1} as ammonium sulfate at seeding (10 June 1994). These sites are managed by the farm owners, and the monitoring of N_2O emissions was superimposed on the management practices generally employed by the farmers in this study region.

At each study site, two spatial sampling units were used: shoulder and footslope complexes (as discussed in section 3.4). On each landform complex, at least ten sampling points were selected from a grid sampling design with 15-m spacing (e.g., Figs. 3.1 and 3.2). From a denitrification study conducted earlier in the Black soil zone, these number of samples were considered sufficient in representing the activity of a given landform complex (Van Kessel et al., 1993).

5.2.2 Temporal sampling scheme

To assess the seasonal pattern of N_2O emission, sufficient frequency of sampling had to be undertaken to characterize the rate of the process under different

environmental conditions throughout the years of study (Table 5.1). During the summer of 1993, measurements were taken on successive days after three particular rainfall events to monitor the length in time of N_2O emission after rainfall. This information was used as the basis for sampling timing in the succeeding measurements. Measurements for N_2O emissions during the summer of 1994 were taken thrice a month, particularly after a significant rainfall event ($\geq$ 5 mm). In fall, when the soil water content was low, measurements were taken once a month until the activity was undetectable. Measurements were resumed at approximately weekly interval during the spring thaw. On any given sampling day when N_2O emissions were measured at several sites, these sites were sampled at the same time of the day (between 10:00 a.m. to 2:00 p.m.) to facilitate comparison of their N_2O emission activity.

5.2.3 N_2O concentration analysis and flux measurement

Direct in-field measurement of N_2O emission was carried out using a sealed chamber method (Fig. 5.1). This sealed chamber has similar specifications to the closed chamber designed by Hutchinson and Mosier (1981), except that it was not provided with a vent. On each sampling day, the sealed chamber was inserted into the surface of the soil. Gas samples were withdrawn through the injection port using a 20-mL syringe and stored in 20-mL vacutainers (pre-evacuated to 40 Pa) (Becton Dickson and Co., Rutherford, NJ). The gas samples were then transported to the laboratory for analysis. The standard N_2O gases were also stored in vacutainers to have similar storage and handling procedures with the gas samples. Nitrous oxide standards were obtained from Linde (Union Carbide Canada Limited, Toronto, ON). Calibration curves were established on each day of analysis, and 0.99 correlation coefficients were obtained between standard N_2O concentration and peak area. The N_2O concentration was analyzed by a gas chromatograph (HP 5710A) equipped with ^{63}Ni electron

Table 5.1. Dates of N_2O emission measurements at each site.

Sampling dates	Clay loam			Fine sandy loam	Sandy		
	Cropped	Fallow	Pasture	Cropped	Cropped	Pasture	Forest
1993							
17 May	x						
28 May			x				
12 June	x						
13 June	x						
14 June	x						
15 June	x						
26 June	x		x				
27 June	x		x				
6 July	x		x				
7 July	x	x					
19 August	x	x					
21 October	x	x	x				
25 November	x	x	x				
1994							
17 March	x	x	x				
24 March	x	x	x				
29 March	x	x	x				
5 April	x	x	x				
9 April	x	x	x				
18 April	x	x	x				
25 April	x	x	x				
18 May	x		x	x			
23 May	x		x	x			
14 June	x		x	x			
16 June	x		x	x			
30 June	x		x-fs †	x	x	x	x-fs
8 July	x		x-fs	x	x	x-fs	x
19 July	x		x	x	x	x-fs	x-fs
30 July	x		x-fs	x	x	x	x-fs
8 August	x		x-fs	x	x	x-fs	x
18 August	x		x	x	x	x-fs	x-fs
29 August	x		x-fs	x	x	x	x-fs
20 September	x		x	x	x	x-fs	x-fs
4 October	x		x-fs	x	x	x	x-fs
8 November	x		x-fs	x	x	x	x-fs
1995							
14 March	x		x	x	x	x	x
21 March	x		x	x	x	x	x
13 April	x		x	x	x	x	x
18 April	x		x	x	x	x	x
21 April	x		x	x	x	x	x
26 April	x		x	x	x	x	x
3 May	x		x	x	x	x	x
12 May	x		x	x	x	x	x
19 May	x		x	x	x	x	x

† N_2O emission was measured only on the footslope complex.

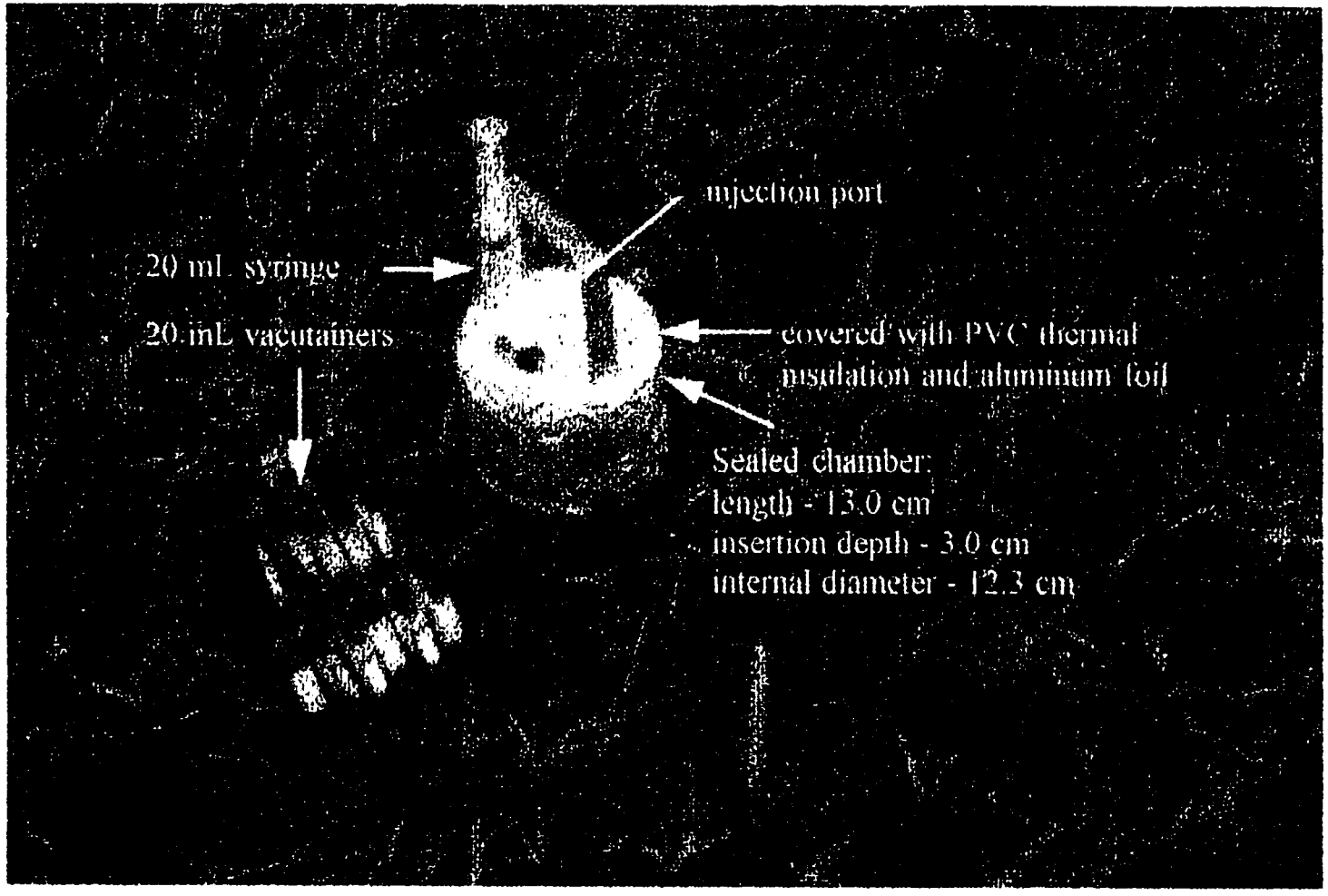

Fig. 5.1. Sealed chamber method of measuring N_2O emission in the field.

capture detector (operated at 300 °C) and Porapak Q column (SUPELCO, Oakville, ON; 200 μm mesh, 3.05 m long, 0.32 cm diam., and in an oven temperature of 60 °C).

The vertical N_2O flux density (μg N_2O-N m^{-2} d^{-1}) above the soil was determined by measuring the change in N_2O concentration beneath the sealed chambers at 2 h and 4 h of trapping and by using the estimation model established by Hutchinson and Mosier (1981) (Eq. 1; section 4.2). As pointed out by Livingston and Hutchinson (1995), there is no single chamber design, deployment period or sampling and analytical approach applicable in all situations. In this relatively low-flux area, this deployment period was long enough for the concentration increase to be measurable yet also short enough to minimize the feedback effect of the chamber air to the subsurface concentration gradient.

5.2.4 Other measurements

At each selected N_2O-sampling point, other soil properties were also assessed periodically. On all N_2O-sampling days, except when the soil was covered with snow, the soil water content was measured by the gravimetric method. The soil samples were oven dried at 105 °C for 24 h, and the bulk densities were used to calculate the volumetric moisture content (Gardner, 1986). Soil mineral N (NH_4^+ and NO_2^- + NO_3^-) and soluble organic C were measured once a month in all sites, except in the clay loam, unfertilized canola and fallow sites where these parameters were measured only in the beginning and in the end of the 1993 growing season. The mineral N was extracted by shaking 50 g of unprocessed (i.e., moist) soil samples with 200 mL of 2M KCl for 1 h, after which NH_4^+ and NO_2^- + NO_3^- were determined by using mineral N autoanalyzer (Technicon Autoanalyzer II, Tarrytown, NY). Total soluble C and soluble

inorganic C were extracted by shaking 10 g of field-moist soil with 0.5M K_2SO_4 for 1 h, and were analyzed using soluble C analyzer (Beckman Tocomaster Model 915B, Fullerton, CA). Soluble organic C was calculated as the difference between total soluble C and soluble inorganic C. These soil properties were measured on samples from 0 to 15-cm depth.

A climate station was set up at the clay loam area, in between the pasture and cultivated sites, and standard meteorological measurements were recorded throughout the years of study. Air temperature (at 1.5 m above the ground) was measured using thermistors. Rainfall was measured with a tipping bucket rain gauge (Model RG2501, Sierra Misco, Berkeley, CA). The data were summarized daily using a data logger and periodically transferred to a computer for processing.

5.2.5 Statistical analyses

Exploratory data analysis (EDA) as described by Pennock et al. (1992) was used in the first stage of statistical analyses. The EDA showed that the N_2O fluxes for each sampling date at each site were generally non-normally distributed (Appendix 1). Hence, all the succeeding statistical analyses were carried out using nonparametric methods. Nonparametric statistical methods are based on ranked data rather than on the original data values. The use of ranked data eliminates some of the problems associated with highly skewed distributions.

At each study site, the differences in N_2O emissions between landform complexes across time were assessed using repeated-measures one-way analysis of variance. Crowder and Hand (1990) discussed the applications of repeated-measures analysis in determining differences between experimental units on a variable measured repeatedly over a certain period of time. This test was carried out by ranking the

individual sampling points in a site (e.g., clay loam, unfertilized canola site), based on their corresponding N_2O fluxes, separately for each sampling date. Repeated-measures analysis was conducted to the whole data sets of rank values during the sampling period specified for a site. In repeated-measures analysis, if the mean square error of the test for differences between experimental units (i.e., landform complexes in a given site) is significant, this indicates that the landform complexes differ in N_2O emissions over the period of time being considered. The temporal consistency of these differences is signified by the mean square error for the time factor; if the mean square error for the time factor is insignificant, then the difference between the experimental units is consistent over time. The level of significance adopted in landscape-scale study is at $\alpha = 0.20$ (Van Kessel, 1993; Pennock et al., 1994), as the use of a rigorous significant level is unwise given the high degree of variability inherent to uncontrolled, field-based designs. High variability greatly increases the probability of a Type II error (i.e., of failing to detect differences in N_2O emissions between the landform complexes when differences do occur) if an unrealistically rigorous α level is selected (Peterman, 1990).

The differences in N_2O emissions among sites were assessed using Kruskal-Wallis H test (Siegel and Castellan, 1988). This comparison was carried out separately for each landform complex because within a site the landform complexes differed in N_2O emissions. If a difference was detected at a particular sampling date, the multiple-comparison extension of Kruskal-Wallis H test was used to determine the nature of differences among the sites. The results of the multiple-comparison test were then used as the basis for ranking the sites in terms of their N_2O emission activity. For sampling days when there was no significant differences among the sites, the sites were given a tie rank value. The temporal consistency of the ranking order among the sites was assessed using the Kendall coefficient of concordance, W (Siegel and Castellan, 1988).

5.3 Results

5.3.1 Landscape- and seasonal-scale patterns

Generally, highly skewed frequency distributions were observed in our data sets, which led to large coefficients of variation (CV > 100 %; Appendix 1). Large CVs both spatially and temporally have also been reported in plot-scale studies (Mosier and Hutchinson, 1981; Goodroad and Keeney, 1984), and appear to be inherent to N_2O emission process when measured *in situ*. In this study, the interest was on the variability between landform complexes, and whether the differences are temporally consistent. The repeated-measures analysis by ranks was used for this purpose (Table 5.2). The spatial variance was significant in all sites except in the clay loam, pasture site (i.e., during May 1993-April 1994 and summer-fall 1994 sampling periods) and in the sandy, forest site. Thus, within most of the study sites, the landform complexes differed significantly in N_2O emission activity. In the sites where a significant landscape-scale pattern was observed, generally higher N_2O emissions occurred on the footslope than on the shoulder complex (Figs. 5.2, 5.3, 5.5, 5.6, and 5.7). The temporal variance of the spatial domains was not significant in all sites (Table 5.2). These results indicate that the ranking order of the individual sampling points in a site for a particular sampling day was consistent throughout the sampling period or, in other words, that the landscape-scale pattern was generally consistent over time.

The seasonal pattern of N_2O emission showed that fluxes were increasing towards the early summer, decreasing towards the end of summer, and virtually ceased by the onset of frost in fall (Figs. 5.2 to 5.8). In the clay loam, fertilized wheat site, the first application of N fertilizer (when the area had just received the first summer rainfall; Fig. 5.9) did not increase N_2O emission, but the N fertilizer applied in June 1994 (when rainfall was high) triggered N_2O emission (Fig. 5.2B). Nitrogen fertilization followed by rainfall increased N_2O emissions due to the increase in N availability (from

Table 5.2. Assessment of the differences in N_2O emissions between landform complexes across time using repeated-measures analysis by ranks.

Site	Sampling period	Difference between spatial domains		Temporal difference of the spatial domains	
		Variance†	Signif. F	Variance	Signif. F
	1993 - 1994				
Clay loam					
Unfertilized canola	May - April	2421	0.002	12	0.995
Fallow	July - April	180	0.067	2	0.998
Pasture§	May - April	26	0.441	0	1.000
	1994 - 1995				
Clay loam					
Fertilized wheat	May - May	227	0.155	8	0.987
Pasture§	May - May	243	0.065	7	0.986
	(summer - fall)‡	36	0.425	1	0.998
	(spring)	497	0.001	4	0.991
Fine sandy loam					
Fertilized canola	May - May	1965	0.000	12	0.926
Sandy					
Fertilized oat	June - May	224	0.020	2	1.000
Pasture	June - May	369	0.003	5	0.998
Forest	June - May	1	0.743	0	1.000

† Mean square error of the test for differences between landform complexes within sites, considering all the N_2O measurements taken during the specified sampling period.

‡ Analyzed seasonally to determine when was the difference between landform complexes being observed.

§ In the clay loam, pasture site, the shoulder complex was occupied by bromegrass and the footslope complex was dominated by aspen.

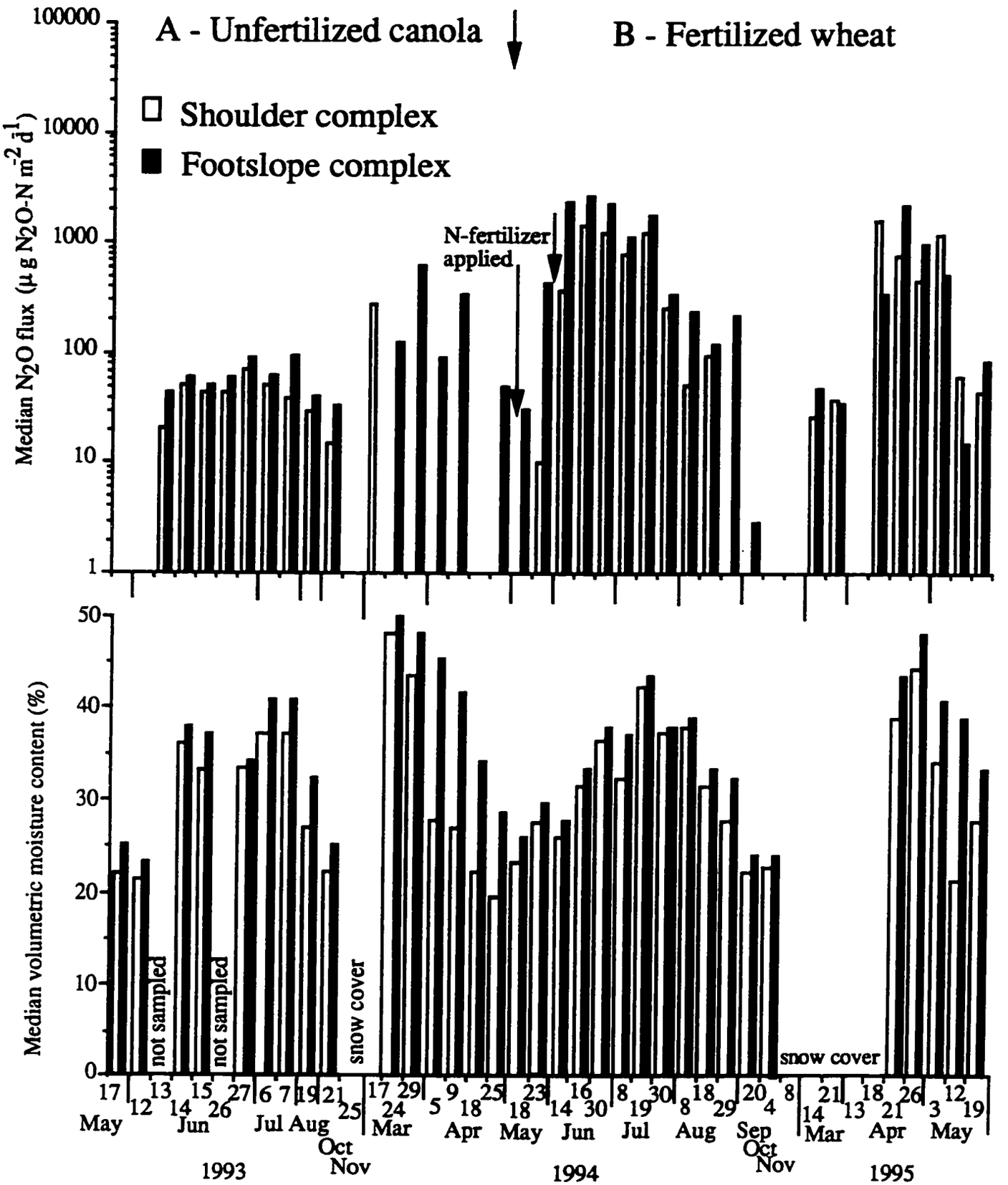

† sampling days marked with snow cover refer to conditions where either all or some sampling points were still covered with snow.

Fig. 5.2. Landscape- and seasonal-scale patterns of N_2O emissions and soil moisture contents in the clay loam, cropped site.

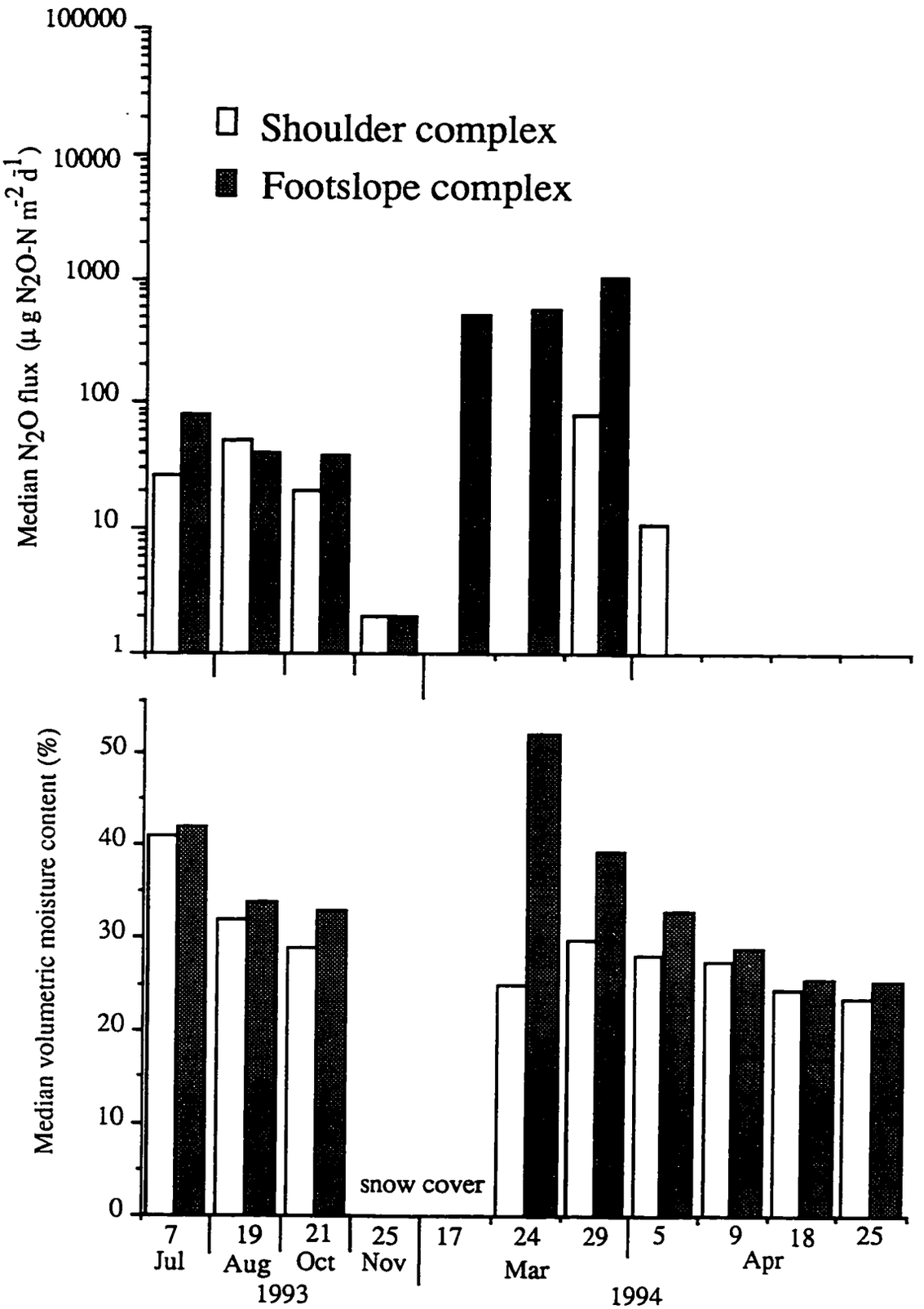

† sampling days marked with snow cover refer to conditions where either all or some sampling points were still covered with snow.

Fig. 5.3. Landscape- and seasonal-scale patterns of N_2O emissions and soil moisture contents in the clay loam, fallow site.

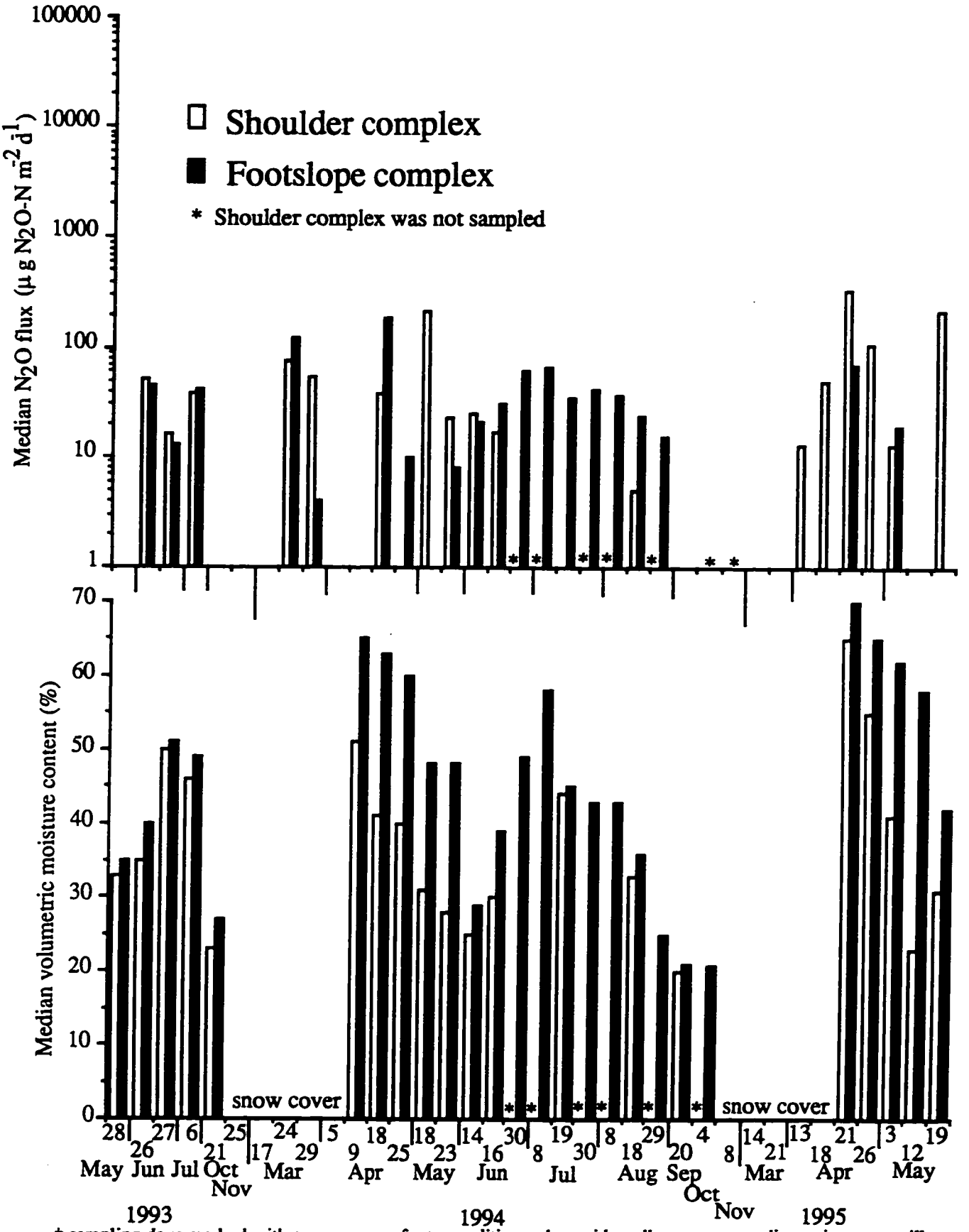

† sampling days marked with snow cover refer to conditions where either all or some sampling points were still covered with snow.

Fig. 5.4. Landscape- and seasonal-scale patterns of N_2O emissions and soil moisture contents in the clay loam, pasture site.

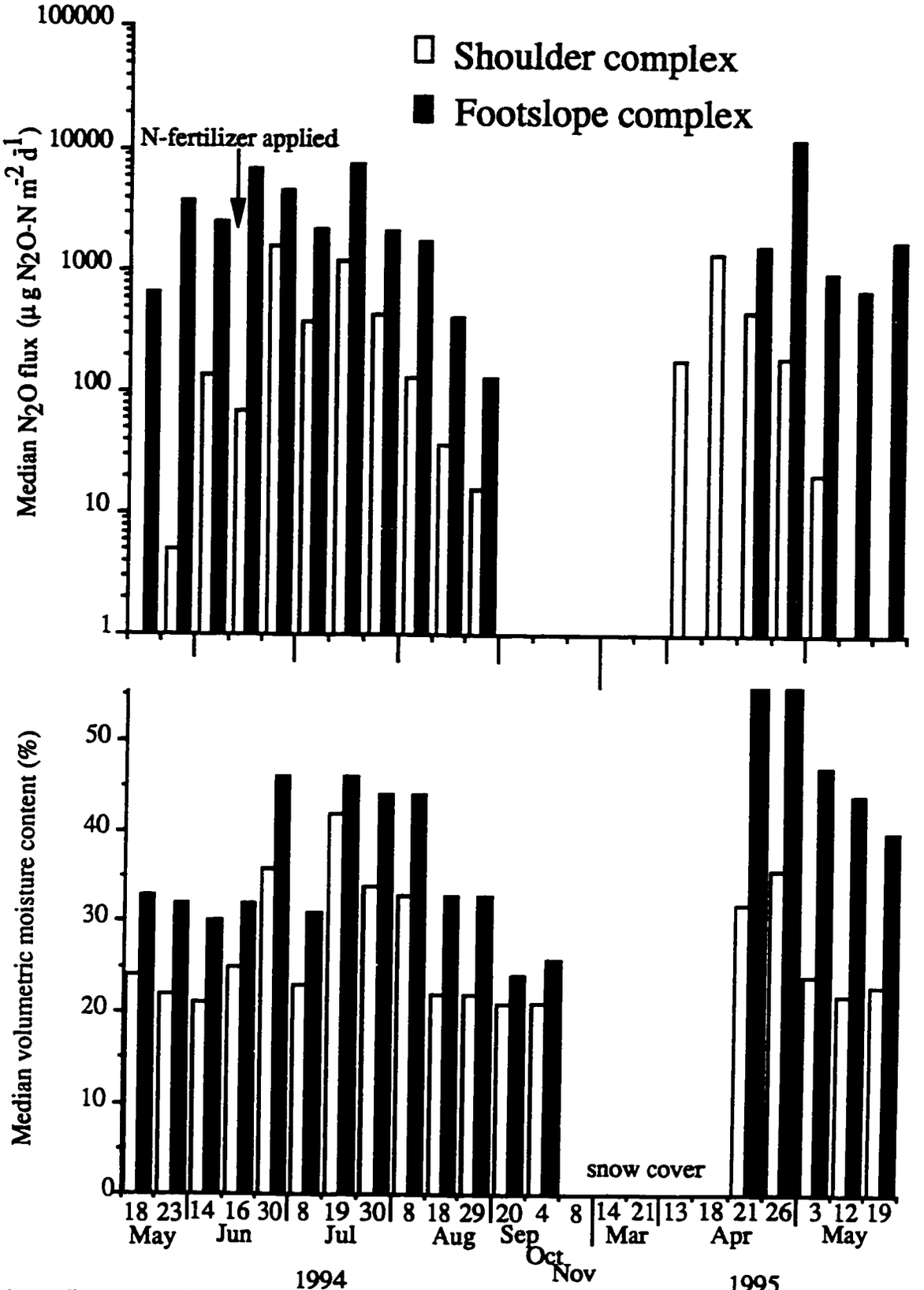

† sampling days marked with snow cover refer to conditions where either all or some sampling points were still covered with snow.

Fig. 5.5. Landscape- and seasonal-scale patterns of N_2O emissions and soil moisture contents in the fine sandy loam, fertilized canola site.

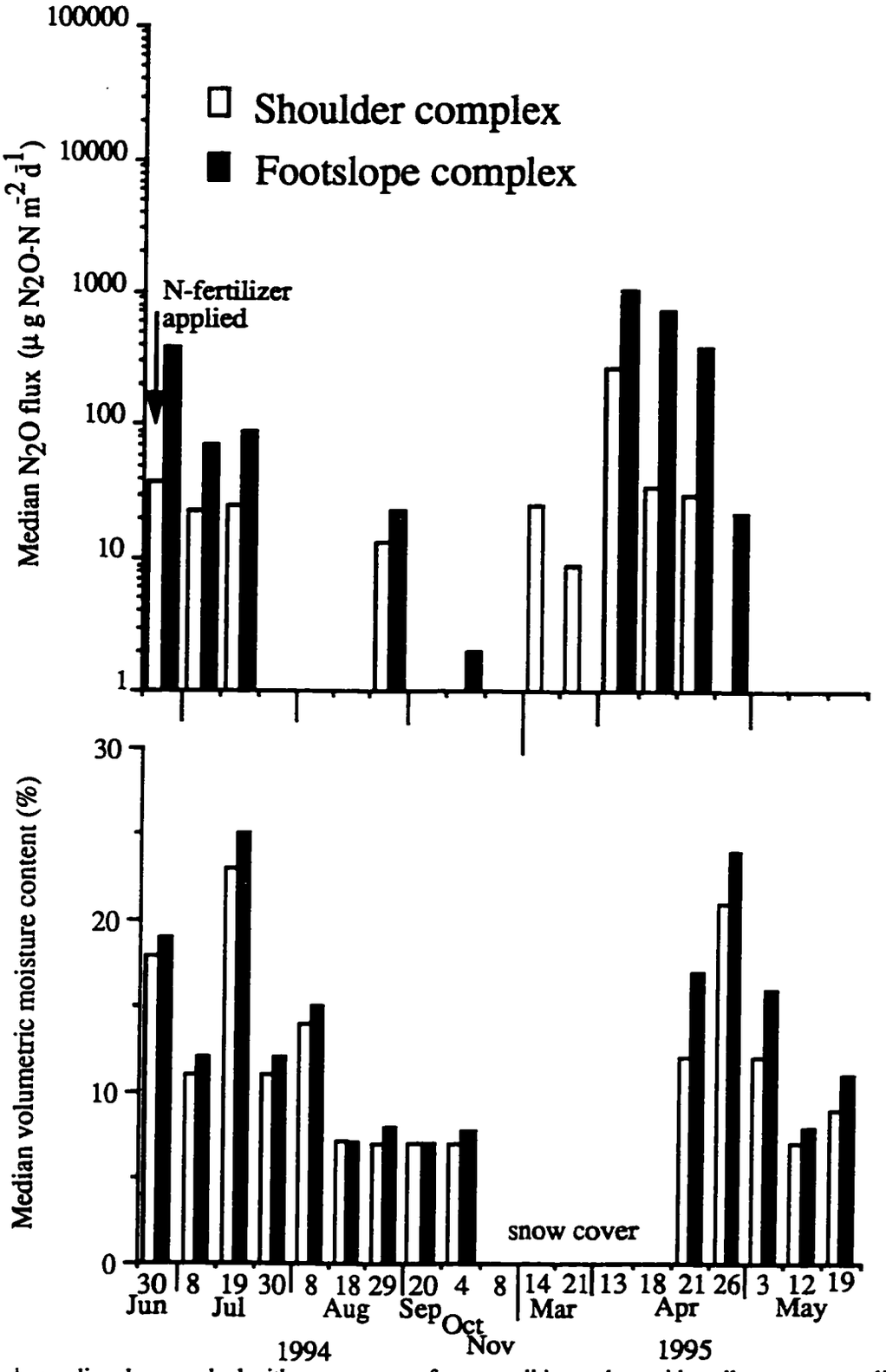

† sampling days marked with snow cover refer to conditions where either all or some sampling points were still covered with snow.

Fig. 5.6. Landscape- and seasonal-scale patterns of N_2O emissions and soil moisture contents in the sandy, fertilized oat site.

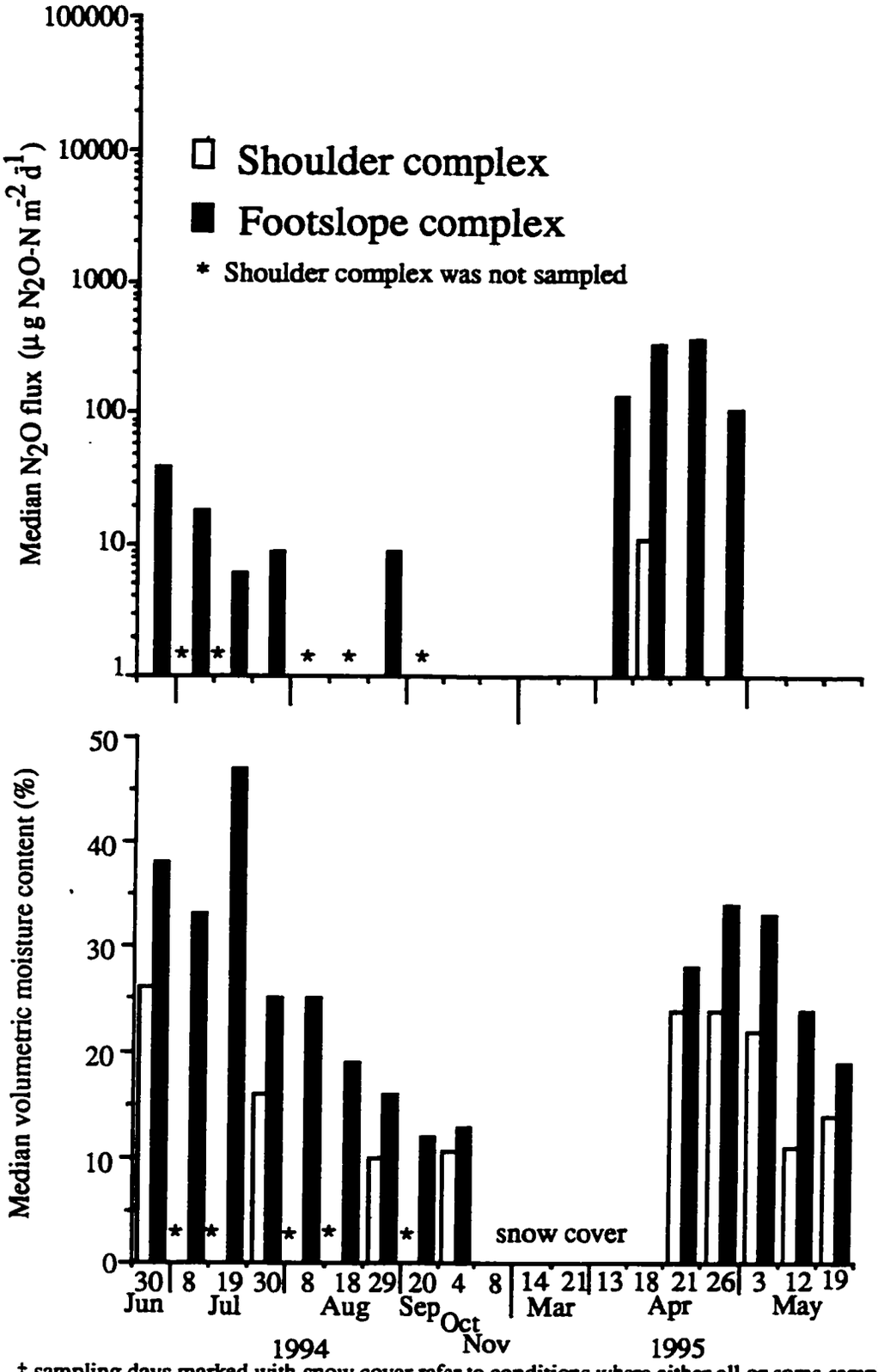

† sampling days marked with snow cover refer to conditions where either all or some sampling points were still covered with snow.

Fig. 5.7. Landscape- and seasonal-scale patterns of N_2O emissions and soil moisture contents in the sandy, pasture site.

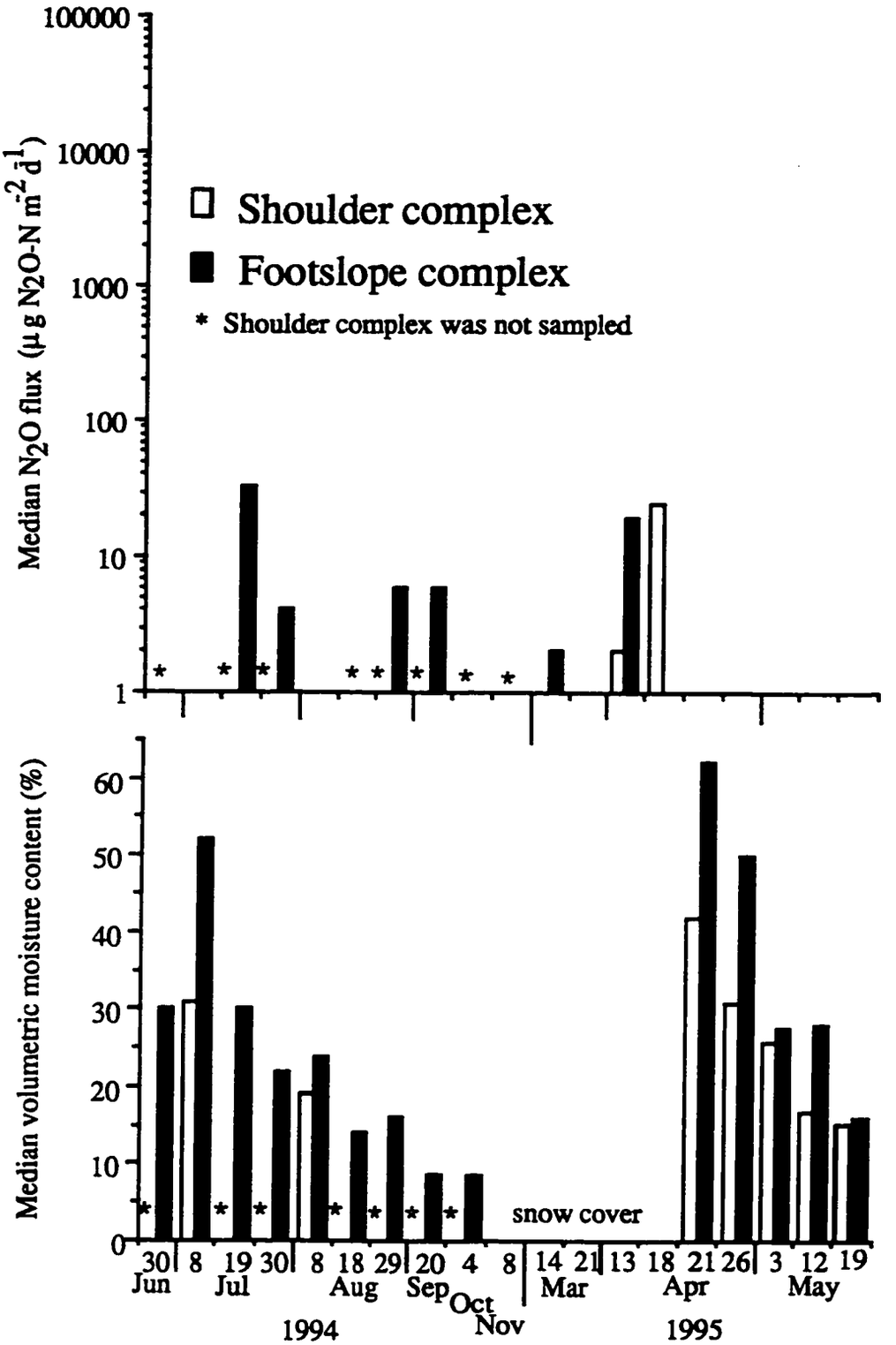

† sampling days marked with snow cover refer to conditions where either all or some sampling points were still covered with snow.

Fig. 5.8. Landscape- and seasonal-scale patterns of N_2O emissions and soil moisture contents in the sandy, forest site.

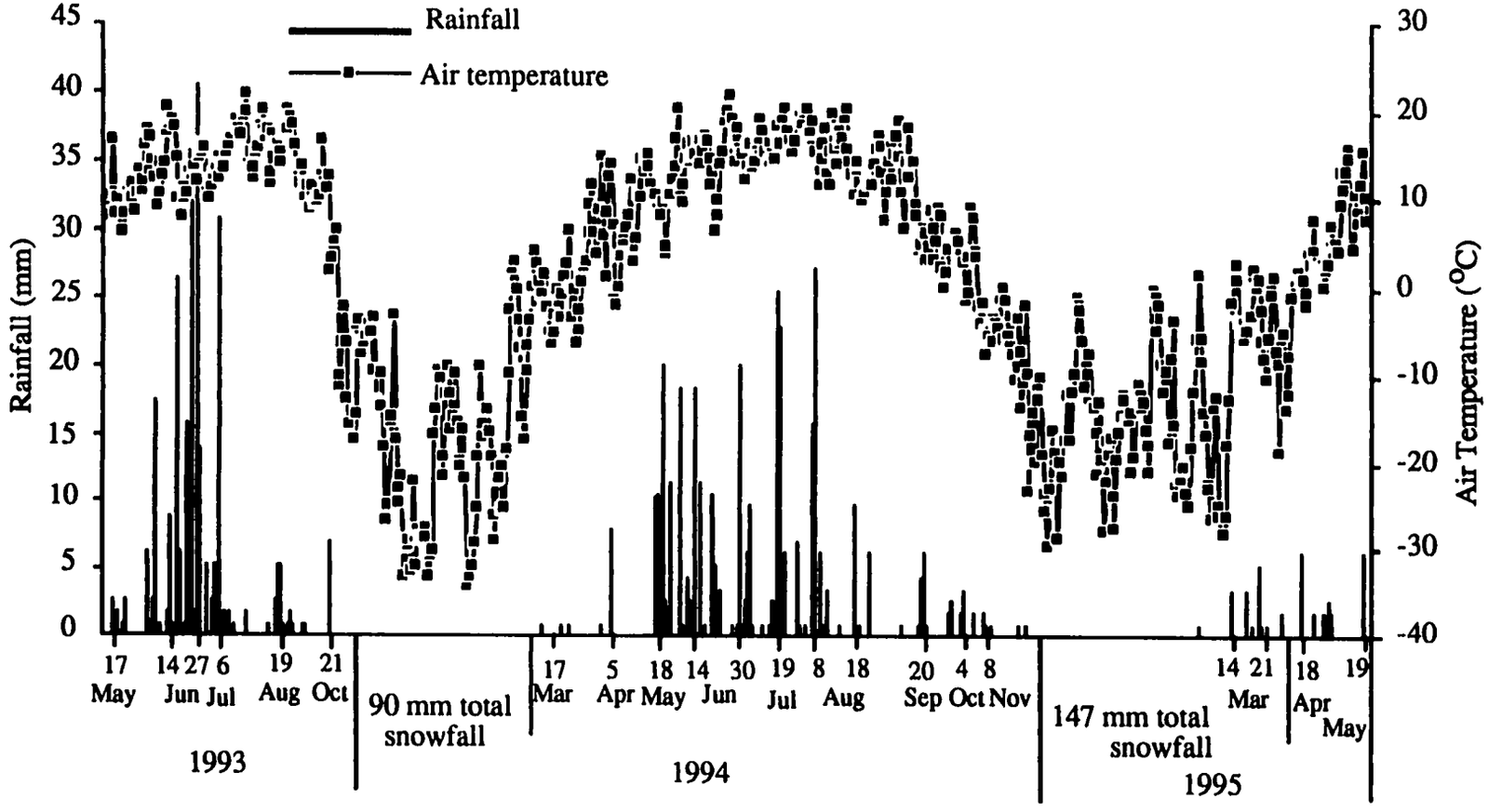

Fig. 5.9. Daily total rainfall and average air temperature measured at the clay loam area.

N fertilizer application) and anaerobiosis in the soil (from increased soil water content due to rainfall). In the fine sandy loam, fertilized canola site, considerable increase in N_2O emissions were observed after N fertilizer application (Fig. 5.5). At this site, although the median values representing the N_2O emission on the footslope complex were already high before fertilization, there were more sampling points with zero to very low fluxes before fertilization than after fertilization. In the sandy, fertilized oat site, although N_2O emission was not measured prior to fertilization, higher N_2O fluxes were observed during the earlier sampling days (close to the date of N fertilization) than during the later sampling days (Fig. 5.6). The large efflux of N_2O lasted for about six weeks after fertilization (Figs. 5.2B, 5.5, and 5.6), and coincided with the normal period of high rainfall and temperature (Fig. 5.9). McKenney et al. (1980) and Mosier et al. (1983) also found that increase in N_2O emissions occurred for about six weeks after fertilization, and that after this time emissions are reduced to about the base-line level, independent of the amount of fertilizer applied.

A large pulse of N_2O emission activity was observed during the spring thaw (Figs. 5.2 to 5.8). Sequential occurrence of spring N_2O emission activity was observed between landform complexes, particularly in the cropped sites. Between the second to the third sampling in spring (about two weeks since melting of snow began), the shoulder complex had higher N_2O fluxes than the footslope complex (Figs. 5.2, 5.5, and 5.6); this also coincided with the earlier disappearance of snow on the shoulders (which had less accumulation of snow) than on the footslopes. However, the maximum spring activity on the shoulder was lower than on the footslope complex. In addition, because in these sites there were only two to three sampling days in spring that the shoulders had higher emissions than the footslopes, these observations were masked in the analysis of landscape-scale pattern (i.e., repeated-measures analysis) by

the higher fluxes predominantly observed on the footslopes than on the shoulders during most of the sampling days.

In 1995, the spring pulse of activity in the sandy sites (Figs. 5.6 to 5.8) occurred about a week earlier than in the clay loam and fine sandy loam sites (Figs. 5.2B, 5.4, and 5.5). The spring activity in the sandy sites was observed as soon as the snow started to melt. The spring thaw in 1994 began in mid-March, whereas in 1995 it started in mid-April. Consequently, the N_2O emission activity during the spring of 1994 was also observed earlier (Figs. 5.2A, 5.3, and 5.4) than during the spring of 1995 (Figs. 5.2B, 5.4 to 5.8).

5.3.2 Effects of land use and soil texture

Figure 5.10 shows the ranges of the median values of N_2O fluxes on each landform complex at the study sites during their specified sampling period. The comparison of N_2O emissions among sites was carried out on each sampling day, based on the activity of the individual sampling points, using Kruskal-Wallis H test. The consistency of the nature of differences among sites throughout the sampling period was assessed using Kendall coefficient of concordance, as outlined earlier in section 5.2.5. During May 1993-April 1994 sampling period for the clay loam sites, the cultivated sites showed higher N_2O emissions than the pasture site. The difference in N_2O emission activity among these land use types were particularly distinct on the footslope complex, as indicated by a high *W* value (Table 5.3). During May 1994-May 1995 sampling period, within a similar textural area, the fertilized cropped sites showed higher N_2O emissions than the uncultivated sites (pasture and forest sites), except in the sandy sites where the fertilized oat and pasture sites did not differ in N_2O fluxes (Table 5.3). In the sandy, fertilized oat and pasture sites, although their median fluxes at the landform complex level showed clear differences (Figs. 5.6 and 5.7), the ranking

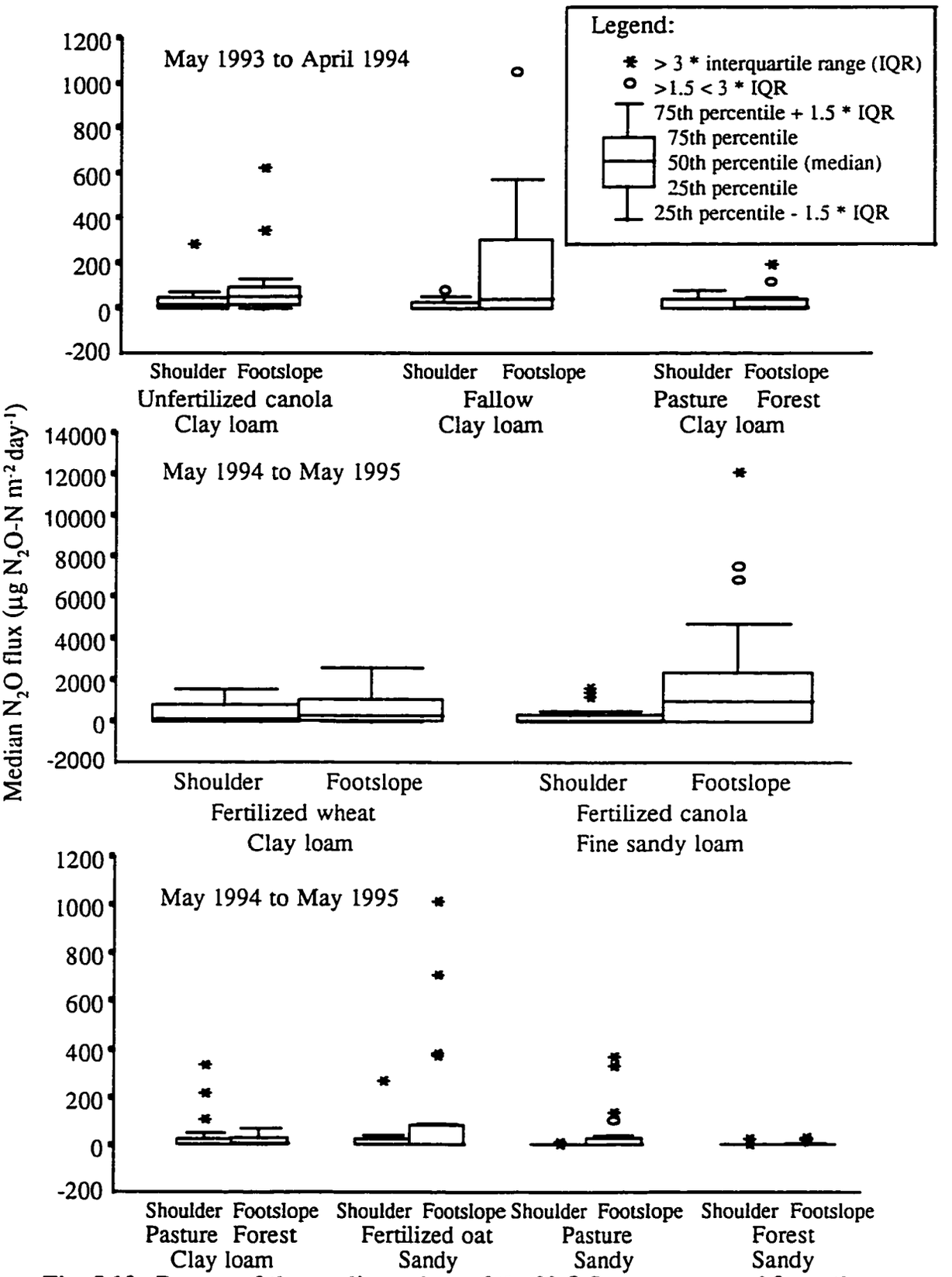

Fig. 5.10. Ranges of the median values of the N_2O fluxes measured from the study sites.

Table 5.3. Comparison of N_2O emission activity among sites, as indicated by the mean ranks based from multiple comparison extension of Kruskal-Wallis H test.

	Mean Rank†						Coefficient of Concordance, (W)‡
May 1993 - April 1994	Clay loam, unfertilized canola	Clay loam, fallow	Clay loam, pasture§				
Footslope	2.5 a	2.3 a	1.2 b				0.63 **
Shoulder complex	2.5 a	1.8 a	2.0 a				0.08 ns
May 1994 - May 1995	Clay loam, fertilized wheat	Clay loam, pasture§	Fine sandy loam, fertilized canola	Sandy, fertilized oat	Sandy, pasture	Sandy, forest	
Footslope complex	5.1 a	3.1 b	5.4 a	2.9 b	2.8 b	1.7 c	0.48 *
summer 1994	5.4 a	3.3 b	5.6 a	2.6 bc	2.2 cd	1.9 d	0.60 **
spring 1995	4.8 a	2.9 bc	5.2 a	3.2 b	3.4 b	1.5 c	0.40 *
Shoulder complex¶	5.7 a	4.1 c	5.0 b	2.2 d	2.2 d	1.6 e	0.67 **

*, ** - significant at $\alpha = 0.05$, and 0.01, respectively; ns - not significant.

† Values are the average of the ranking order among sites (referred by row); mean ranks within rows followed by the same letter(s) are not significantly different from each other at $\alpha \leq 0.20$.

‡ Values were corrected for ties; the value of *W* varies between 0 (no agreement) and 1 (perfect agreement).

§ In the clay loam, pasture site, the shoulder complex was occupied by bromegrass and the footslope complex was dominated by aspen.

¶ Comparison during summer 1994 was precluded from the test by the large number of sampling points that had no detectable activity.

of individual sampling points from which Kruskal-Wallis H test is based were not that different due to the wide range of fluxes observed at these sites. Between the uncultivated sites, the forest site had lower activity than the pasture site. On the footslope complex, the low *W* value during May 1994-May 1995 sampling period was contributed by the low *W* value in spring 1995 (Table 5.3). During this period, the ranking among sites was affected by their differences in time of occurrence of the spring pulse of N_2O emission activity. In general, the *W* values signified a strong agreement of the ranking order among the land use types studied in this region.

Comparison of N_2O emissions among the textural areas showed that the sandy sites had lower activity than the fine sandy loam and clay loam sites (Table 5.3). The N_2O emissions on the footslope complex in the clay loam, fertilized wheat site were generally comparable with the fine sandy loam, fertilized canola site (Table 5.3), although during the first few weeks after fertilizer application and in early spring sampling the latter showed higher emissions than the former (Figs. 5.2B and 5.5). The anhydrous ammonia fertilizer, applied in the fine sandy loam site, has been reported to emit more N_2O than urea, which was applied in the clay loam site (Breitenbeck et al., 1980). In the fine sandy loam site, a more pronounced slope gradient also existed than in the clay loam site. The effect of slope can also be shown by the higher proportion of Gleysols compared to Orthic Chernozemic soils occurring in the footslopes of the fine sandy loam site (section 3; Table 3.4) than that of the clay loam site (section 3; Table 3.2). On the shoulder complex, a more distinct difference in N_2O emissions with regards to texture was observed; the fine sandy loam site showed lower activity than the clay loam site (Table 5.3).

5.4 Discussion

5.4.1 Hotspots of N_2O emission

The nature of a predictive relationship for N_2O evolution depends on the relative importance of the landscape-scale response to change in the governing conditions compared to the random response of individual sampling points (Parkin and Robinson, 1989). Several studies on denitrification have noted a random response associated with microsites in the soil mass. These microsites of high activity have been referred to as "hotspots", and identified as a major factor influencing spatial variability (Parkin, 1987). Christensen et al. (1990a) defined hotspots as soil cores that yield denitrification rates more than five standard deviations above the overall mean and considered them to belong to a different population. In the present study, the hotspots of N_2O emission activity in a site on a particular sampling day were identified by analyzing the N_2O flux data in that site as a whole (i.e., considering all sampling points together from the two landform complexes; Appendix 1). Nonparametric statistics were used to define the hotspots (i.e., extreme outliers) - as a N_2O flux on a particular sampling point that was greater than the median + 3 times the interquartile range. During the May 1993-April 1994 period for the three sites in the clay loam area, 10% of all the samples taken were identified as hotspots, of which 75% occurred on the footslope and 25% on the shoulder complex. During the May 1994-May 1995 period, 9% of all the measurements were identified as hotspots, of which 72% occurred on the footslope and 28% on the shoulder complex. When the N_2O flux data were analyzed separately for each landform complex in a site, the number of hotspots further decreased as most of the hotspots identified from the whole-site analysis were included within the 75th percentile ranges of N_2O emission activity of the landform complexes.

These results reinforce the earlier observations of Pennock et al. (1992) and Van Kessel et al. (1993) that the occurrence of hotspots followed a distinct landscape-

scale pattern with a higher number on the footslope than on the shoulder complex. Therefore, hotspots of N_2O emission activity can be considered to be of limited importance in terms of quantifying N_2O flux at the landscape scale when an appropriate spatial sampling scheme is used (i.e., stratifying a landscape into spatial units that reflect distinctive domains of N_2O evolution). Because hotspots constituted only a minimal number in proportion to the total number of samples taken, their occurrence is also not a hindrance to deriving a spatially-based predictive relationship for N_2O emission if appropriate statistical measures (e.g., median), which are resistant to the effects of a few extreme values, are used.

5.4.2 Landscape-scale pattern

Distinct N_2O fluxes were associated with each landform complex, showing the indirect control of topography on N_2O emission. The lower N_2O emission activity associated with the shoulder compared to the footslope complex reflects the influence of topographically-induced water redistribution and generally drier condition of the soils on the upper than on the lower landscape positions. This was shown clearly by the parallel landscape-scale patterns of N_2O emissions and soil water contents (Figs. 5.2 to 5.8). Throughout the specified sampling periods, the soil water contents in the footslopes were higher than in the shoulders, with the average difference of 7 % , 13 %, and 6 % (v/v) in the clay loam, fine sandy loam, and sandy sites, respectively. This study showed that in an area of similar geomorphological characteristics and vegetation type, topography can be taken as a proxy variable at the landscape level to represent the many factors, which control N_2O emission.

In the sandy, forest site, the N_2O emissions between landform complexes were not statistically distinct when analyzed throughout the sampling period due to the many sampling days when N_2O emission was undetectable (Fig. 5.8). In the clay loam,

pasture site, the N_2O fluxes on the shoulders and footslopes did not differ (i.e., during May 1993-April 1994 and summer-fall 1994 sampling periods, as shown in Table 5.2), which suggests complex interactions among topography, vegetation (bromegrass on shoulders and aspen on footslopes) and possibly soil factors (e.g., low mineral N contents). Spatial variation in N and C dynamics in a landscape has not only been related to topography but also to differences of vegetation in the landscape (Burke et al., 1989; Smith et al., 1994).

In addition, in the clay loam, pasture site, the shoulders had higher N_2O fluxes than the footslopes during the spring of 1995 (Fig. 5.4), as shown in the analysis of landscape-scale pattern (Table 5.2). This could be due to the higher soil water contents in the shoulders during the spring thaw than during the summer months. In a study of N_2O emission from semi-arid shrubsteppe ecosystem, low N_2O fluxes were observed during dry months due to low soil moisture and intense competition for available N among microorganisms and plants (Mummey et al., 1994). On the other hand, the footslope complex was subjected to longer saturated-to-waterlogged condition during the spring thaw of 1995 than during the spring thaw of 1994 due to higher snowfall that occurred in winter of 1994-1995 (a water equivalent of 147 mm) than in the winter of 1993-1994 (90 mm). For most grass or forest ecosystems, NH_4^+ is typically the dominant N species rather than NO_3^-. Studies have shown that nitrification is a significant source of N_2O in undisturbed semiarid ecosystems (Parton et al., 1988b; Mummey et al., 1994). The prolonged saturated condition on the footslope complex during the spring of 1995 might have hindered nitrification and/or caused further reduction of N_2O to N_2 (Keller, 1994), which probably led to the lower N_2O emissions on this position in spring of 1995 than of 1994.

5.4.3 Seasonal fluctuations

The seasonal pattern of N_2O emission was largely influenced by the rainfall pattern. The high N_2O emission during the early summer was due to the occurrence of high and frequent rainfall events (Fig. 5.9). During the years of study, 67 % of the total annual rainfall (388 mm in 1993 and 401 mm in 1994) had occurred from late May to mid-July. The decrease in N_2O emission activity from late summer to fall undoubtedly reflects the decrease in soil moisture, which was due to the intermittent occurrence of low levels of rainfall.

This study showed that a large pulse of N_2O emission occurred during the spring thaw, and this is consistent with the findings of others (Goodroad and Keeney, 1984; Parsons et al., 1991; Groffman et al., 1993a; Burton and Beauchamp, 1994). The spring pulse of activity has been attributed primarily to high soil moisture (Groffman et al., 1993a). It was also observed from the study sites that available N and C were higher in spring than in summer and fall (Table 5.4). High N and C availability also occurred in spring due to low plant activity and the lysis of microbial cells, as a result of freezing and thawing (Groffman and Tiedje, 1989a). High N_2O emissions during spring thaw can also result from changes in solubility of N_2O, production of N_2O near the soil surface, and diffusion from depth of accumulated N_2O during winter (Goodroad and Keeney, 1984; Burton and Beauchamp, 1994).

In the cropped sites, the occurrence of earlier spring activity on the shoulders than on the footslopes was attributed to factors such as the redistribution of snow by wind from the shoulders to the footslopes, with a thinner snow cover on shoulders which melted earlier, and earlier thawing of the soil on the shoulders than on the footslopes. Hence, N_2O emission was detected first on the shoulder followed by the footslope complex. Earlier fluxes of N_2O on shoulders did not occur in the pasture and

Table 5.4. Seasonal average† of total mineral N and soluble organic C.

Site	Total mineral N‡ (μg g-1)			Soluble organic C (μg g^{-1})		
	Summer	Fall	Spring	Summer	Fall	Spring
1993 - 1994						
Clay loam						
Unfertilized canola	4	7	20	20	22	52
Fallow	15	20	40	61	45	65
Pasture	7	7	28	100	109	325
1994 - 1995						
Clay loam						
Fertilized wheat	14	16	41	18	12	24
Pasture	9	3	32	71	21	368
Fine sandy loam						
Fertilized canola	8	16	57	16	33	63
Sandy						
Fertilized Oat	7	3	5	22	26	25
Pasture	9	6	10	71	91	130
Forest	10	1	15	100	30	281

† For each site, the median values of all the sampling points on a particular sampling day were obtained, and these values were averaged among the sampling days within the season.

‡ NH_4^+ was the dominant N species in the pasture and forest sites, while NO_3^- + NO_2^- were the dominant N species in the cropped sites.

forest sites, where the presence of pasture vegetation and trees had minimized snow redistribution. The earlier pulse of spring activity in the sandy sites than in the clay loam and fine sandy loam sites could be partly attributed to the presence of macropores in sandy soils that would allow diffusion of gases to be less restricted. Burton and Beauchamp (1994) pointed out that diffusion of N_2O during spring thaw is restricted by the snow layer and the water accumulating on the soil surface during the early portion of the thaw event. During the early spring thaw, the clay loam and fine sandy loam sites remained wet longer than the sandy sites. This could also be attributed to the differences in the characteristics of the soils occurring in the clay loam and fine sandy loam sites from that in the sandy sites, particularly in the footslope areas (refer to section 3.3.1). The Btg horizons present in the Gleysolic soils in the footslopes of the clay loam and fine sandy loam sites could induce slowing down of water movement within the profile and thereby lengthening the duration of anaerobic condition in the upper soil layers. It is evident that the N_2O emissions in the sandy sites lasted only towards the end of April 1995, whereas in the clay loam and fine sandy loam sites activity was still observed until mid-May 1995. These results also showed the importance of the proper timing of sampling during the spring period when considerable portion of annual N_2O emissions occur.

In addition to intra-annual variation, significant changes in N_2O emission activity from year to year were also observed. The N_2O emission activity during the spring was higher in 1995 than in 1994. This could be due to the occurrence of higher snowfall and consequently higher amount of stored soil water in spring 1995 than in spring 1994. In the clay loam, fertilized wheat site, the high N_2O emission activity during the spring of 1995 may also have resulted from residual effects of fertilization and/or enhanced N mineralization of crop residues due to fertilization compared when it was unfertilized the previous year. These results imply that changes in management

and/or climate could have an important effect on the annual budget of N_2O emissions from this region.

5.4.4 Controls on N_2O emission

The landscape- and seasonal-scale patterns of N_2O emission observed in this study signified that the factors controlling N_2O emission vary systematically from local to regional scale within a given climatic region. Figure 5.11 shows a conceptual basis for linking the relationships between the large-scale controllers and proximal factors of N_2O emission. This study showed that the most important proximal control of N_2O emission is soil water. Certainly, the parallel spatial and temporal patterns of N_2O emissions and soil water contents found in this study would support this argument. Soil water functions to promote N_2O production by reducing O_2 diffusion, promoting diffusion of mineral N and soluble C to microbiologically active sites (Vermes and Myrold, 1992), and also by directly stimulating microbial activity (Davidson and Swank, 1986). Several studies have demonstrated the hierarchy of importance of soil water and available N and C, as factors controlling N_2O emission at the micro scale; limited O_2 supply is first necessary and as O_2 supply gradually diminishes, availability of N and C becomes increasingly important (Mosier and Hutchinson, 1981; Burton and Beauchamp, 1985; Van Kessel et al., 1993). At the landscape scale, these factors are, in turn, influenced by topography and soil type. As discussed previously (section 3) and as found in earlier studies, soils vary systematically with topography because of the influence of hillslope morphology on the surface- and subsurface-water movement (Pennock et al., 1987). These topography-related differences in soil and water distribution in the landscape have also been shown to influence the spatial variation in soil N and C cycling processes (Schimel et al., 1985a; Groffman et al., 1993b). The

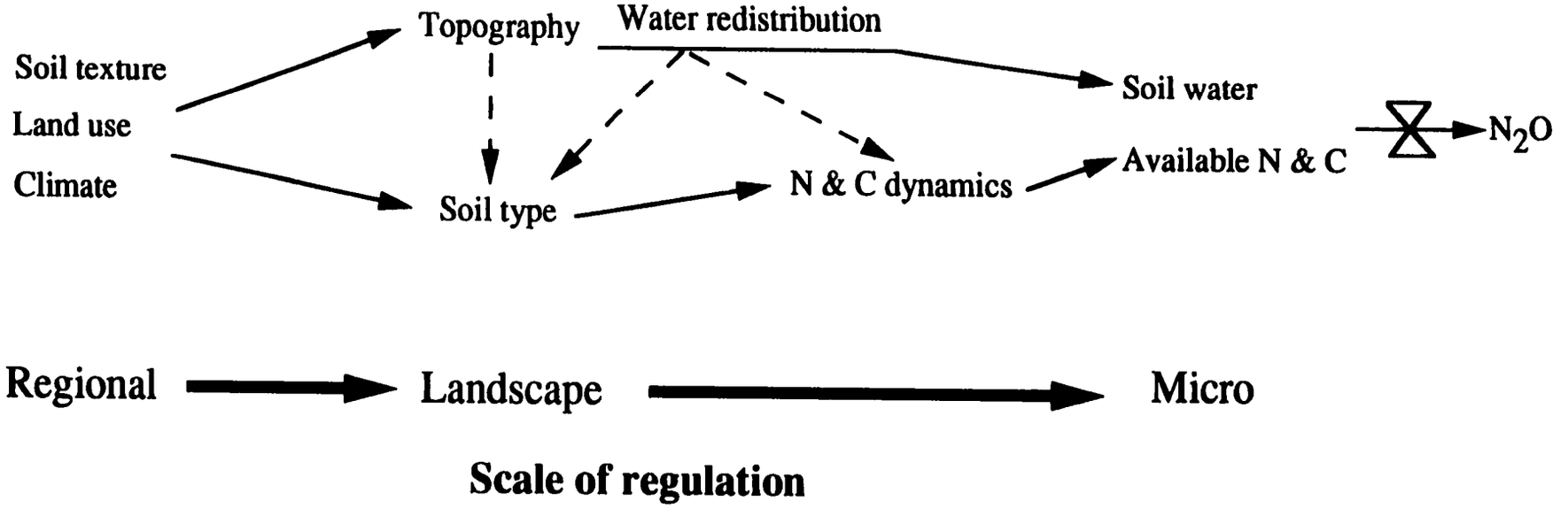

Fig. 5.11. Conceptual links between large-scale controllers and proximal factors of N_2O emission.

generally consistent landscape-scale pattern of N_2O emissions observed in this study indicates that the spatial sampling scheme had accounted for the variation of soil characteristics and moisture redistribution in the landscape.

In the study region, soil texture indirectly affects N_2O emission through its influence on the differences of soil fertility, of plant community structure, and eventually of N and C levels in the area. Most importantly, it affects N_2O emission more directly through its control on the differences of soil water regime. As shown in other studies conducted in semiarid ecosystems, soil water potential is the primary factor controlling differences in patterns of N cycling (Matson et al., 1991; Smith et al., 1994; Mummey et al., 1994). On the other hand, different land use conditions have been shown to differ in denitrification (Groffman et al., 1993a) and nitrification activities (Hutchinson and Davidson, 1993), and therefore it is not surprising in this study to observe differences in N_2O emissions among the land use types. The low N_2O emissions in the forest and pasture sites reflected the tight and conservative N cycling in uncultivated ecosystems (Hutchinson and Davidson, 1993; Smith et al., 1994). The high N_2O emissions in the cropped sites were due at least partly to the application of N fertilizers. However, it should be pointed out that among the cropped sites the effect of fertilization on N_2O emission was only favored in soils with high moisture contents. This was shown by the relatively low N_2O emissions in the sandy cropped site. On the other hand, precipitation and temperature are the climatic factors considered important in influencing the seasonal pattern of N_2O emission. The high rainfall and temperature during the early summer favored high N_2O emissions. The pulse of activity in spring was also related to the melting of snow and thawing of the soil, which is affected by temperature. Groffman et al. (1993a) stated that the ecological or large-scale controls of N_2O emission may vary from region to region

depending on the geomorphic process(es) that contributed to the differences of soils in an area. In this glaciated region, soil texture and land use were indicated as useful integrative variables for extrapolating N_2O fluxes to a regional scale within a particular climatic zone.

6. ANNUAL ESTIMATES OF NITROUS OXIDE EMISSIONS AT THE LANDSCAPE SCALE

6.1 Introduction

In areas where seasonal fluctuations of N_2O emission are observed, the estimation of annual fluxes from non-continuous daily measurements continues to pose a challenge for researchers. One of the models used in estimating annual N_2O emission is the process-oriented DNDC model (Li et al., 1992). This model is driven by daily-time step climatic variables (i.e., daily rainfall and temperature), and N_2O emission is simulated daily. Another daily-time step simulation model is the NGAS (Parton et al., 1996). The annual N_2O fluxes were simulated using relatively simple relationships controlled by WFPS, soil texture, soil temperature, soil NH_4^+ and NO_3^- levels, pH, and soil respiration. In Wyoming sagebrush steppe, where N_2O emission was neither related to soil water nor temperature, annual N_2O fluxes were estimated by simple interpolation of the fluxes measured at discrete sampling days (Matson et al., 1991). A similar approach was used in estimating annual N_2O emission from forest in Massachusetts (Bowden et al., 1990), and in determining annual denitrification losses from forest in Michigan (Groffman and Tiedje, 1989b) and Oregon (Vermes and Myrold, 1992). This method is appropriate when the frequency of sampling is considered sufficient in characterizing the seasonal variation of N_2O emission. In Saskatchewan, Elliott and de Jong (1992) estimated annual denitrification losses by establishing regression models that related denitrification losses to daily soil moisture and air temperature.

The key in achieving reliable estimates of annual N_2O emissions is the knowledge of the factor(s) that result in systematic variation across seasons. The present study demonstrated that the landscape and seasonal patterns of N_2O emissions are tractable, with rainfall as the main factor governing seasonal variation in N_2O fluxes through its effect on soil moisture contents which, in turn, affect the soil O_2 status. The inclusion of the effect of rainfall would improve the accuracy of annual flux estimates and facilitate extrapolation of fluxes in years of differing rainfall conditions. The objective of this component of the study was to obtain annual estimates of N_2O emissions for the investigated landscapes.

6.2 Materials and Methods

6.2.1 Predictive relationships for N_2O emission

The first step in quantitatively analyzing the N_2O flux data was to determine which soil and environmental factors were correlated with N_2O emissions. The independent variables considered included WFPS (which is calculated as the ratio of the volumetric moisture content to the total pore space), mineral N, soluble organic C, rainfall, and daily air temperature. The WFPS was used instead of the volumetric moisture content because it has the advantage of being largely comparable among soils of different texture (Davidson and Schimel, 1995). The correlation analysis was performed for each landform complex in each study site. This analysis was based on the median values of N_2O emissions and independent variables on a particular sampling day and was carried out for the data obtained during the whole sampling period for each study site. The analysis based on the central tendency values (i.e., median) afforded more meaningful interpretation than the analysis based on the entire data set.

Regression equations were developed to predict N_2O emissions from WFPS. These equations included only the data gathered from May to October. The N_2O fluxes

and WFPS measured from mid-Mar to April were excluded in the regression analysis, because spring thaw emissions indicated different conditions governing the fluxes, whereas the N_2O emissions during the growing season were closely related to soil moisture and rainfall (as discussed in section 5.4.3). Separate equations were obtained for different land use types to reflect their differences in substrate availability and thereby eliminating the need for substrate parameters in the regression equations. The pasture regression equation included the data from the sandy, pasture site and the clay loam, pasture site on the shoulder complex (occupied by bromegrass). The forest regression equation included the data from the sandy, forest site and the clay loam, pasture site on the footslope complex (dominated by aspen). The regression equation for the unfertilized cropland considered the data from clay loam, unfertilized canola and fallow sites. For the fertilized cropland sites, predictive relationships were established separately for the sandy and for the clay loam and fine sandy loam sites.

The regression models were linked to a simple soil moisture model. The N_2O emissions from May to October were estimated from the WFPS, which was calculated from the soil water contents predicted daily using the Versatile Soil Moisture Budget (VSMB; Baier and Robertson, 1966). The soil variables that drive the VSMB are soil texture, saturation moisture content, field capacity, and permanent wilting point. These variables were measured from 0 to 15-cm depth (Table 6.1). The particle size analysis was carried out using the modified pipette method (Indorante et al., 1990). The saturation moisture content was assumed to be equal to the total porosity, which was calculated from bulk density. The moisture contents at field capacity and permanent wilting point were determined by equilibrating soil samples in pressure chambers at 33 kPa and 1500 kPa, respectively (Klute, 1986).

The driving climatic variables used in the VSMB were daily rainfall, and daily minimum and maximum air temperatures. The VSMB was run for the climatic data

Table 6.1. Soil physical characteristics measured at 0 to 15-cm depth.

Representative sites	Land use	Landform complex	Sand†	Silt†	Clay†	Saturation moisture content†	Field capacity‡	Permanent wilting point‡
			<-------- % -------->			<---------- % (v/v) ---------->		
Clay loam	cropped	shoulder	31	37	32	50	39	22
		footslope	31	38	31	56	40	21
	fallow	shoulder	31	37	32	50	39	22
		footslope	31	38	31	56	40	21
	pasture	shoulder	26	42	32	55	41	25
		footslope	22	48	30	67	41	28
Fine sandy loam	cropped	shoulder	52	27	21	49	30	18
		footslope	48	29	23	54	31	19
Sandy	cropped	shoulder	88	6	6	50	13	7
		footslope	85	8	7	54	14	7
	pasture	shoulder	87	8	5	44	13	7
		footslope	82	12	6	63	16	9
	forest	shoulder	87	7	6	60	15	9
		footslope	85	9	6	58	16	9

† Values reported were the median of the selected sampling points for measurement of N_2O emission on each landform complex at each site.

‡ Values reported were the mean of the three sampling points selected on each landform complex at each site.

recorded during the years of study and for the 3 climatic scenarios (dry/cold, normal, wet/warm years), which were developed based from the 50-year climatic record of the climate station located within the study region (Prince Albert, Saskatchewan, Canada). The dry/cold, normal, and wet/warm scenarios were used to represent the minimum, average, and maximum potential for N_2O emissions, respectively. The differences in the predicted N_2O fluxes from these climatic scenarios were based solely on the predictive relationships developed between N_2O fluxes and WFPS.

The temperature scenarios were developed by taking the percentile distributions of the daily minimum and maximum air temperatures of the 50-year data for each day (e.g., Julian day 1 has 50 records of minimum and maximum air temperatures, and the percentile values for this day were determined). The cold, normal, and warm year scenarios are characterized by minimum and maximum air temperatures at the 25th, 50th, and 75th percentile distributions for each day, respectively. For the rainfall scenarios, the percentile distributions of the rainfall data on a daily basis are not appropriate to use because, unlike temperature data, rainfall data are not continuous values (e.g., the chance for rain on the same day in 50 years is very low, and thus the percentile values will likely be zero). Instead, the total annual rainfall for each year was used in determining the percentile distributions of the 50-year rainfall record. The dry, normal, and wet years are characterized by annual rainfall values at 25th, 50th, and 75th percentile distribution, respectively. Since the VSMB model is driven by daily rainfall data, five specific years were chosen to represent for each classified dry, normal, and wet years. Hence, a particular rainfall-temperature scenario (i.e., dry/cold year) is depicted by 5 representative years of a categorized rainfall scenario (i.e., dry year), and these years have the same daily minimum and maximum air temperature values derived from the temperature scenario (i.e., cold year). In total, there were fifteen years representing the three climatic scenarios (five for each climatic scenario).

6.2.2 Versatile Soil Moisture Budget

The VSMB was adapted from the modified version of de Jong and Bettany (1986) and Elliott and de Jong (1992). For the years under study, simulations were run starting from that day in May 1993/1994 (for the clay loam and fine sandy loam sites) or in June 1994 (for the sandy sites) when the soil moisture contents were measured at these sites (used as the initial moisture content) up to October (1993 and 1994) when frost occurred. For the years representing the different climatic scenarios, the same initial moisture contents were assumed for the study sites, and simulations were run from May to October. Maximum and minimum daily air temperatures were used to predict latent evaporation following method I of Baier and Robertson (1965). Latent evaporation was converted to potential evapotranspiration using a crop factor which depended on the nature of the crop and its growth stage (Krogman and Hobbs, 1976). Evapotranspiration extracted water until the permanent wilting point was reached. Texture and land use were used as the basis for partitioning the rainfall into infiltration and runoff, referring to the Soil Conservation Service Method discussed by Schwab et al. (1993). Following rain, soil moisture was allowed to increase to the saturation moisture content and drainage occurred when the soil was between saturation and field capacity. For the clay loam and fine sandy loam soils, it was assumed that 75% of the moisture excess of the field capacity drained in 24 h and that field capacity was reached in 2 d (similar to the conditions assumed by Elliott and de Jong (1992)). For the sandy soil, it was assumed that 100 % of the moisture excess of the field capacity drained in 24 h. At the end of each day, the gains and losses of water were summed and new moisture contents were calculated.

6.3 Results and Discussion

6.3.1 Predictive relationships for N_2O emission

The measured WFPS was the factor most strongly correlated to N_2O emission (Table 6.2). Related to this factor is the rainfall, which was observed to give high correlation coefficients with N_2O emissions in the unfertilized cropped, pasture, and forest sites. In the fertilized cropped sites, rainfall did not show significant correlations because of the confounding effects of fertilization. For example, a particular rainfall level occurring before the fertilization showed much lower N_2O fluxes than with the same rainfall level occurring after fertilization. It is not surprising, however, to observe that there was no clear relationships of N_2O emissions with soil mineral N and soluble C, because these pools turn over rapidly and are end products of several competing processes. Other findings have also shown that it is difficult to directly correlate *in situ* N_2O fluxes to soil mineral N contents, and that N_2O emissions are related more to the soil N turnover rate rather than mineral N pool size (Schimel et al., 1989; Matson and Vitousek, 1990; Davidson and Hackler, 1994; and Mosier et al., 1996). Of the measures used for air temperature (i.e., maximum, minimum, and average air temperatures), only the maximum air temperatures showed significant correlation with N_2O emissions and that was in the clay loam, forest (footslope) site. The lack of significant relationship of N_2O emission with temperature has also been observed in other studies (Myrold, 1988; Parsons et al., 1991), and in this study was a probable consequence of the high N_2O fluxes even at low temperatures in spring. Davidson and Swank (1986) and Elliott and de Jong (1992) also showed that the effects of temperature were confounded by moisture; when soil moisture was favorable, temperature was important and vice versa.

It is clear, however, that a reliable method of temporally interpolating fluxes could be achieved by relating the N_2O emissions with WFPS. Other studies have used

Table 6.2. Pearson correlation§ analysis between N_2O emissions and soil and environmental factors.

Site	N_2O vs.	Measured WFPS	NH_4^+	$NO_3^- + NO_2^-$	Soluble organic C	Rainfall	Max. air temperature
Clay loam							
Unfertilized	shoulder	0.79 **	-0.14 ns	-0.93 *	(.)	0.62 *	0.00 ns
canola	footslope	0.71 **	-0.43 ns	-0.67 ns	(.)	0.55 *	-0.23 ns
Fallow	shoulder	0.88 **	0.34 ns	-0.40 ns	(.)	0.48 ns	0.15 ns
	footslope	0.29 ns	0.15 ns	-0.98 *	(.)	0.72 *	-0.24 ns
Pasture¶	shoulder	0.44 ‡	-0.35 ns	-0.01 ns	-0.14 ns	0.56 **	0.09 ns
Forest¶	footslope	0.59 *	0.64 ‡	0.73 †	0.40 ns	0.56 **	0.62 **
Fertilized	shoulder	0.49 *	0.49 ns	-0.64 ns	-0.23 ns	0.42 †	0.02 ns
wheat	footslope	0.50 †	-0.19 ns	-0.78 ns	-0.08 ns	0.28 ns	0.18 ns
Fine sandy loam							
Fertilized	shoulder	0.71 ***	0.65 ns	-0.26 ns	-0.66 ns	0.36 ns	0.21 ns
canola	footslope	0.56 *	0.29 ns	0.21 ns	-0.63 ns	0.10 ns	0.12 ns
Sandy							
Fertilized	shoulder	0.40 ‡	0.04 ns	0.57 ns	-0.65 ns	0.40 ns	-0.20 ns
oat	footslope	0.50 †	-0.44 ns	0.68 ns	-0.25 ns	0.16 ns	-0.23 ns
Pasture	whole site	0.33 ‡	0.58 ns	0.89 ‡	-0.10 ns	0.39 *	-0.17 ns
Forest	whole site	0.02 ns	-0.19 ns	(.)	-0.31 ns	0.40 †	0.16 ns

*, **, ***, †, ‡ - significant at $\alpha = 0.05$, 0.01, 0.001, 0.10, and 0.20 respectively; ns - not significant.

(.) Coefficient cannot be determined. In the clay loam, unfertilized canola and fallow sites, soluble organic C was only measured in May and October 1993. In the sandy, forest site, $[NO_3^- + NO_2^-]$ were close to zero.

§ This test was used because correlations were done on the central tendency values (i.e., median) of the variables.

¶ In the clay loam, pasture site, the shoulder complex was occupied by bromegrass and the footslope complex was dominated by aspen.

a simpler approach; the average value of the N_2O fluxes measured across the seasons was multiplied by the number of days in a season or in a year to get the seasonal or annual estimate (Matson and Vitousek, 1990), with the assumption that there was no month-to-month variation in the mean flux. Similar method was used by Mosier et al. (1996), in which N_2O meaurements were taken at weekly interval in four years. This method is inappropriate for the present study because of the clear seasonal fluctuations observed in the study sites (section 5.3.1) , which are also shown by the wide ranges of the median values of N_2O fluxes (Fig. 5.10). Simple interpolation of measured fluxes at discrete sampling days (using trapezoidal quadrature method of calculation) would also result in an underestimation of seasonal or annual fluxes because those sampling days did not likely represent the day-to-day variation of fluxes, which is probably caused largely by the wetting and drying cycles in the soil, especially during summer to fall when N_2O fluxes and soil moisture contents were influenced by rainfall pattern (section 5.4.3). The trapezoidal quadrature calculation, however, is considered appropriate for determining the total N_2O emission in spring (i.e., mid-March to April) because the data from spring clearly showed the beginning, peak, and end of the spring pulse of activity, which also reflected the occurrence of snow melting and soil thawing (sections 5.3.1 and 5.4.3). Also, it is difficult to predict N_2O emissions from WFPS during spring using a simplified soil moisture model (i.e., VSMB) that does not deal with detailed soil water dynamics during the spring thaw period.

The predictive relationships between N_2O emissions and WFPS, measured from May to October, are shown in Figs. 6.1 to 6.3. For the pasture and forest sites, the regression equations were developed by combining the N_2O flux data in the sandy and clay loam soils (Fig. 6.1). The ranges of N_2O emissions from these land use types in the different textural sites were of a similar order of magnitude, and regressing the

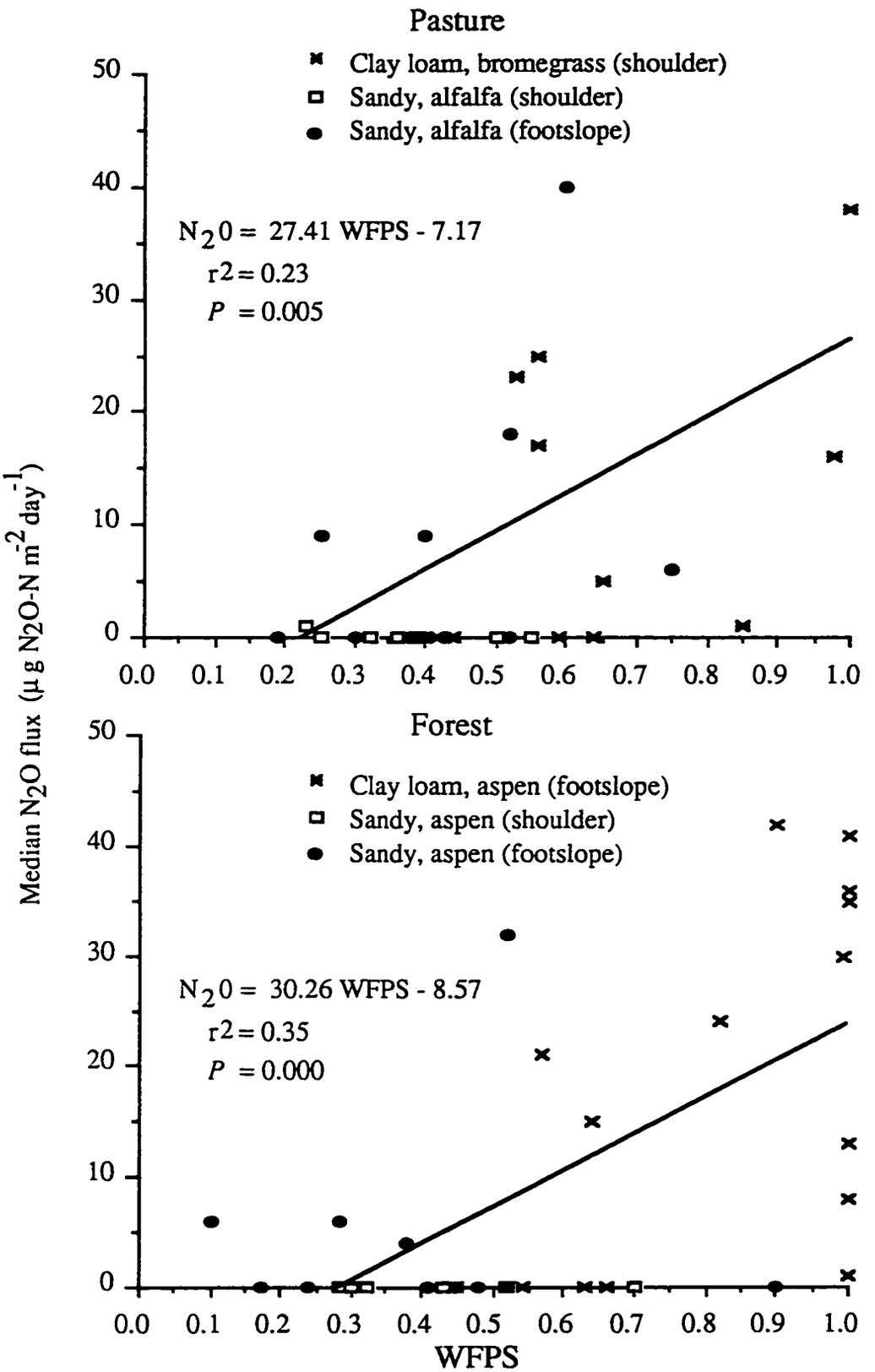

Fig. 6.1. Relationships between field-measured N_2O emissions and water-filled pore space in the pasture and forest sites.

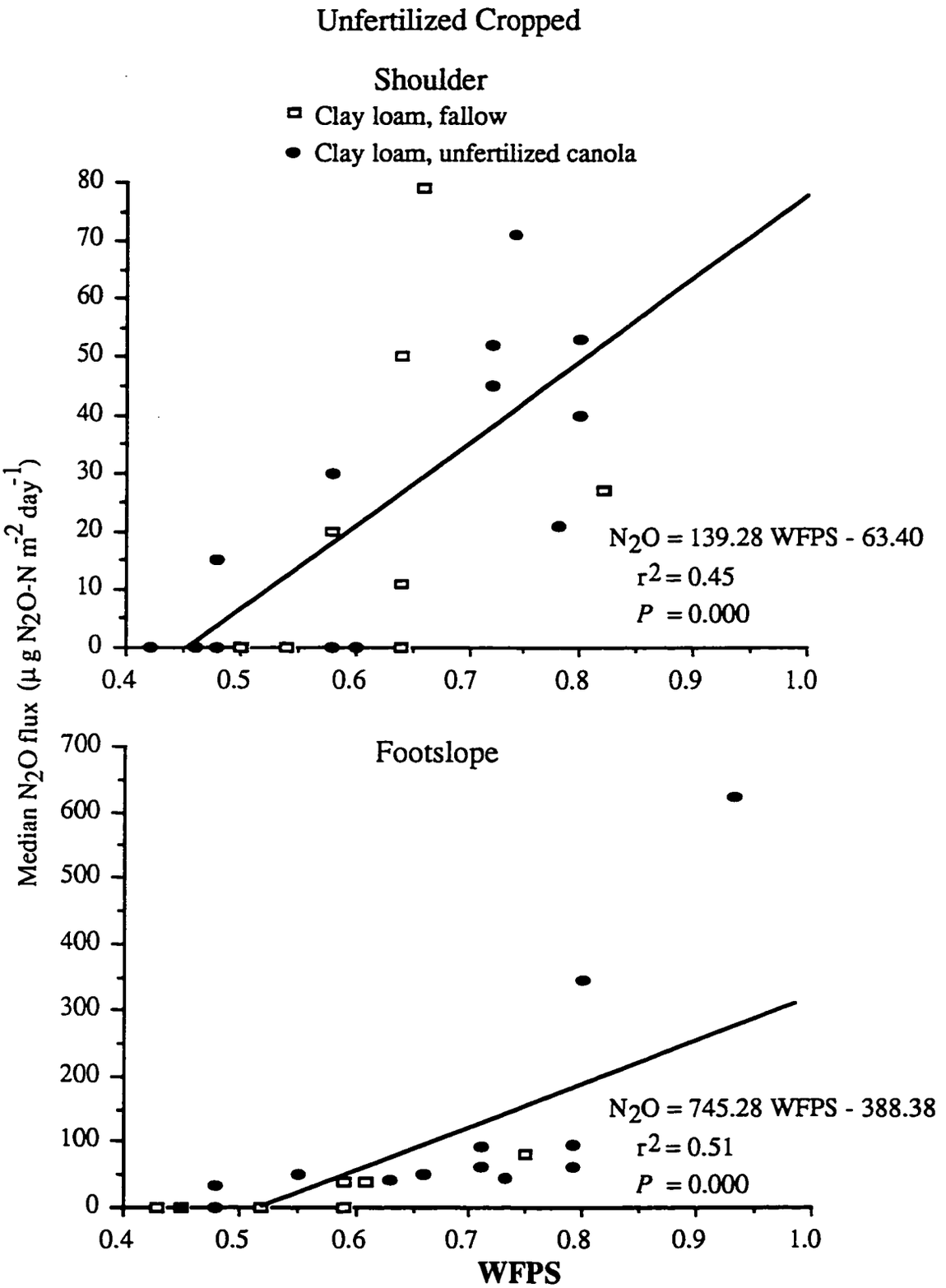

Fig. 6.2. Relationships between field-measured N_2O emissions and water-filled pore space in the unfertilized cropped sites.

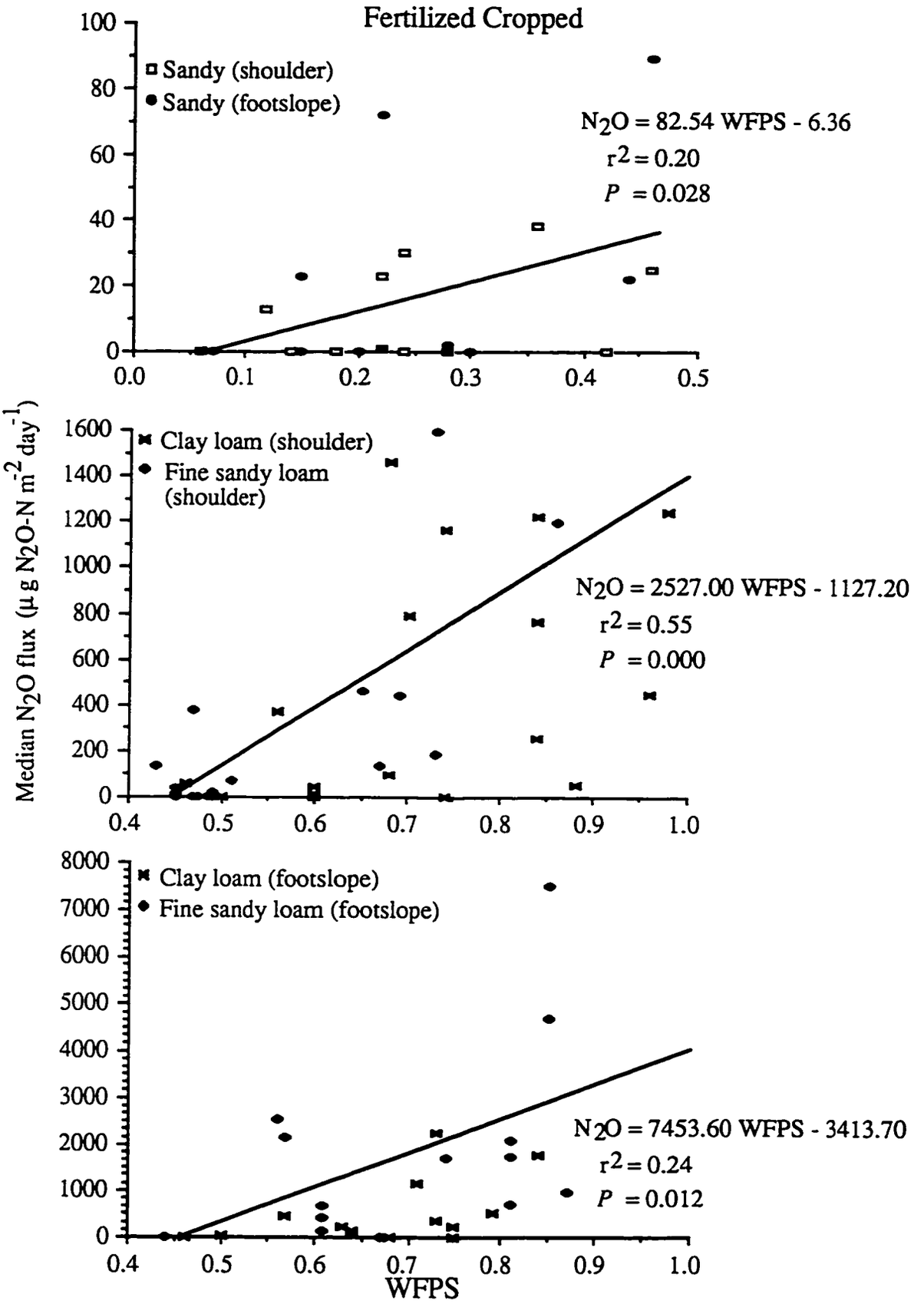

Fig. 6.3. Relationships between field-measured N_2O emissions and water-filled pore space in the fertilized cropped sites.

N_2O fluxes with WFPS across the textural sites provided a range of conditions in terms of the differences in soil moisture regimes, thereby resulting to better predictive relationships than when only considering the data in one particular site (as shown in the correlation analysis in Table 6.2).

The regression equations for the unfertilized cropland included the N_2O flux data from the clay loam, unfertilized canola and fallow sites (Fig. 6.2). These sites were located in a similar landscape, had the same cropping history, and were only divided into two respective land uses in 1993 for N_2O emission study (sections 3.2.1 and 5.2.1). Also, their N_2O emission activity at the landform complex level did not differ (Table 5.3).

For the fertilized cropland, separate regression equations were developed for the sandy and the clay loam and fine sandy loam sites (Fig. 6.3). In the sandy site, generally low N_2O fluxes occurred at about 0.15 to 0.45 WFPS. In the clay loam and fine sandy loam sites, high N_2O fluxes were observed at about 0.45 to 0.95 WFPS. The model developed by Parton et al. (1996) on the effect of WFPS to N_2O emission in soils of differing texture showed that for the same level of N_2O flux the coarse-textured soils need to be at higher WFPS than the fine-textured soil. The results from the present study, however, are obtained from sites located in the same climatic region, which means that the study sites generally received similar levels of rainfall at any given rainfall event. Hence, it is not possible for the sandy soils to get WFPS similar to that of the clay loam and fine sandy loam soils during a given rainfall event. The effect of soil texture on N_2O emission is also not only through its direct control on the soil water regimes of the sites but also through its indirect influence on the substrate availability, as indicated by the lower levels of N and organic C in the sandy than in the clay loam and fine sandy loam soils (Table 3.12; discussed in section 5.4.4). Hence, the sandy

site showed a lower range of N_2O emissions and WFPS than the clay loam and fine sandy loam sites.

The r^2 values of the regression equations, although low, are considered respectable, in reference to what others have obtained from field-based studies of N_2O emission. Mosier et al. (1996) obtained r^2 values of 0.23 and 0.29 between N_2O fluxes and WFPS (measured from May to October in semiarid Colorado) from fertilized and unfertilized pastures, respectively. In the present study, for the years under study and for the developed climatic scenarios, estimates of N_2O emissions from May to October were obtained by summing the predicted daily N_2O fluxes from the regression equations, in which the WFPS were calculated from the VSMB-simulated soil moisture content.

6.3.2 Estimates of annual N_2O fluxes

In general, the predicted WFPS (calculated from the VSMB-predicted soil moisture contents) were highly correlated with the measured WFPS (calculated from the measured soil moisture contents) (Table 6.3). The measured N_2O emissions were also compared with the predicted values from the regression and DNDC models. In a separate study, the DNDC model was used to predict the N_2O fluxes from these sites (unpublished data of Smith et al., 1996). Considering all the sites, the correlation analysis conducted for the shoulder complex showed correlation coefficients of 0.57 ($P \leq 0.001$) and 0.64 ($P \leq 0.001$) between the measured and predicted N_2O fluxes from the regression and DNDC models, respectively. For the footslope complex, correlation coefficients of 0.72 ($P \leq 0.001$) and 0.60 ($P \leq 0.001$) were obtained between the measured and predicted N_2O fluxes from the regression and DNDC models, respectively.

Table 6.3. Pearson correlation‡ analysis between the measured and predicted water-filled pore space.

Site	Landform complexes	No. of sampling days (May to Oct.)	Pearson correlation coefficient
Clay loam			
Unfertilized canola	shoulder	9	0.67 **
	footslope	9	0.57 *
Fallow	shoulder	7§	0.40 ns
	footslope	7§	0.88 **
Pasture¶	shoulder	15	0.67 **
Forest¶	footslope	21	0.81 ***
Fertilized wheat	shoulder	16	0.72 ***
	footslope	16	0.58 *
Fine sandy loam			
Fertilized canola	shoulder	16	0.37 †
	footslope	16	0.43 †
Sandy			
Fertilized oat	shoulder	12	0.72 **
	footslope	12	0.79 ***
Pasture	shoulder	7	0.65 †
	footslope	12	0.62 *
Forest	shoulder	5	0.80 *
	footslope	12	0.74 **

*, **, ***, † - significant at $\alpha = 0.05$, 0.01, 0.001, and 0.10, respectively; ns - not significant.

‡ This test was used because the values representing the measured water-filled pore spaces were the central tendency values (i.e., median).

§ For the clay loam, pasture site, the correlation analysis included sampling days in April 1994 because there were only three sampling days from July to Oct 1993.

¶ In the clay loam, pasture site, the shoulder complex was occupied by bromegrass and the footslope complex was dominated by aspen.

In Table 6.4, the percent increase in N_2O emissions during May to October from the simulated wet/warm year compared to that of the dry/cold year is only about 20 - 30 % in the clay loam cropland, and even less (10 -15 %) in the fine sandy loam cropland, sandy cropland, and clay loam uncultivated sites. It should be pointed out that this simulated effect of climate was based on the regression models that only consider the effect of WFPS on N_2O emissions. Another important effect of climate on N_2O emission is its regulation on N turnover rate (which could relate to changes in substrate availability), which could probably be depicted clearly only by using a process-oriented simulation model. Prediction of the N_2O emissions during spring of the different climatic scenarios was not attempted because the WFPS during spring could not be predicted reliably using the VSMB, which does not deal with detailed soil water dynamics during the spring thaw period.

The denitrification estimates (measured by C_2H_2 incubation method) of Elliott and de Jong (1992) from a fertilized, loam-textured Black Chernozemic cropland range from 1.0 - 1.4 kg N ha^{-1} on the shoulder and 7.6 - 12.8 kg N ha^{-1} on the footslopes. In the present study, the estimates of N_2O emissions on the shoulders at the clay loam and fine sandy loam, fertilized cropped sites were comparable to their estimates of total denitrification losses (Table 6.4). However, the estimates of N_2O emissions on the footslopes were about an order of magnitude lower than their estimates of total denitrification losses. Assuming that the methods of measurement used by Elliott and de Jong (1992) and used in the present study did not influence the differences of these estimates, these findings implied that on the footslopes, where reduced-O_2 conditions are common, N_2O emissions could be lower than total denitrification losses because of further reduction of N_2O to N_2. The estimates of annual N_2O emissions from the pasture sites were about half of the estimates from other studies: 0.100 kg N_2O-N ha^{-1}

Table 6.4. Estimates of N_2O emission during the years of study (1993 to 1995) and under the different climatic scenarios using regression models.

Site	Landform complexes	Years of study			Dry/cold	Normal	Wet/warm
		May to Oct	Spring†	Total	<-- (May to Oct.; mean ± S.E.)‡ -->		
		<---------- g N_2O-N ha^{-1} ---------->					
Clay loam							
Unfertilized	shoulder	73	10	83	60 ± 4	73 ± 1	80 ± 3
canola	footslope	149	74	223	135 ± 8	150 ± 8	178 ± 13
Fallow	shoulder	36	5	41	§	§	§
	footslope	180	116	296	§	§	§
Pasture¶	shoulder				19 ± 1	20 ± 2	22 ± 2
	(1993 - 94)	23	13	36			
	(1994 - 95)	23	24	47			
Forest¶	footslope				17 ± 1	18 ± 1	19 ± 1
	(1993 - 94)	19	23	42			
	(1994 - 95)	20	4	24			
Fertilized	shoulder	1513	167	1680	1224 ± 54	1363 ± 34	1477 ± 38
wheat	footslope	2789	223	3012	2073 ± 88	2327 ± 81	2634 ± 136
Fine sandy loam							
Fertilized	shoulder	1137	112	1249	994 ± 22	1026 ± 21	1120 ± 40
canola	footslope	2710	823	3533	2298 ± 51	2384 ± 54	2662 ± 108
Sandy							
Fertilized oat	shoulder	32	42	74	32 ± 1	33 ± 1	36 ± 1
	footslope	33	187	220	33 ± 1	34 ± 1	38 ± 1
Pasture	shoulder	1	1	2	1 ± 0	1 ± 0	3 ± 1
	footslope	4	53	57	3 ± 1	4 ± 1	6 ± 1
Forest	shoulder	1	1	2	1 ± 0	2 ± 0	3 ± 1
	footslope	1	3	4	1 ± 0	2 ± 0	3 ± 1

† The total N_2O emissions in spring (March to April of 1994 and 1995) were calculated by interpolating the N_2O fluxes measured at discrete sampling days.

‡ Calculated from the estimates of the five representative years in each climatic scenario.

§ The regression model for the clay loam, fallow site was the same as that for the clay loam, unfertilized canola site.

¶ In the clay loam, pasture site, the shoulder complex was occupied by bromegrass and the footslope complex was dominated by aspen.

yr^{-1} for Wisconsin prairie (Goodroad and Keeney, 1984), and 0.142 kg N_2O-N ha^{-1} yr^{-1} for Colorado shortgrass steppe (averaged from fertilized and unfertilized pastures; Mosier et al., 1996). The estimates of annual N_2O emissions from the forest sites were within the range of the estimates from pine and hardwood forest in the northeastern U.S., which were 0.010 ± 0.015 and 0.017 ± 0.017 kg N_2O-N ha^{-1} yr^{-1}, respectively (Bowden et al., 1990).

In the unfertilized cropped sites (clay loam, unfertilized canola and fallow sites), the averaged contributions of spring emissions to annual N_2O fluxes were 11 % and 36 % on the shoulders and footslopes, respectively. In the clay loam and fine sandy loam, fertilized cropped sites, the spring emissions accounted for an average of 9 % and 15 % of the annual N_2O fluxes on the shoulders and footslopes, respectively. In the sandy, fertilized oat site, the spring emission contributed 57 % and 85 % of the annual N_2O fluxes on the shoulders and footslopes, respectively. In the uncultivated sites (pasture and forest sites), the averaged contributions of spring emissions to annual N_2O fluxes were 47 % on the shoulders and 60 % on the footslopes. Therefore, the N_2O emissions in spring were of greater importance in the annual N_2O flux estimates from the low-flux sites (pasture, forest, unfertilized cropped, and sandy, fertilized cropped sites) than from the high-flux sites (clay loam and fine sandy loam, fertilized cropped sites).

The fertilizer-induced N_2O emission (% N_2O-N = {[annual N_2O flux from fertilized cropland - annual N_2O flux from unfertilized cropland] / fertilizer rate}) was calculated from the clay loam site, where emissions during both unfertilized (1993 growing season) and fertilized (1994 growing season) conditions were determined. The fertilizer rate applied in this site (a total of 85 kg N ha^{-1}; section 5.2.1) is a typical level that farmers used for this type of soil in the study region. Assuming that the

annual N_2O flux during the unfertilized condition in 1993 remained similar for 1994 when the site was fertilized, the estimate of emitted N_2O from N fertilization (Table 6.4) comprised 2 % and 3 % on the shoulders and footslopes, respectively. In a study conducted in Ontario, Canada, 0.25 % of applied N was emitted as N_2O from a sandy loam soil within 80 days of measurement (McKenney et al., 1980). On the other hand, from a study conducted in Colorado, N_2O emissions amounted to 1-2 % of the applied N from a clay loam soil utilized to irrigated cereal crops (Mosier and Hutchinson, 1981; Mosier et al., 1982; Mosier et al., 1986; Bronson et al., 1992). These studies were conducted in relatively flat areas. The present study suggested that estimates of fertilizer-induced N_2O emissions could be improved by considering in the investigation scheme the differences of activity at different topographical positions in a landscape.

The relationships between annual N_2O fluxes (total flux during years of study; Table 6.4) and soil texture (as exemplified by % sand; Table 6.1), soil total N (Table 3.10), and soil total organic C (Table 3.11) were examined for the fertilized cropped landscapes (Fig. 6.4). The percentage sand was used as an index of the gradient of soil moisture regimes in the study region. The soil total N and organic C, being the long-term integrative products of physical and biological factors, were used as indices of the gradient of soil fertility in the study region. The present study showed that soil texture, total N and organic C explained most of the variations of annual N_2O emissions from fertilized cropped landscapes in this study region. Similar results were also obtained by Groffman and Tiedje (1989a), who showed that soil texture and drainage accounted for 86 % of the variation of annual denitrification losses in temperate forest landscapes. These findings confirmed that increasing the scale of investigation in both time (annual losses rather than daily fluxes) and space (landscape and regional rather than field or plot scale) is useful for overcoming the variability problem of N_2O emission. The

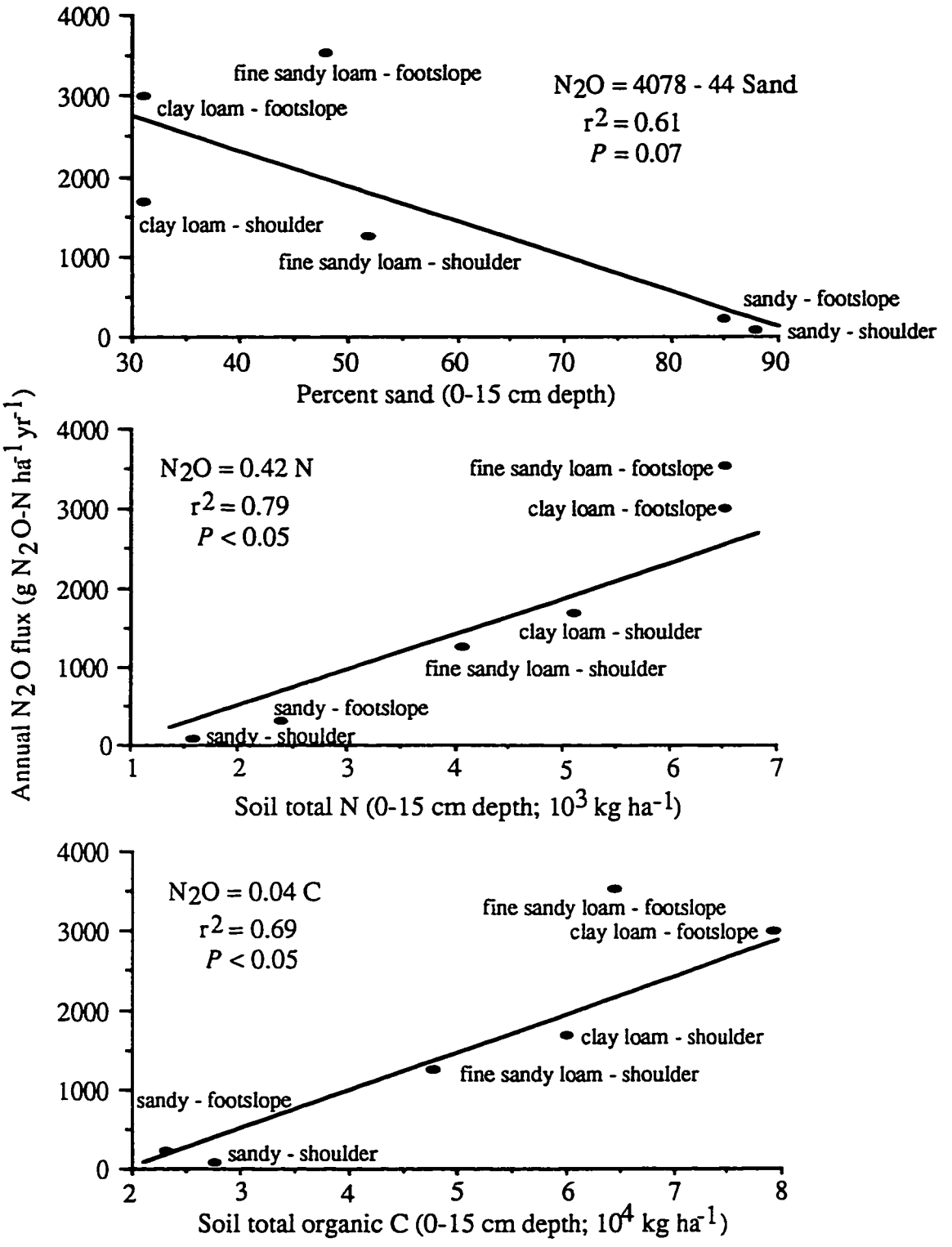

Fig. 6.4. Relationships between annual N_2O fluxes and percent sand, total N, and total organic C from fertilized cropped landscapes.

approach used in this study is consistent with the concept outlined by O'Neill (1988) on the theory of "coherent levels" - defined as "the scale at which predictive power is maximized". If the coherent level for N_2O emission is at the landscape or regional scale, these results would be a great aid for producing large-area estimates of N_2O fluxes.

7. SPATIAL EXTRAPOLATION OF NITROUS OXIDE EMISSIONS

7.1 Introduction

A reliable method of spatial extrapolation requires the implementation of mechanistic studies of N_2O emission across a range of sites in a region to gain an understanding of how the regulating factors of N_2O emission vary systematically from local to regional scales. This mechanistic knowledge subsequently provides the framework for the extrapolation of N_2O fluxes (Schimel et al., 1988; Matson et al., 1989; Matson and Harriss, 1995). Several studies that investigated N_2O emissions at the regional scale have used this conceptual approach where the region was examined through consideration of the gradients of factors that control N_2O fluxes across the region. For example, Matson and Vitousek (1987) showed that N_2O fluxes in tropical forests are positively related to indices of nitrogen turnover in the soil, and that both vary as a function of soil type; based on this information, they stratified tropical forests on the basis of soil type, climate and disturbance to organize previous N_2O flux measurements and to develop an estimate of the tropical N_2O source (Matson and Vitousek, 1990).

In the present study, the observed differences in N_2O emissions among soil textures and land use types indicate the appropriateness of the regional stratification scheme employed. Soil texture was the main physical factor investigated since this is the distal factor that controls the differences in soil moisture regimes in the study region. Soil moisture (as assessed by volumetric moisture content and WFPS) was, in turn, shown to be the important proximal factor controlling N_2O emission. Land use

was used as a surrogate variable to relate to the differences in N availability in the study region. The regional estimates of N_2O emission activity can be achieved by using the techniques of remote sensing (for land use characterization) and geographic information systems (for soil data available from soil survey) to extrapolate the landscape-scale estimates of annual N_2O fluxes. The objective of this component of the study was to obtain regional-scale estimates of N_2O emission.

7.2 Materials and Methods

The 'measure and multiply' method was used in scaling-up annual N_2O fluxes from landscape to regional scale. This method was employed using GIS technology where the maps of the ecological variables proven to control N_2O emissions (i.e., soil texture and land use) were overlaid to form discrete spatial classes or cells. The aerial coverage of each class was determined, and these spatial classes were filled with their corresponding annual N_2O fluxes. This technique is expressed in equation form as:

$$F = \Sigma [Ai\ Fi]$$

where F is the total flux, Ai is the area of the spatial class i (i.e., specific soil texture and land use characteristics), and Fi is the annual flux from spatial class i.

7.2.1 Remote sensing for land use classification

The different land use types in the study region were characterized using satellite imagery. A LANDSAT 5 thematic mapper image was acquired on a cloud-free day (9 August 1991) for LANDSAT track 37 and frame 23 (LANDSAT reference grid). A cloud-free image is necessary to avoid the problem of atmospheric scattering (radiance from the atmosphere), which reduces scene contrast. The image was obtained from RADARSAT International Inc. (Richmond, BC). The sun's elevation and azimuth at the image center are 48° and 141°, respectively. The image is a map-

oriented subscene registered on UTM projection and contained bands 3 (red, 0.63-0.69 μm), 4 (near infrared, 0.76-0.90 μm) and 5 (middle infrared, 1.55-1.75 μm). It is composed of 2535 rows and 2955 columns of pixels, and its size is approximately 63 km by 74 km. The Earth Resources Data Analysis Systems (ERDAS; ERDAS Inc., Atlanta, GA) software was used in the image processing and classification.

Prior to image classification, the image has to be pre-processed in order to get radiometric and geometric characteristics as close as possible to the original scene (Estes et al., 1983). The image was radiometrically corrected when purchased. Image rectification was then performed to remove geometric distortions in the image. This process corrects pixel locational errors, thereby placing ground features in their correct positions throughout the image. In image rectification, it is essential to have well-distributed and accurate ground control points (GCP), as they are used to establish the geometric transformations required to match the image to the map. Depending on the number of GCP used, their location relative to one another, and the distortion of the image, polynomial equations may be required to express the needed transformation. The aim is to derive geometric equations for which there is the least possible amount of error when used to transform source coordinates of the GCP into reference coordinates. The image was rectified using 27 GCP, with cubic convolution resampling to 25-m^2 pixels.

After the image was corrected, image enhancement was carried out to improve feature detectability. Of all the image enhancement techniques explored (i.e., multispectral band ratioing, simulated natural color, spectral ratios for vegatation monitoring, and contrast stretching), linear contrast stretching was found to be the most effective in detecting the different land use patterns in the study region. This technique is shown by the schematic representation in Fig. 7.1. The range of digital numbers (DN) is linearly expanded between 0 and 255. Linear contrast stretching increases the

difference between digital numbers of image features, thereby increasing the contrast between features (Jensen, 1986).

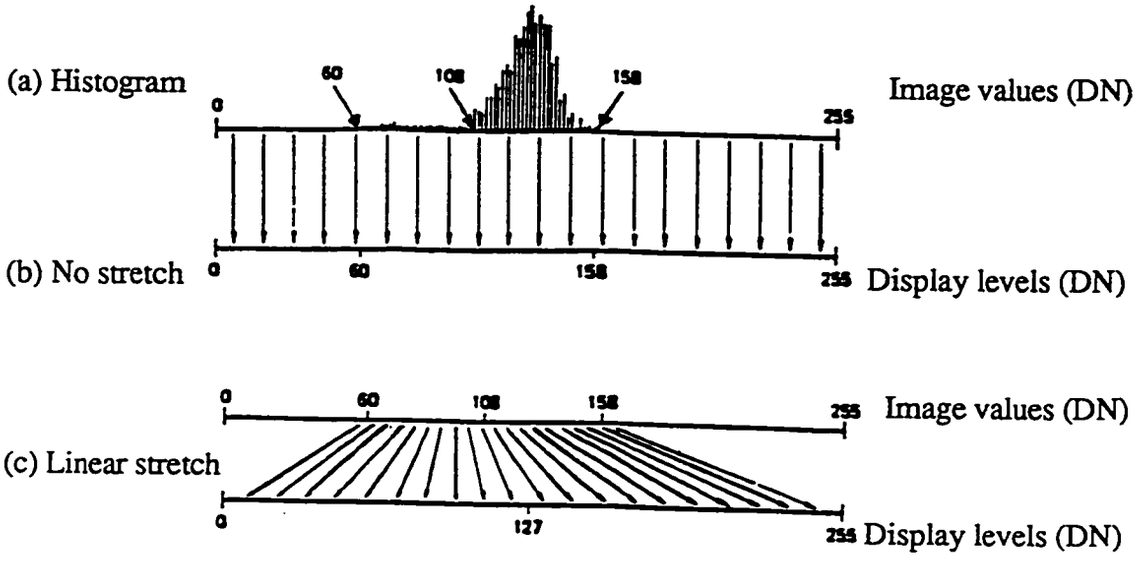

Fig. 7.1. Schematic representation of linear contrast stretching (From Jensen, 1986).

The image was classified using a combination of supervised and unsupervised classification methods. The development of spectral classes began with unsupervised classification of the composite image of bands 3, 4, and 5. Using the 'iterative self-organizing data analysis technique' for clustering in ERDAS, ten spectral classes were first identified, and these classes were related to the training samples. Training samples are areas of known land use types, which were identified from reconnaissance observation of the study region and from aerial photographs of 1:30000 scale. With reference to the spectral information of the training samples, the ten spectral classes were generalized into five classes corresponding to five spatial features of interest in the study region (i.e., cropped, fallow, pasture/hay land, forest, and water bodies). This

simplification was required to accommodate the land use types (i.e., cropped, fallow, pasture, and forest) from which N_2O emissions had been measured. Finally, the accuracy of the classified image was evaluated by 'ground truthing'. One hundred ground points of known land use type were noted from aerial photographs and reconnaissance survey. These ground points were not the same 'ground truths' that were used as training samples during the image classification.

7.2.2 Geographic Information System database

A GIS database of soil information (i.e., soil association, soil texture, parent material, slope, topographic phases, and land capability) was created for the study region using the Spatial Analysis Systems (SPANS; INTERA TYDAC Tech. Inc., Ottawa, ON). The data were taken from other GIS products (i.e., ARC/INFO, PAMAP), and from soil survey maps (Table 7.1). The maps were encoded to the GIS framework through the use of a graphic digitizer, and the indexing of spatial entities was achieved by the use of vector and grid data structures. The data from other GIS products and from the digitized maps were combined into a common format in SPANS. The information on particular soil characteristics (i.e., soil texture) was generalized in order to reduce complexity and to identify the more general patterns and trends. In GIS terminology, the type of generalization process used is called qualitative classification. The soil texture information of the study region was grouped together based upon similarity. For example, sandy-, medium-, and moderately fine-to-fine-textured areas included soil textures ranging from gravely to sand, fine sandy loam to loam, and clay loam to clay, respectively. A geographic image of soil texture in the study region was then generated (Fig. 7.2). Finally, the land use information was integrated with the GIS database, and a matrix of soil texture and land use types was created.

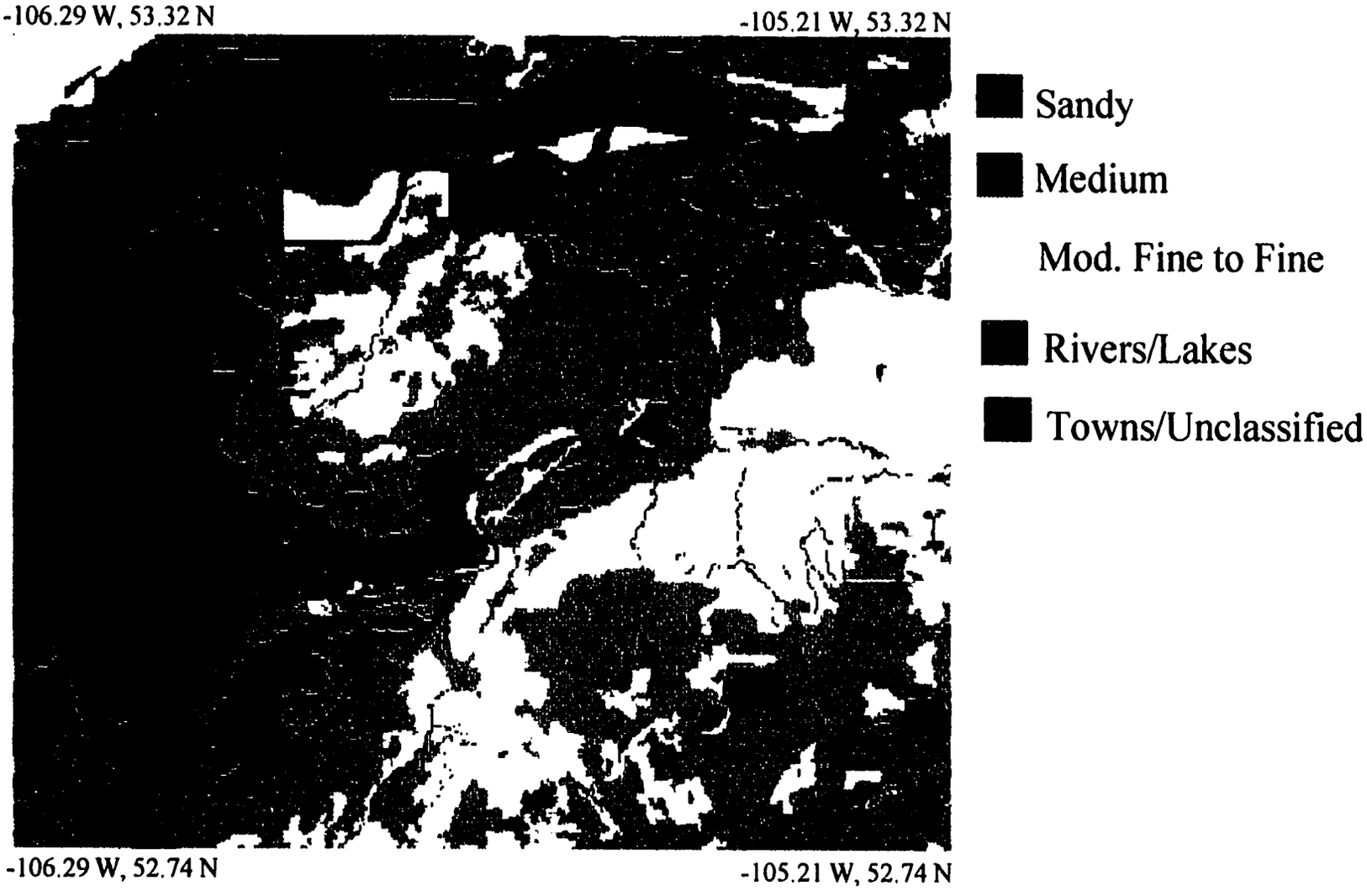

Fig. 7.2. Soil texture characteristics of the study region.

Table 7.1. Sources of the soil information database created for the study region.

Soil surveys of the rural municipalities	Information format
401 - Hoodoo	PAMAP
430 - Invergordon	PAMAP
431 - St. Louis	ARC/INFO
459 - Kinistino	ARC/INFO
460 - Birch Hills	ARC/INFO
461 - Prince Albert	ARC/INFO
463 - Duck Lake	Soil map of Saskatoon sheet 73B (1:126,720)
493 - Shellbrook	Northern Provincial Forest Reserve - Shellbrook map sheet 73G (1:126,720)
Southwest of Northern Provincial Forest Reserve	ARC/INFO and soil map of Pasquia Hills 63E (1:126,720)

7.3 Results and Discussion

7.3.1 Land use characterization

The distinctiveness of the spectral reflectance (indicated by the digital numbers) of the identified land use types was assessed statistically. Representative pixels were systematically selected from the classified image (Fig. 7.3) by sampling pixels at 50-pixel interval. Table 7.2 shows the comparison of the digital numbers of the pixels representing each land use type. Water bodies showed the lowest digital numbers, which decrease as the spectral wavelength increase. The reflectance observed at the red

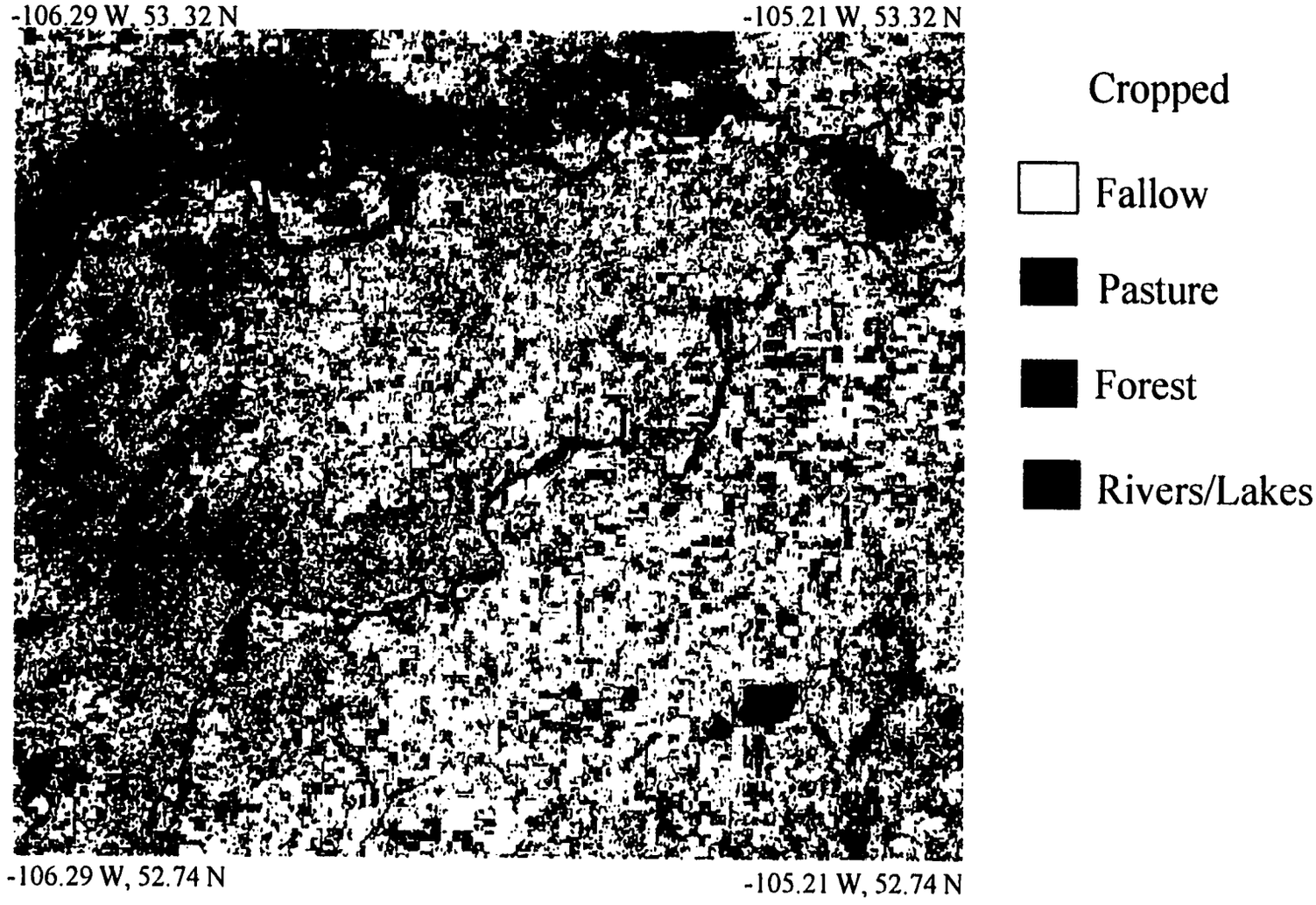

Fig. 7.3. Land use pattern in the study region determined from LANDSAT thematic mapper image.

Table 7.2. Comparison of the spectral characteristics of the different land use types in the study region.

Land use type	No. of sample pixels	Median digital numbers†		
		Red	Near infrared	Middle infrared
Water	53	48 b	52 e	8 e
Forest	689	52 b	72 c	61 d
Pasture/hay land	432	54 ab	76 b	99 b
Cropped	867	60 a	79 a	71 c
Fallow	159	63 a	67 d	125 a

† The differences in digital numbers among land use types was assessed using multiple comparison extension of Kruskal-Wallis H test. Medians in each column followed by the same letter(s) are not significantly different $\alpha = 0.05$.

and near infrared bands was contributed by the pixels representing shallow water areas, which indicated that the reflectance was due to the suspended sediments or the bottom. The fallow areas showed increase in digital numbers with the increase in wavelength. This reflectance characteristics agreed with the spectral response curve of a bare soil (section 2.7.1).

In the near infrared band, the cropped areas showed the highest digital numbers, followed by the pasture/hay land and forest areas. This band has been observed to give the greatest distinction among vegetation types (Arai, 1992). The high reflectance of the cropped areas was due to the dense vegetative cover, as the crops were in full vegetative stage during the image acquisition. Trolier and Philipson (1986) indicated that similarity in reflectance could exist between the cropped and pasture areas, depending on the image acquisition date. In their study, the distinction between cropped and pasture areas was aided by associating field features (i.e., field size and

boundary) and known field practices (i.e., harvest or cutting time). In the present study, the aerial photographs of the study region, taken on the same date as the satellite image, were used as additional reference in identifying the training samples for the pasture/hay land areas during the image classification. On 9 August 1991, the known pasture/hay land areas (training samples) had already been cut, as indicated by presence of hay bales on the aerial photographs. It is assumed that harvest of pasture and hay had occurred for all pasture/hay land areas in the study region. Hence, the pasture areas should have less vegetative cover than the cropped areas at the time when the image was taken. As a result of this classification basis, the classified pasture/hay land areas showed lower digital numbers in the near infrared band than the cropped areas, but they have higher digital numbers in the middle infrared band than the cropped areas due to the influence of the spectral reflectance of the soil. The forest areas had the lowest digital numbers among the vegetated areas at the near and middle infrared bands. This low reflectance was attributed to the presence of shadow and wood (Townshend, 1984). It is obvious from these spectral characteristics that the different land use types were more effectively defined by basing the classification on the composite image of bands 3, 4, and 5 rather than on a single band image. Overall, a classification accuracy of 85 % was obtained, based on the ground truth data.

7.3.2 Regional estimates of N_2O emissions

The calculation of the regional N_2O emissions (Table 7.3) is bounded by a number of assumptions:

(1) The N_2O fluxes of the studied cropped, fallow, pasture and forest sites in the three textural areas represent the typical N_2O emission activity of the agricultural and natural landscapes in the study region.

(2) The proportion of the shoulder and footslope complexes at each study sites holds true for the landscapes in the study region that these study sites are representing.
(3) The N_2O emission from the sandy, fallow area was not measured. It is assumed that the proportion of the annual N_2O fluxes in the clay loam, fallow to clay loam, fertilized cropped (wheat) sites is similar for the sandy, fallow to the sandy, fertilized cropped (oat) sites.
(4) The classified cropped areas from the satellite image are assumed to be all fertilized, as N fertilization is the typical practice of farmers from this study region.
(5) Since N_2O fluxes from fallow, pasture and forest sites are generally low, the estimates of N_2O fluxes for the medium-textured area with these land use types are assumed to be similar with that of the moderately fine- to fine-textured area (which was represented by the clay loam site).
(6) The estimate for pasture in medium- to fine-textured areas is represented by the bromegrass-grown shoulder position in the clay loam site, and the estimate for forest in medium- to fine-textured areas was taken from the aspen-dominated footslope position in the clay loam site.

The areal coverage of the different textural areas and land use categories (Table 7.3) was determined from the combined texture-land use geographic image (Fig. 7.4). The average annual fluxes for fertilized cropped, fallow, pasture, and forest areas in this region, weighted by their areal extents in the different textural areas, were 2010, 125, 40, and 15 g N_2O-N ha^{-1} yr^{-1}, respectively. The weighted-average annual flux from the fertilized cropped landscapes is comparable to the weighted-average annual flux from tropical forest (1825 g N_2O-N ha^{-1} yr^{-1}; Matson and Vitousek, 1990). Considering all the textural areas, the pasture and forest covered 49 % of the total area in the study region and contributed 1.4 % of the total regional flux. The fertilized cropped areas covered only 44 % of the regional area, but contributed 98 % of the

Table 7.3. Annual N_2O fluxes, areal extent, and extrapolated N_2O fluxes for different landscapes in a Black soil region of central Saskatchewan.

Land use - Soil texture†		Landscape scale			Regional scale	
		Proportion (%)‡	Annual flux§ (kg N_2O-N ha^{-1} yr^{-1})	Weighted annual flux	Area (km^2)¶	Total annual flux (Mg N_2O-N yr^{-1})
Fertilized cropped						
Sandy				0.162	285	4.62
	shoulder	40	0.074			
	footslope	60	0.220			
Medium				2.368	991	235.67
	shoulder	50	1.249			
	footslope	50	3.533			
Moderately fine - Fine				2.279	613	139.70
	shoulder	55	1.680			
	footslope	45	3.012			
Fallow						
Sandy				0.012#	81	0.10
Medium - Fine				0.168	217	3.65
	shoulder	50	0.041			
	footslope	50	0.296			
Pasture						
Sandy				0.041	236	0.97
	shoulder	30	0.002			
	footslope	70	0.057			
Medium - Fine				0.042††	544	2.28
Forest						
Sandy				0.003	796	0.24
	shoulder	45	0.002			
	footslope	55	0.004			
Medium - Fine				0.033††	555	1.83
Total					**4318**	**389.06**

† The medium- and moderately fine-to-fine-textured areas were represented by the studied fine sandy loam and clay loam landscapes, respectively.

‡ Percentage proportion of the shoulder and footslope complexes are reported in Tables 3.2 to 3.7.

§ The values are reported in Table 6.4 (total flux during the years of study).

¶ Total area was determined from the combined texture-land use geographic image (Fig. 7.4).

The value was based on the assumption that the proportion of the annual N_2O fluxes in the clay loam, fallow to fertilized cropped (wheat) sites is similar for the sandy, fallow to fertilized cropped (oat) sites (i.e., 0.168/2.279 = 0.074; 0.074 * 0.162 = 0.012).

†† The values were taken from the estimates at the clay loam, bromegrass (shoulder) and clay loam, aspen (footslope) and are averages of the estimates from two years.

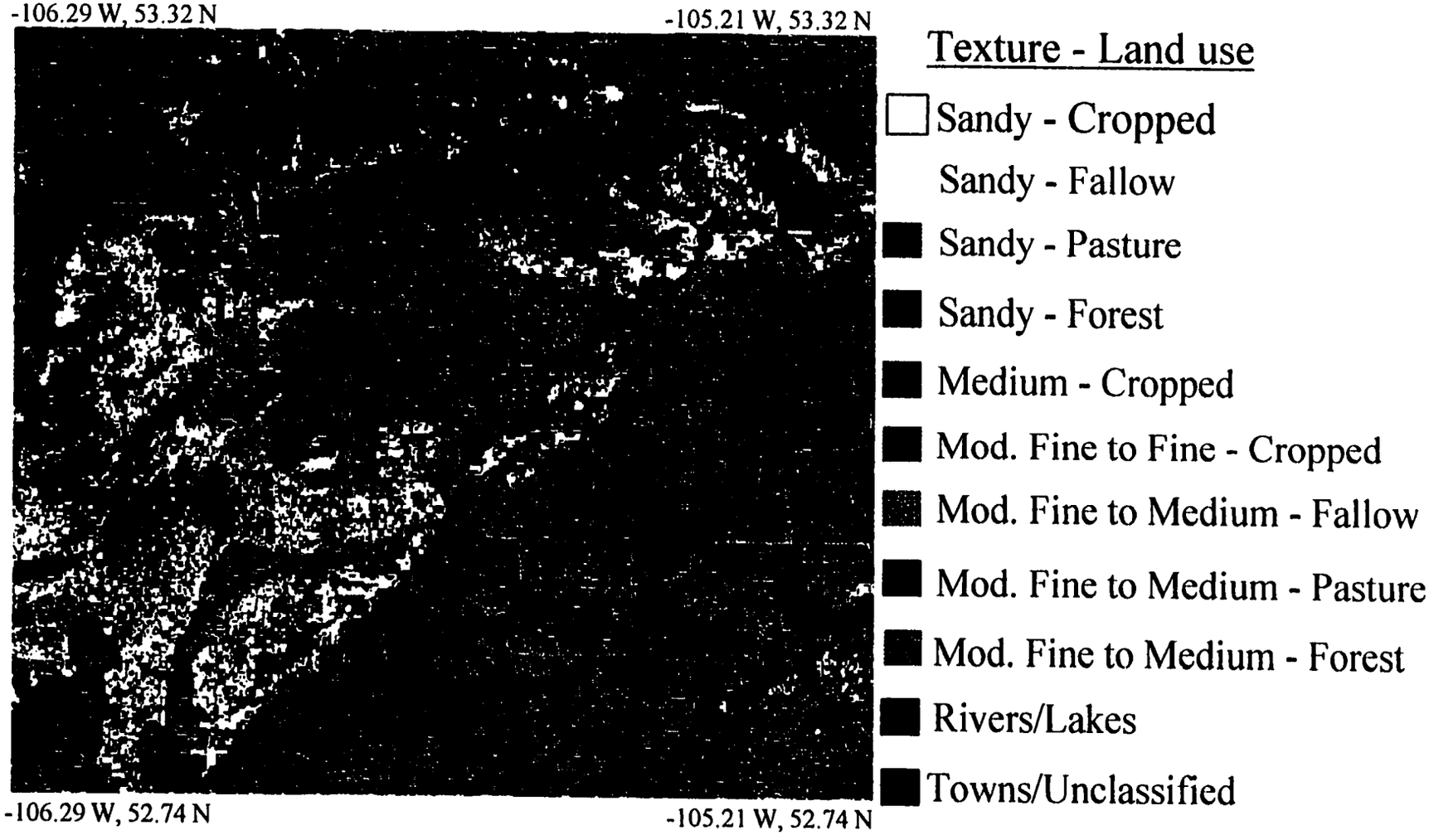

Fig. 7.4. Soil texture and land use characteristics of the study region.

regional flux. The weighted-average annual fluxes for the medium- to fine-textured and sandy-textured areas were 1310 and 40 g N_2O-N ha^{-1} yr^{-1}, respectively.

In this study region, the proportions of the area covered by the sandy-textured and the medium- to fine-textured areas were 30 % and 70 %, respectively. In the whole Black soil zone of the three Prairie Provinces, about 5 % is covered by sandy-textured area and about 10 % is covered by fine-textured area ($\geq$ 40 % clay; E. de Jong, personal communication). In this fine-textured area, no estimates of N_2O emissions measured directly on the field are yet published. If the estimate of N_2O emission from the whole Black soil zone is needed, from the present study region the weighted average annual flux during the years of study was 900 g N_2O-N ha^{-1} yr^{-1}. However, further refinement of this regional estimate can be achieved by investigating N_2O emissions over a much wider array of agricultural production systems, particularly in the fine-textured areas, to encompass different management practices and extent of N fertilization.

For the purpose of extrapolating this regional estimate of N_2O emission to the Black soil zone of Saskatchewan (7.8×10^6 ha; Agriculture Canada, 1992), the projected total annual flux is 7×10^9 g N_2O-N yr^{-1}. If a similar regional estimate is assumed for the whole Black soil zone of the Prairie Provinces of Canada (18.6×10^6 ha; H. Rostad, personal communication), a total annual flux of 2×10^{10} g N_2O-N yr^{-1} is calculated. This value is an order of magnitude less than the calculated flux (1.1×10^{11} g N_2O-N yr^{-1}) from the U. S. and Eurasian deserts and semi-deserts (total area of 4.92×10^8 ha with an average flux of 210 g N_2O-N ha^{-1} yr^{-1}; Matson et al., 1991), an order of magnitude less than the estimate for native, temperate grasslands (1.6×10^{11} g N_2O-N yr^{-1} with a total land area of 11.5×10^8 ha and an average flux of 142 g N_2O-N ha^{-1} yr^{-1}; Mosier et al, 1996), and two orders of magnitude less than the range of estimates from tropical forests ($2.5 - 7.5 \times 10^{12}$ g N_2O-N yr^{-1} with a total

area of 14.8 x 10^8 ha; McElroy and Wofsy, 1986; Matson and Vitousek, 1990). The scarcity of N_2O flux data from subhumid, cold continental regions of Canada leads to uncertainty of the importance of this ecozone in contributing to the annual global N_2O production (14 x 10^{12} g N_2O-N yr^{-1}). However, although the calculation of N_2O flux for the Black soil zone is based on the data collected over a small region, it does suggest that such ecozone represent a relatively small contribution of the estimated global N_2O emissions from terrestrial sources.

8. GENERAL DISCUSSION AND CONCLUSIONS

To obtain reliable estimates of annual N_2O fluxes at the landscape and regional scale, it is necessary to employ investigation techniques that reduce random variation within experimental units and that characterize the factors controlling the systematic variation within the landscape and across the region. A conceptual tool, which hypothesized the link of N_2O-controlling factors from local to regional scale, was used as the basis of the investigation approach employed. The selection of sampling sites was governed by the present understanding of the regional controls on N_2O emission. Both field-based research (Groffman and Tiedje, 1989a; Mosier et al., 1996) and existing models of N_2O emission (Parton et al., 1996; Potter et al., 1996) suggest that the texture of the parent sediments and land use exert a strong, indirect control on N_2O emissions at the regional scale. To reflect these factors, landscapes with specific soil texture-land use characteristics were identified to cover the range of conditions across the region and were considered as the experimental units at the regional level. At the landscape level, based on the soil-landform relations and soil physical and biochemical characteristics (section 3.3), the shoulder and footslope complexes were considered as the experimental units (discussed in section 3.4) in order to account for the functional differences of these distinct spatial units in the landscape.

Results demonstrated that the spatial and temporal variability of N_2O emission is controlled by definable factors, which are linked as a continua on scale from local to regional (section 5.4.4). Examination of the relationships between N_2O emission and soil factors at the landform complex level showed that soil water (as assessed by

volumetric moisture content and WFPS) was the factor dominantly controlling N_2O emission. At the landscape level, topography was the basic factor controlling N_2O emission through its influence on water redistribution and differences of soils in the landscape. This is clearly evident by the parallel landscape-scale patterns of N_2O fluxes and soil water contents, particularly in sites where both landform complexes were grown to the same vegetation or crop types. The N_2O fluxes and water contents on the footslope complex were consistently higher than on the shoulder complex. The landscape-scale differences in soils also affect differences in N_2O emission; in the clay loam and fine sandy loam sites, the presence of Btg horizon of soils in the footslopes indicated significant N_2O emissions due to its horizonation effect on water percolation.

The seasonal fluctuations of N_2O emissions were also similar to the seasonal patterns of soil water contents which, in turn, were affected by the distribution of rainfall. The N_2O emission activity increased towards the early summer, decreased towards the late summer, and virtually ceased by the onset of frost in fall. The high N_2O fluxes in early summer were attributed to the frequent occurrence of high rainfall levels, while the low N_2O fluxes towards fall were due to the intermittent occurrence of low rainfall levels. The presence of frozen soil layer and snow cover in fall might have prevented gas efflux during this period and presumably also during winter. High N_2O fluxes were again observed in spring as a consequence of high soil water (Figs. 5.2 to 5.8) and substrate availability (Table 5.4), and probably also due to diffusion from depth of accumulated N_2O during winter.

The differences in N_2O emissions among the textural areas and land use types signified the appropriateness of stratifying a region based on ecological factors that are proven to influence dynamics of N cycling at a large scale. Soil texture was used in stratifying the region because it exerts a strong influence on the differences in soil

moisture regimes in the region. In the study region, the fine-textured landscapes showed higher N_2O emissions and soil water contents than the sandy-textured landscapes for a similar type of land use (e.g. fertilized cropped landscapes; Figs. 5.2, 5.5, 5.6, 6.3). Fine-textured soils can hold more water than sandy-textured soils, such that the former would have a more extensive anaerobic condition during a given rainfall event or spring thaw than the latter (spring emissions discussed in section 5.4.3). Soil texture should also indirectly affect N_2O emission through its influence on the differences in soil fertility, plant community structure, and eventually of N and C levels in the area. Studies have shown that fine-textured soils supported vegetation of high litter quality and a more dynamic soil N cycle, with high rates of mineralization and nitrification (Pastor et al., 1984; Burke et al., 1989), which could lead to high N_2O fluxes.

Land use was also used in stratifying the region because different land uses reflects differences in N cycling. Long-term agricultural soils may have progressively reduced potentials for biogenic gas emissions (Groffman et al., 1993a), which is probably due to decrease in organic matter availability or nutrient reserve after years of cultivation. As observed from this study, increased N_2O emissions from the agricultural landscapes were largely caused by N fertilization. This study also showed low N_2O emissions from the pasture and forest landscapes. Uncultivated soils may actually have high potential for N mineralization (Walley et al., 1996), but the high C availability in these soils usually results in a conservative N cycle (little NO_3^- accumulation) and low gaseous N emissions (Hutchinson and Davidson, 1993). In addition, if N_2O emission in undisturbed ecosystems is largely contributed by nitrification (Parton et al., 1988b; Mummey et al., 1994), autotrophic nitrifiers are also considered poor competitors for NH_4^+ relative to the heterotrophic microorganisms (Verhagen and Laanbroek, 1991). For example, where the available organic matter

fraction has a high C:N ratio, microbial heterotrophs will readily immobilize NH_4^+ ions in the soil solution, leaving little for nitrifiers.

The N_2O emissions during May to October were estimated by establishing regression models that related N_2O fluxes to WFPS. The WFPS was the factor most correlated to N_2O emission. A clear seasonal difference in soil mineral N and soluble C was also observed (Table 5.4), which might have also contributed to the seasonal fluctuations of N_2O emissions. However, the relationships between N_2O emission and soil mineral N and soluble C were not significant. Land use was the surrogate variable used to represent the differences in N and C availability, and the regression models were developed for each land use type. Estimates of N_2O emissions from May to October were obtained by summing the predicted daily N_2O fluxes from the regression equations, in which the WFPS were calculated from the VSMB-simulated soil water content. For the determination of the total spring flux (i.e., mid-Mar to April), the trapezoidal quadrature calculation was considered appropriate because the data from spring clearly showed the beginning, peak, and end of the spring pulse of activity, which also reflected the occurrence of snow melting and soil thawing (sections 5.3.1 and 5.4.3). It is also difficult to predict N_2O emissions from WFPS during spring using only simplified soil moisture model (i.e., VSMB) that does not deal with detailed soil water dynamics during the spring thaw period.

During the years of study, the landscape-scale estimates of annual N_2O emissions from the fertilized-cropped sites were 2.28, 2.37, and 0.16 kg N_2O-N ha^{-1} in the clay loam, fine sandy loam, and sandy areas, respectively. In the clay loam (fertilized wheat) and fine sandy loam (fertilized canola) sites, the spring emissions accounted for 9 % of the annual emissions on the shoulders and for 15 % of the annual emissions on the footslopes. In the sandy, fertilized oat site, the spring emission contributed 57 % and 85 % of the annual N_2O fluxes on the shoulders and footslopes,

respectively. These annual N_2O emissions constituted 2.5 %, 3.6 %, and 0.3 % of the amount of N applied in the clay loam, fine sandy loam, and sandy sites, respectively. The pasture sites had annual N_2O emissions of 0.042 and 0.041 kg N_2O-N ha^{-1} in the clay loam and sandy areas, respectively. The estimates of annual N_2O emissions from the pasture sites were about half of the estimates from other studies: 0.100 kg N_2O-N ha^{-1} yr^{-1} for Wisconsin prairie (Goodroad and Keeney, 1984), and 0.142 kg N_2O-N ha^{-1} yr^{-1} for Colorado shortgrass steppe (averaged from fertilized and unfertilized pastures; Mosier et al., 1996). The forest sites had annual N_2O emissions of 0.033 kg N_2O-N ha^{-1} in the clay loam area and 0.003 kg N_2O-N ha^{-1} in the sandy area. The estimates of annual N_2O emissions from the forest sites were within the range of the estimates from pine and hardwood forest in the northeastern U.S., which were 0.010 ± 0.015 and 0.017 ± 0.017 kg N_2O-N ha^{-1} yr^{-1}, respectively (Bowden et al., 1990). In the pasture and forest sites, the averaged contributions of spring emissions to annual N_2O fluxes were 47 % on the shoulders and 60 % on the footslopes. Therefore, the N_2O emissions in spring were of greater importance in the annual N_2O flux estimates from the low-flux sites (pasture, forest, and sandy, fertilized cropped sites) than from the high-flux sites (clay loam and fine sandy loam, fertilized cropped sites). Considering the annual N_2O fluxes in the fertilized cropped landscapes, their relationships with % sand, soil total N and organic C showed that N_2O emissions vary systematically among sites arrayed along gradients of soil moisture regimes and soil fertility in the region.

Regional estimates of N_2O emission activity were obtained using a GIS database of soil texture and land use characteristics (derived from satellite imagery) of the study region. Since the true geographic locations of the GIS database are known, the spatial dimension of each spatial class (i.e., area of specific soil texture and land use

characteristics) could be determined. The annual N_2O fluxes of the investigated landscapes were used to represent the categorized soil texture-land use areas in the region. During the years of study, the average annual N_2O fluxes for the medium- to fine-textured and sandy-textured areas, weighted by their aerial extents in the different land use types, were 1.31 and 0.04 kg N_2O-N ha^{-1} yr^{-1}, respectively. On the other hand, the average annual N_2O fluxes for the fertilized-cropped, fallow, pasture, and forest areas, weighted by their areal extent in the different textural areas, were 2.01, 0.12, 0.04, 0.02 kg N_2O-N ha^{-1} yr^{-1}, respectively. The weighted average flux for the study region, considering the soil texture and land use types being studied, was 0.90 kg N_2O-N ha^{-1} yr^{-1}. This estimate is higher compared to the weighted average of 0.21 g N_2O-N ha^{-1} yr^{-1} for a Wyoming sagebrush steppe ecosystem (Matson et al., 1990) and about half of the weighted average for tropical forest region (1.82 kg N_2O-N ha^{-1} yr^{-1}; Matson and Vitousek, 1990).

The total N_2O emission for the study region was 390 x 10^3 kg N_2O-N yr^{-1}, and 98 % was contributed by fertilized cropped landscapes although they only occupy 44 % of the regional area. Improved accuracy of the regional estimate can then be achieved by investigating N_2O emissions over a much wider array of agricultural production systems to encompass different management practices and extent of N fertilization. Large efflux of N_2O from N fertilization occurred generally within six weeks following the application, and the temporal sampling approach used should sufficiently account for this activity. Proper timing of sampling during the spring period is also equally important because although the contribution of spring emissions to annual emissions in the fertilized cropped sites was relatively low (i.e., clay loam and fine sandy loam sites), it is evident that large efflux occured during the relatively short period of the spring thaw. The contribution of spring emissions to annual

emissions may also increase with change in management practices (e.g., increase in rate of N fertilization) and climate (e.g., high snowfall and warm spring), which can result in increased N availability, a longer period of high soil moisture contents, and increased in microbial activity.

The use of N fertilizers in agriculture during the last four decades is one of several explanations for the increase in atmospheric N_2O concentration. Nitrogen fertilizer use and biological N fixation are projected to increase continuously during the next 100 years to meet food demands (Hammond, 1990). Although emissions of CO_2 dominate the anthropogenic radiative forcing of climate, evidence has shown that since the 1960s N_2O has made progressively larger contributions (Shine et al., 1990). Furthermore, the imbalance in the global budget of N_2O (i.e., total flux of sources is lower than the total sinks) could possibly be due to underestimation of N_2O emissions resulting from N fertilization and biological N fixation. From this study, the annual N_2O emissions constituted 2.7 % (weighted average in the region) of the applied N. From a no-till corn field in Tennessee, Thornton and Valente (1996) also reported N_2O emissions of 2.6 to 3.0 % of the applied N. Bouwman (1994) conducted an inventory of fertilizer-induced N_2O emissions from different climatic regions, soils, crops, fertilizer types and rates, and he recommended a global estimate of 1.25 % yr^{-1} for direct N_2O emission from fertilized fields. Results from the present study suggest that N_2O emissions from fertilized soil may be considerably higher than previously thought, and these high emissions may, in part, explain some of the reasons for the shortfall in the global N_2O budget. The effect of N input is usually only partially traced in the environment. Very little of the ~80 x 10^{12} g N yr^{-1} added as fertilizer worldwide remains in the soil-plant system (Duxbury et al., 1993; Mosier, 1994). Most of it is ultimately denitrified, and only a small proportion has to be released as

N_2O to have a substantial effect on the global N_2O budget. A complete accounting of the fertilizer N, biologically fixed N, and N mineralized from organic matter is difficult to achieve, but needed if the aim is to accurately assess the impact of increased use of N in agricultural systems on terrestrial N_2O emissions.

Overall, I believe that this study contributes a substantial progress in estimating N_2O emission at the regional scale, and enhances a mechanistic understanding of the factors controlling N_2O emission. The approach used in this study might also aid in improving research tools for those attempting to quantify regional-level nutrient fluxes or storage. This approach also can be useful for the development or adaptation of simulation models that predict ecosystem processes and trace gas fluxes. Further studies are needed in order to predict N_2O emission from agricultural soils based on N application, soil, crop, management, and climatic conditions. Saskatchewan is a particularly apt location for such studies in that the wide but gradual vegetation and climatic gradients are clearly reflected in the soils.

9. LITERATURE CITED

Acton, D.F., and J.G. Ellis. 1978. The soils of the Saskatoon Map Area 73-B. Saskatchewan Institute of Pedology Pub. S4. Saskatchewan, Canada.

Agriculture Canada. 1992. Soil landscapes of Canada: Saskatchewan soil inventory. Publ. No. 5243/B. Land Resource Research Center, Research Branch, Agriculture Canada. Ottawa, ON.

Ambus, P., and S. Christensen. 1994. Measurement of N_2O emission from a fertilized grassland: An analysis of spatial variability. J. Geophys. Res. 99:16549-16555.

Ambus, P., and S. Christensen. 1995. Spatial and seasonal nitrous oxide and methane fluxes in Danish forest-, grassland-, and agro-ecosystems. J. Environ. Qual. 24:993-1001.

Ambus, P., H. Clayton, J.R.M. Arah, K.A. Smith, and S. Christensen. 1993. Similar N_2O flux from soil measured with different chamber techniques. Atmospheric Environ. 27A:121-123.

Anthony, W.H., G.L. Hutchinson, and G.P. Livingston. 1995. Chamber measurement of soil-atmosphere gas exchange: Linear vs. diffusion-based flux models. Soil Sci. Soc. Am. J. 59:1308-1310.

Arah, J.R.M. 1990. Diffusion-reaction models of denitrification in soil microsites. p. 245-258. *In* N.P. Revsbech and J. Sorensen (eds.) Denitrification in soil and sediment. Plenum, New York.

Arah, J.R.M., and K.A. Smith. 1989. Steady-state denitrification in aggregated soils: A mathematical model. J. Soil Sci. 40:139-149.

Arai, K. 1992. A supervised Thematic Mapper classification with a purification of training samples. Int. J. Rem. Sens. 13:2039-2049.

Baier, W., and G.W. Robertson. 1965. Estimation of latent evaporation from simple weather observations. Can. J. Plant Sci. 45:276-284.

Baier, W., and G.W. Robertson. 1966. A new versatile soil moisture budget. Can J. Plant Sci. 46:299-315.

Blackmer, A.M., and M.E. Cerrato. 1986. Soil properties affecting formation of nitric oxide by chemical reactions of nitrite. Soil Sci. Soc. Am. J. 50:1215-1218.

Blackmer, A.M., S.G. Robins, and J.M. Bremner. 1982. Diurnal variability in rate of emission of nitrous oxide from soils. Soil Sci. Soc. Am. J. 46:937-942.

Bottner, P. 1985. Response of microbial biomass to alternate moist and dry conditions in a soil incubated with ^{14}C- and ^{15}N-labeled plant material. Soil Biol. Biochem. 17:329-337.

Bouwman, A.F. 1990. Exchange of greenhouse gases between terrestrial ecosystems and the atmosphere. p. 61-127. *In* A.F. Bouwman (ed.) Soils and the greenhouse effect. John Wiley and Sons, New York.

Bouwman, A.F. 1994. Direct emission of nitrous oxide from agricultural soils. National Institute of Public Health and Environmental Protection. Report No. 773004004. Bilthoven, Netherlands.

Bowden, R.D., P.A. Steudler, J.M. Melillo, and J.D. Aber. 1990. Annual nitrous oxide fluxes from temperate forest soils in the Northeastern United States. J. Geophys. Res. 95:13997-14005.

Bowden, W. B., W. H. Mcdowell, C. E. Asbury, and A. M. Finley. 1992. Riparian nitrogen dynamics in two geomorphologically distinct rain forest watersheds: Nitrous oxide fluxes. Biogeochemistry 18:77-99.

Bowman, R.A. and D.D. Focht. 1974. The influence of glucose and nitrate concentrations upon denitrification rates in sandy soils. Soil Biol. Biochem. 6:297-301.

Brasseur, G., and M.H. Hitchman. 1988. Stratospheric response to trace gas perturbation. Science 240:634-637.

Breitenbeck, G.A., A.M. Blackmer, and J.M. Bremner. 1980. Effects of different nitrogen fertilizers on emission of nitrous oxide from soil. Geophys. Res. Lett. 7:85-88.

Bremner, J.M., and A.M. Blackmer. 1978. Nitrous oxide: Emission from soils during nitrification of fertilizer nitrogen. Science 199:295-296.

Bronson, K.F., A.R. Mosier, and S.R. Bishnoi. 1992. Nitrous oxide emissions in irrigated corn as affected by nitrification inhibitors. Soil Sci. Soc. Am. J. 56:161-165.

Burke, I.C., W.A. Reiners, and R.O. Olson. 1989. Topographic control of vegetation in a mountain big sagebrush steppe. Vegetatio 84:77-86.

Burton, D.L., and E. G. Beauchamp. 1985. Denitrification rate relationships with soil parameters in the field. Commun. Soil Sci. Plant Anal. 16:539-549.

Burton, D.L., and E.G. Beauchamp. 1994. Profile nitrous oxide and carbon dioxide concentrations in a soil subject to freezing. Soil Sci. Soc. Am. J. 58:115-122.

Christensen, S., S. Simkins, and J.M. Tiedje. 1990a. Spatial variation in denitrification: Dependency of activity centers on the soil environment. Soil Sci. Soc. Am. J. 54:1608-1613.

Christensen, S., S. Simkins, and J.M. Tiedje. 1990b. Temporal patterns of soil denitrification: Their stability and causes. Soil Sci. Soc. Am. J. 54:1614-1618.

Crowder, M.J., and D.J. Hand. 1990. Analysis of repeated measures. 1st ed. Chapman and Hall, New York. 257p.

Crutzen, P.J., and D.H. Ehhalt. 1977. Effects of nitrogen fertilizers and combustion in the stratospheric ozone layer. Ambio 6:112-117.

Davidson, E.A. 1991. Fluxes of nitrous oxide and nitric oxide from terrestrial ecosystems. p. 219-235. *In* J.E. Rogers and W.B. Whitman (eds.) Microbial production and consumption of greenhouse gases: Methane, nitrogen oxides, and halomethanes. Am. Soc. Microbiol., Washington, DC.

Davidson, E.A., and J.L. Hackler. 1994. Soil heterongeneity can mask the effects of ammonium availability on nitrification. Soil Biol. Biochem. 26:1449-1453.

Davidson, E.A., and J.P. Schimel. 1995. Microbial processes of production and consumption of nitric oxide, nitrous oxide and methane. p. 327-357. *In* P.A. Matson and R.C. Harriss (eds.) Biogenic trace gases: Measuring emissions from soil and water (Methods in ecology series). Blackwell Sci. Publ., Cambridge, Massachussets.

Davidson, E.A., J.M. Stark, and M.K. Firestone. 1990. Microbial production and consumption of nitrate in an annual grassland. Ecology 71:1968-1975.

Davidson, E. A., and W. T. Swank. 1986. Environmental parameters regulating gaseous nitrogen losses from two forested ecosystems via nitrification and denitrification. Appl. Environ. Microbiol. 52:1287-1292.

De Jong, E., and J.R. Bettany. 1986. The versatile soil moisture budget - Basic version. Department of Soil Science, University of Saskatchewan, Saskatoon, SK.

Denmead, O.T. 1979. Chamber systems for measuring nitrous oxide emission from soils in the field. Soil Sci. Soc. Am. J. 43:89-95.

Denmead, O.T., J.R. Freney, and J.R. Simpson. 1979. Studies of nitrous oxide emission from a grass sward. Soil Sci. Soc. Am. J. 43:726-728.

Denmead, O.T., and M.R. Raupach. 1993. Methods of measuring atmospheric gas transport in agricultural and forest systems. p. 19-44. *In* L.A. Harper, A.R. Mosier, J.M. Duxbury, and D.E. Rolston (eds.) Agricultural ecosystem effects on trace gases and global climate change. ASA Spec. Publ. 55. ASA, CSSA, and SSSA, Madison, Wisconsin.

Duxbury, J.M., L.A. Harper, and A.R. Mosier. 1993. Contributions of agroecosystems to global climate change. p. 1-18. *In* L.A. Harper, A.R. Mosier, J.M. Duxbury, and D.E. Rolston (eds.) Agricultural ecosystem effects on trace gases and global climate change. ASA Spec. Publ. 55. ASA, CSSA, and SSSA, Madison, Wisconsin.

Duxbury, J.M., and P.K. McConnaughey. 1986. Effect of fertilizer source on denitrification and nitrous oxide emission in a maize field. Soil Sci. Soc. Am. J. 50:644-648.

Eichner, M.J. 1990. Nitrous oxide emissions from fertilized soils: Summary of available data. J. Environ. Qual. 19:272-280.

Elkins, J.W., and R. Rossen. 1989. Summary report 1988: Geophysical monitoring for climatic change. NOAA, ERL, Boulder, Colorado.

Elliott, J.A., and E. de Jong. 1992. Quantifying denitrification on a field scale in hummocky terrain. Can. J. Soil Sci. 72:21-29.

Estes, J.E., E.J. Hajic, and L.R. Tinney. 1983. Fundamentals of image analysis: Analysis of visible and thermal infrared data. p. 1039-1040. *In* R.N. Colwell

(ed.) Manual of remote sensing. Am. Soc. Photogram. Rem. Sens. Falls Church, Virginia.

Firestone, M.K. 1982. Biological denitrification. p. 289-326. *In* F.J. Stevenson (ed.) Nitrogen in agricultural soils. ASA, Madison, Wisconsin.

Firestone, M.K., and E.A. Davidson. 1989. Microbiological basis of NO and N_2O production and consumption in soil. p. 7-21. *In* M.O. Andreae and D.S. Schimel (eds.) Exchange of trace gases between terrestrial ecosystems and atmosphere. John Wiley & Sons, Chichester, England.

Firestone, M.K., R.B. Firestone, and J.M. Tiedje. 1980. Nitrous oxide from soil denitrification: Factors controlling its biological production. Science 208:749-751.

Focht, D.D. 1974. The effect of temperature, pH, and aeration on the production of nitrous oxide and gaseous nitrogen - A zero order kinetic model. Soil Sci. 118:173-179.

Focht, D.D. 1992. Diffusional constraints on microbial processes in soil. Soil Sci. 154:300-307.

Folorunso, O.A., and D.E. Rolston. 1984. Spatial variability of field-measured denitrification gas fluxes. Soil Sci. Soc. Am. J. 48:1214-1219.

Fung, T., and E. LeDrew. 1987. Application of principal components analysis to change detection. Photogram. Engin. Rem. Sens. 53:1649-1658.

Gardner, W.H. 1986. Water content. p. 493-541 *In* A. Klute (ed.) Methods of soil analysis: Part I, Physical and mineralogical methods. 2nd ed. Agronomy No. 9. ASA, Madison, Wisconsin.

Goodroad, L.L., and D.R. Keeney. 1984. Nitrous oxide emission from forest, marsh, and prairie ecosystems. J. Environ. Qual. 13:448-452.

Groffman, P.M. 1991. Ecology of nitrification and denitrification in soil evaluated at scales relevant to atmospheric chemistry. p. 201-217. *In* J.E. Rogers and W.B. Whitman (eds.) Microbial production and consumption of greenhouse gases: Methane, nitrogen oxides, and halomethanes. Am. Soc. Microbiol., Washington, DC.

Groffman, P.M., C.W. Rice, and J.M. Tiedje. 1993a. Denitrification in a tallgrass prairie landscape. Ecology 74:855-862.

Groffman, P.M., and J.M. Tiedje. 1989a. Denitrification in north temperate forest soils: Spatial and temporal patterns at the landscape and seasonal scales. Soil Biol. Biochem. 21:613-620.

Groffman, P.M., and J.M. Tiedje. 1989b. Denitrification in north temperate forest soils: Relationship between denitrification and environmental factors at the landscape scale. Soil Biol. Biochem. 21:621-626.

Groffman, P.M., D.R. Zak, S. Christensen, A.R. Mosier, and J.M. Tiedje. 1993b. Early spring nitrogen dynamics in a temperate forest landscape. Ecology 74:1579-1585.

Gupta, R.P. 1991. Remote sensing geology. Springer-Verlag, New York. 356p.

Hahn, J. and P.J. Crutzen. 1981. The role of fluxed nitrogen in atmospheric photochemistry. Proc. R. Soc. London. B196:219-240.

Hammond, A.L. 1990. World resources 1990-91. A report by The World Resources Institute. Oxford University Press, Oxford, England. 383 p.

Harris, R.F. 1982. Energetics of nitrogen transformations. p. 833-890. *In* F.J. Stevenson (ed.) Nitrogen in agricultural soils. ASA, Madison, Wisconsin.

Henderson, T.L., M.F. Baumgardner, D.P. Franzmeier, D.E. Scott, and D.C. Coster. 1992. High dimensional reflectance analysis of soil organic matter. Soil Sci. Soc. Am. J. 56:865-872.

Hillel, D. 1982. Introduction to soil physics. 2nd ed. Academic Press, London. 364p.

Houghton J.T., B.A. Callander, and S.K. Varney. 1992. Climate change 1992. The supplementary report to the IPCC Scientific Assessment. Cambridge University Press, Cambridge, England.

Hutchinson, G.L., and E.A. Brams. 1992. NO versus N_2O emissions from an NH_4^+-amended Bermuda grass pasture. J. Geophys. Res. 97:9889-9896.

Hutchinson, G.L., and E.A. Davidson. 1993. Processes for production and consumption of gaseous nitrogen oxides in soil. p. 79-93. *In* L.A. Harper, A.R. Mosier, J.M. Duxbury, and D.E. Rolston (eds.) Agricultural ecosystem effects on trace gases and global climate change. ASA Spec. Publ. 55. ASA, CSSA, and SSSA, Madison, Wisconsin.

Hutchinson, G.L., and G.P. Livingston. 1993. Use of chamber systems to measure trace gas fluxes. p. 63-78. *In* L.A. Harper, A.R. Mosier, J.M. Duxbury, and D.E. Rolston (eds.) Agricultural ecosystem effects on trace gases and global climate change. ASA Spec. Publ. 55. ASA, CSSA, and SSSA, Madison, Wisconsin.

Hutchinson, G.L., and A.R. Mosier. 1979. Nitrous oxide emission from an irrigated cornfield. Science 205:1125-1127.

Hutchinson, G.L., and A.R. Mosier. 1981. Improved soil cover method for field measurement of nitrous oxide fluxes. Soil Sci. Soc. Am. J. 45:311-316.

Indorante, S.J., L.R. Follmer, R.D. Hammer, and P.G. Koenig. 1990. Particle-size analysis by a modified pippette procedure. Soil Sci. Soc. Am. J. 54:560-563.

Intergovernmental Panel on Climate Change. 1990. Climate change: The intergovernmental panel on climate change (IPCC) scientific assessment. Cambridge University Press, Cambridge, England.

Jensen, J. R. 1986. Introductory digital image processing : A remote sensing perspective. Prentice-Hall Publishing Company, Englewood Cliffs, New Jersey.

Keller, M. 1994. Controls on soil-atmosphere fluxes of nitrous oxide and methane: effects of tropical deforestation. p. 123-138. *In* R.G. Zepp (ed.) Biogenic emissions and environmental effects of climate change. John Wiley & Sons, Chichester, England.

Keller, M., W.A. Kaplan, and S.C. Wofsy. 1986. Emissions of N_2O, CH_4, and CO_2 from tropical soils. J. Geophys. Res. 91:11791-11802.

Khalil, M.A.K., and R.A. Rasmussen. 1992. The global sources of nitrous oxide. J. Geophys. Res. 97:14651-14660.

Kimball, B.A. 1983. Canopy gas exchange: Gas exchange with soil. p. 215-226. *In* H.M. Taylor, W.R. Jordan, and T.R. Sinclair (eds.) Limitations to efficient water use in crop production. ASA, CSSA, and SSSA, Madison, Wisconsin.

Kimball, B.A., and E.R. Lemon. 1972. Theory of soil air movement due to pressure fluctuations. Agric. Meteorol. 9:163-181.

Klute, A. 1986. Water retention: Laboratory methods. p. 635-660. *In* A. Klute (ed.) Methods of soil analysis: Part I, Physical and mineralogical methods. 2nd ed. Agronomy No. 9. ASA, Madison, Wisconsin.

Knowles, R. 1982. Denitrification. Microbiol. Rev. 46:43-70.

Krogman, K.K., and E.H. Hobbs. 1976. Scheduling irrigation to meet crop demands. Agriculture Canada, Ottawa, ON. Publ. 1590. 18p.

Leffelaar, P.A., and W.W. Wessel. 1988. Denitrification in a homogeneous closed system: Experiment and simulation. Soil Sci. 146:335-349.

Li, C., S.E. Frolking, and T.A. Frolking. 1992. A model for nitrous oxide evolution from soil driven by rainfall events: I. Model structure and sensitivity. J. Geophys. Res. 97:9759-9776.

Linn, D. M., and J. W. Doran. 1984. Effect of water-filled pore space on carbon dioxide and nitrous oxide production in tilled and nontilled soils. Soil Sci. Soc. Am. J. 48:1267-1272.

Livingston, G.P., and G.L. Hutchinson. 1995. Enclosure-based measurement of trace gas exchange: Applications and sources of error. p. 14-51. *In* P.A. Matson and R.C. Harriss (eds.) Biogenic trace gases: Measuring emissions from soil and water (Methods in ecology series). Blackwell Sci. Publ., Cambridge, Massachussets.

Martikainen, P.J. 1985. Nitrous oxide emission associated with autotrophic ammonium oxidation in acid coniferous forest soil. Appl. Environ. Microbiol. 50:1519-1525.

Matson, P.A., and R.C. Harriss. 1995. Trace gas exchange in an ecosystem context: Multiple approaches to measurement and analysis. p. 1-13. *In* P.A. Matson and R.C. Harriss (eds.) Biogenic trace gases: Measuring emissions from soil and water (Methods in ecology series). Blackwell Sci. Publ., Cambridge, Massachussets.

Matson, P.A., and P.M. Vitousek. 1987. Cross-system comparisons of soil nitrogen transformations and nitrous oxide flux in tropical forest ecosystems. Global Biogeochem. Cycles 1:163-170.

Matson, P.A., and P.M. Vitousek. 1990. Ecosystem approach to a global nitrous oxide budget. BioScience 40:667-672.

Matson, P.A., P.M. Vitousek, and D.S. Schimel. 1989. Regional extrapolation of trace gas flux based on soils and ecosystems. p. 97-108. *In* M.O. Andreae and

D.S. Schimel (eds.) Exchange of trace gases between terrestrial ecosystems and the atmosphere. Dahlem Workshop Report, John Wiley and Sons, Chichester, England.

Matson, P.A., C. Volkmann, K. Coppinger, and W.A. Reiners. 1991. Annual nitrous oxide flux and soil nitrogen characteristics in sagebrush steppe ecosystems. Biogeochemistry 14:1-12.

Matthias, A.D., A.M. Blackmer, and J.M. Bremner. 1980. A simple chamber technique for field measurement of emissions of nitrous oxide from soils. J. Environ. Qual. 9:251-256.

Matthias, A.D., D.N. Yarger, and R.S. Weinbeck. 1978. A numerical evaluation of chamber methods for determining gas fluxes. Geophys. Res. Lett. 5:765-768.

McClaugherty, C.A., J. Pastor, J.D. Aber, and J.N. Melillo. 1985. Forest litter decomposition in relation to soil nitrogen dynamics and litter quality. Ecology 66:266-275.

McConnaughey, P.K., and D.R. Bouldin. 1985. Transient microsite model of denitrification: I. Model development. Soil Sci. Soc. Am. J. 49:886-891.

McElroy, M.B., and S.C. Wofsy. 1986. Tropical forests: Interaction with the atmosphere. p. 33-60. *In* G.T. Prance (ed.) Tropical rain forests and the world atmosphere. Westview Press, Boulder, Colorado.

McKenney, D.J., K.F. Shuttleworth, and W.I. Findlay. 1980. Nitrous oxide evolution rates from fertilized soil: Effects of applied nitrogen. Can. J. Soil Sci. 60:429-438.

Mosier, A.R. 1989. Chamber and isotope techniques. p. 175-187. *In* M.O. Andreae and D.S. Schimel (eds.) Exchange of trace gases between terrestrial ecosystems and atmosphere. John Wiley and Sons, Chichester, England.

Mosier, A.R. 1994. Nitrous oxide emissions from agricultural soils. Fert. Res. 37:191-200.

Mosier, A.R., W.D. Guenzi, and E.E. Schweizer. 1986. Soil losses of dinitrogen and nitrous oxide from irrigated crops in Northeastern Colorado. Soil Sci. Soc. Am. J. 50:344-348.

Mosier, A.R., and G.L. Hutchinson. 1981. Nitrous oxide emissions from cropped fields. J. Environ. Qual. 10:169-173.

Mosier, A.R., G.L. Hutchinson, B.R. Sabey, and J. Baxter. 1982. Nitrous oxide emissions from barley plots treated with ammonium nitrate or sewage sludge. J. Environ. Qual. 11:78-81.

Mosier, A.R., W.J. Parton and G.L. Hutchinson. 1983. Modelling nitrous oxide evolution from cropped and native soils. p. 229-241. *In* R. Hallberg (ed.) Environmental Biogeochemistry. Ecol. Bull. 35. Stockholm.

Mosier, A.R., W.J. Parton, D.W. Valentine, D.S. Ojima, D.S. Schimel, and J.A. Delgado. 1996. CH_4 and N_2O fluxes in the Colorado shortgrass steppe: 1. Impact of landscape and nitrogen addition. Global Biogeochem. Cycles 10:387-399.

Mosier, A.R., D. Schimel, D. Valentine, K. Bronson, and W. Parton. 1991. Methane and nitrous oxide fluxes in native, fertilized and cultivated grasslands. Nature 350:330-332.

Mosier, A.R., M. Stillwell, W.J. Parton and R.G. Woodmansee. 1981. Nitrous oxide emissions from a native short grass prairie. Soil Sci. Soc. Am. J. 45:617-619.

Mummey, D.L., J.L. Smith, and H. Bolton Jr. 1994. Nitrous oxide flux from a shrub-steppe ecosystem: Sources and regulation. Soil Biol. Biochem. 26:279-286.

Myrold, D.D. 1988. Denitrification in ryegrass and winter wheat cropping systems of western Oregon. Soil Sci. Soc. Am. J. 52:412-416.

Nelson, D.W. 1982. Gaseous losses of nitrogen other than through denitrification. p. 327-363. *In* F.J. Stevenson (ed.) Nitrogen in agricultural soils. ASA, Madison, Wisconsin.

O'Neill, R.V. 1988. Hierarchy theory and global change. p. 29-46. *In* T. Rosswall, R.G. Woodmansee, and P. Risser (eds.) Scales and global change: Spatial and temporal variability in biospheric and geospheric processes. John Wiley and Sons, New York.

Parkin, T.B. 1987. Soil microsites as a source of denitrification variability. Soil Sci. Soc. Am. J. 51:1194-1199.

Parkin, T.B. 1993. Spatial variability of microbial processes in soil - A review. J. Environ. Qual. 22:409-417.

Parkin, T.B., and J.A. Robinson. 1989. Stochastic models of soil denitrification. Appl. Environ. Microbiol. 55:72-77.

Parkin, T.B., J.L. Starr, and J.J. Meisinger. 1987. Influence of sample size on measurement of soil denitrification. Soil Sci. Soc. Am. J. 51:1492-1501.

Parsons, L.L., R.E. Murray, and M.S. Smith. 1991. Soil denitrification dynamics: Spatial and temporal variations of enzyme activity, populations, and nitrogen gas loss. Soil Sci. Soc. Am. J. 55:90-95.

Parton, W.J., A.R. Mosier, D.S. Ojima, D.W. Valentine, D.S. Schimel, K. Weier, and A.E. Kulmala. 1996. Generalized model for N_2 and N_2O production from nitrification and denitrification. Global Biogeochem. Cycles 10:401-412.

Parton, W.J., A.R. Mosier, and D.S. Schimel. 1988a. Dynamics of C, N, P, and S in grassland soils: A model. Biogeochemistry 5:109-131.

Parton, W.J., A.R. Mosier, and D.S. Schimel. 1988b. Rates and pathways of nitrous oxide production in a shortgrass steppe. Biogeochemistry 6:45-58.

Pastor, J., J.D. Aber, and C.A. McClaugherty. 1982. Geology, soils and vegetation of Blackhawk Island, Wisconsin. Am. Midland Nat. 108:266-277.

Pastor, J., J.D. Aber, C.A. McClaugherty, and J.M. Melillo. 1984. Aboveground production and N and P cycling along a nitrogen mineralization gradient on Blackhawk Island, Wisconsin. Ecology 65:256-268.

Pearman, G.I., D. Etheridge, F. DeSilva, and P.J. Fraser. 1986. Evidence of changing concentrations of atmospheric carbon dioxide, nitrous oxide, and methane from air bubbles in antarctic ice. Nature 320:248-250.

Pennock, D.J., and and D.F. Acton. 1989. Hydrological and sedimentological influences in Boroll catenas, central Saskatchewan. Soil Sci. Soc. Am. J. 53:904-910.

Pennock, D.J., D.W. Anderson, and E. de Jong. 1994. Landscape-scale changes in indicators of soil quality due to cultivation in Saskatchewan, Canada. Geoderma 64:1-19.

Pennock, D. J., C. van Kessel, R. E. Farrell, and R. A. Sutherland. 1992. Landscape-scale variations in denitrification. Soil Sci. Soc. Am. J. 56:770-776.

Pennock, D. J., B. J. Zebarth, and E. de Jong. 1987. Landform classification and soil distribution in hummocky terrain, Saskatchewan, Canada. Geoderma 40:297-315.

Peterman, R.M. 1990. Statistical power analysis can improve fisheries research and management. Can. J. Fish. Aquatic Sci. 47:2-15.

Poth, M., and D.D. Focht. 1985. ^{15}N kinetic analysis of N_2O production of *Nitrosomonas europaea* : An examination of nitrifier denitrification. Appl. Environ. Microbiol. 49:1134-1141.

Potter, C.S., P.A. Matson, P.M. Vitousek, and E.A. Davidson. 1996. Process modeling of controls on nitrogen trace gas emissions from soils worldwide. J. Geophys. Res. 101:1361-1377.

Prinn, R., D. Cunnold, R. Rasmussen, P. Simmonds, F. Alyea, A. Crawfrod, P. Fraser, and R. Rosen. 1990. Atmospheric emissions and trends of nitrous oxide deduced from 10 years of ALE-GAGE data. J. Geophys. Res. 95:18369-18385.

Reiners, W.A., L.L. Strong, P.A. Matson, I.C. Burke, and D.S. Ojima. 1989. Estimating biogeochemical fluxes across sagebrush-steppe landscapes with thematic mapper imagery. Rem. Sens. Environ. 28:121-129.

Ritchie, G.A.F., and D.J.D. Nicholas. 1972. Identification of the sources of nitrous oxide produced by oxidative and reductive processes from *Nitrosomonas europaea*. Biochem. J. 126:1181-1191.

Robertson, G.P. 1989. Nitrification and denitrification in humid tropical ecosystems: Potential controls on nitrogen retention. p. 55-59. *In* J. Procter (ed.) Mineral nutrients in tropical forest and savanna ecosystems. Blackwell Sci. Publ., Oxford, England.

Robertson, G.P. 1993. Fluxes of nitrous oxide and other nitrogen trace gases from intensively managed landscapes: A global perspective. p. 95-108. *In* L.A. Harper, A.R. Mosier, J.M. Duxbury, and D.E. Rolston (eds.) Agricultural ecosystem effects on trace gases and global climate change. ASA Spec. Publ. 55. ASA, CSSA, and SSSA, Madison, Wisconsin.

Robertson, G.P., M.A. Huston, F.C. Evans, and J.M. Tiedje. 1988. Spatial variability in a successional plant community: Patterns of nitrogen availability. Ecology 69:1517-1524.

Robertson, G.P., and J.M. Tiedje. 1984. Denitrification and nitrous oxide production in successional and old-growth Michigan forest. Soil Sci. Soc. Am. J. 48:383-389.

Rodhe, H. 1990. A comparison of the contribution of various gases to the greenhouse effect. Science 248:1217-1219.

Rolston, D.E., A.N. Sharpley, D.W. Toy, and F.E. Broadbent. 1982. Field measurement of denitrification: III. Rates during irrigation cycles. Soil Sci. Soc. Am. J. 46:289-296.

Ryden, J.C. 1981. N_2O exchange between a grassland soil and the atmosphere. Nature 292:235-237.

Ryden, J.C., and L.J. Lund. 1980. Nature and extent of directly measured denitrification losses from some irrigated vegetable crop production units. Soil Sci. Soc. Am. J. 44:505-511.

Ryden, J.C., L.J. Lund, and D.D. Focht. 1978. Direct in-field measurement of nitrous oxide flux from soil. Soil Sci. Soc. Am. J. 42:731-738.

Salomonson, V.V., P.L. Smith, A.B. Pink, W.C. Webb, and T.J. Lynch. 1980. An overview of progress in the design and implementation of Landsat D systems. I.E.E.E. Trans. Geosci. Rem. Sens. 18:137.

Schimel, D.S., B.H. Braswell, E.A. Holland, R. McKeown, D.S. Ojima, T.H. Painter, W.J. Parton, and A.R. Townsend. 1994. Climatic, edaphic, and biotic controls over storage and turnover of carbon in soils. Global Biogeo. Cyc. 8:279-293.

Schimel, D.S., D.C. Coleman, and K.A. Horton. 1985a. Soil organic matter dynamics in paired rangeland and cropland toposequences in North Dakota. Geoderma 36:201-214.

Schimel, J.P., L.E. Jackson, and M.K. Firestone. 1989. Spatial and temporal effects on plant-microbial competition for inorganic nitrogen in a California annual grassland. Soil Biol. Biochem. 21:1059-1066.

Schimel, D.S., and C.S. Potter. 1995. Process modelling and spatial extrapolation. p. 358-383. *In* P.A. Matson, and R.C. Harriss (eds.) Biogenic trace gases: Measuring emissions from soil and water (Methods in ecology series). Blackwell Sci. Publ., Cambridge, Massachussets.

Schimel, D.S., S. Simkins, T. Rosswall, A.R. Mosier, and W.J. Parton. 1988. Scale and the measurement of nitrogen gas fluxes from terrestrial ecosystems. p. 179-193. *In* T. Rosswall, R.G. Woodmansee, and P.G. Risser (eds.) Scales and global change. SCOPE 35, John Wiley, New York.

Schimel, D.S., M.A. Stillwell, and R.G. Woodmansee. 1985b. Biogeochemistry of C, N and P in a soil catena of the shortgrass steppe. Ecology 66:276-282.

Schwab, G.O., D.D. Fangmeier, W.J. Elliott, and R.K. Frevert. 1993. Soil and water conservation engineering. 4th ed. John Wiley and Sons Inc., New York. 507p.

Seiler, W. and R. Conrad. 1981. Field measurements of natural and fertilizer-induced N_2O release rates from soils. J. Air Pollut. Control Assoc. 31:767-772.

Sexstone, A. J., T. B. Parkin, and J. M. Tiedje. 1985. Temporal response of soil denitrification rates to rainfall and irrigation. Soil Sci. Soc. Am. J. 49:99-103.

Sheffield, C. 1985. Selecting band combinations from multispectral data. Photogram. Engin. Rem. Sens. 51:681-687.

Shine, K.P., R.G. Derwent, D.J. Wuebbles, and J.J. Morcrette. 1990. Radiative forcing of climate. p. 47-68. *In* J.T. Houghton, G.J. Jenkins, and J.J. Ephramus (eds.) Climate change: The IPCC scientific assessment. Cambridge University Press, Cambridge, England.

Siegel, S., and N.J. Castellan Jr. 1988. Nonparametric statistics for the behavioral sciences. 2nd ed. McGraw-Hill, New York. 399p.

Smith, C.J. and P.M. Chalk. 1980. Fixation and loss of nitrogen during transformation of nitrite in soils. Soil Sci. Soc. Am. J. 44:288-291.

Smith, J.L., J.J. Halvorson, and H. Bolton Jr. 1994. Spatial relationships of soil microbial biomass and C and N mineralization in a semi-arid shrub-steppe ecosystem. Soil Biol. Biochem. 26:1151-1159.

Smith, K.A. 1990. Anaerobic zones and denitrification in soil: Modelling and meaurement. p. 229-244. *In* N.P. Revsbech and J. Sorensen (eds.) Denitrification in soil and sediment. Plenum, New York.

Smith, K.A., H. Clayton, J.R.M. Arah, S. Christensen, P. Ambus, D. Fowler, K.J. Hargreaves, U. Skiba, G.W. Harris, F.G. Wienhold, L. Klemedtsson, and B. Galle. 1994. Micrometeorological and chamber methods for measurement of nitrous oxide fluxes between soils and the atmosphere: Overview and conclusions. J. Geophys. Res. 99:16541-16548.

Smith, W.N., R.L. Desjardins, P. Rochette, M.D. Corre, C. van Kessel, D.J. Pennock, and E. Pattey. 1996. Testing the DeNitrification-Decomposition model to predict N_2O emissions at two experimental sites in Canada. Presented at the Greenhouse Gases Workshop in University of Guelph, ON.

Spiridonov, H., R. Kuncheva, and E. Misheva. 1981. Results and conclusions from soil and vegetation reflectance coefficient measurements. Adv. Space Res. 1:111-114.

Thorton, F.C., and R.J. Valente. 1996. Soil emissions of nitric oxide and nitrous oxide from no-till corn. Soil Sci. Soc. Am. J. 60:1127-1133.

Tiedje, J.M., R.B. Firestone, M.K. Firestone, M.R. Betlach, H.F. Kaspar and J. Sorensen. 1981. Use of nitrogen-13 in studies of denitrification. p. 295-315. *In*

K.A. Krohn and J.W. Root (eds.) Recent developments in biological and chemical research with short-lived isotopes. Advances in Chemistry. Am. Chem. Soc., Washington.

Tiedje, J.M., A.J. Sexstone, D.D. Myrold and J.A. Robinson. 1982. Denitrification: Ecological niches, competition and survival. Antonie van Leeuwenhoek 48:569-583.

Townshend, J.R.G. 1984. Agricultural land-cover discrimination using thematic mapper spectral bands. Int. J. Rem. Sens. 5:681-698.

Trolier, L. J., and W.R. Philipson. 1986. Visual analysis of Landsat thematic mapper images for hydrologic land use and cover. Photogram. Engin. Rem. Sens. 52:1531-1538.

Van Kessel, C., D. J. Pennock, and R. E. Farrell. 1993. Seasonal variations in denitrification and nitrous oxide evolution at the landscape scale. Soil Sci. Soc. Am. J. 57:988-995.

Verhagen, F.J.M., and H.J. Laanbroek. 1991. Competition for ammonium between nitrifying and heterotrophic bacteria in dual energy-limited chemostats. Appl. Environ. Microbiol. 57:3255-3263.

Vermes, J. F., and D. D. Myrold. 1992. Denitrification in forest soils of Oregon. Can. J. For. Res. 22:504-512.

Walley, F.L., C. van Kessel, and D.J. Pennock. 1996. Landscape-scale variability of N mineralization in forest soils. Soil Biol. Biochem. 28:383-391.

Watson, R.T., H. Rodhe, H. Oeschger, and U. Siegenthaler. 1990. Greenhouse gases and aerosols. p. 7-40. *In* J.T. Houghton, G.J. Jenkins, and J.J. Ephramus (eds.) Climate change: The IPCC scientific assessment. Cambridge University Press, Cambridge, England.

Weiss, R.F. 1981. The temporal and spatial distribution of tropospheric nitrous oxide. J. Geophys. Res. 86:7185-7195.

Weiss, R.F., and B.A. Price. 1980. Nitrous oxide solubility in water and seawater. Mar. Chem. 8:347-359.

Appendix 1. Exploratory data analysis of N_2O emission activity.

Appendix 1.1. Exploratory data analysis for N_2O emission activity from May 1993 to April 1994 in the clay loam, unfertilized canola site.

Sampling date	Median	Mean	Min.	Max.	C.V.	Skewness	No. extreme outliers		No. of sampling points
	<----- μg N_2O-N m^{-2} d^{-1} ----->				(%)		Shoulder	Footslope	
17May93 (land preparation)	0	34	0	886	380	5.43	6	15	91
12Jun93 (first day of precip. following rosetting)	0	4	0	81	276	4.25	7	13	100
13Jun93 (second day of precip. following rosetting)	25	41	0	312	123	3.22	1	1	60
14Jun93 (third day of precip. following rosetting)	56	117	4	2664	302	6.75	2	4	100
15Jun93 (fourth day of precip. following rosetting)	47	114	27	2436	233	7.26	4	5	100
26Jun93 (first day of precip. following budding)	57	114	22	1534	210	5.04	0	3	49
27Jun93 (second day of precip. following budding)	76	114	48	777	100	4.57	0	3	49
6Jul93 (first day of precip. following flowering)	57	255	2	4835	292	5.39	0	5	48
7Jul93 (second day of precip. following flowering)	52	176	0	2995	253	5.70	0	5	48
19Aug93 (precipitation following late pod fill)	40	37	0	76	54	3.50	0	0	20
21Oct93 (after harvest)	28	36	0	293	133	3.72	0	2	49
25Nov93 (onset of frost)	0	7	0	42	164	1.49	0	0	28
17Mar94	92	2057	0	19750	243	2.98	1	2	20
24Mar94	0	734	0	7257	250	2.89	0	3	20
29Mar94	62	1529	0	19955	293	4.06	1	2	20
5Apr94	0	2840	0	23525	232	2.48	0	6	20
9Apr94	47	1944	0	16114	208	2.50	0	4	20
18Apr94	0	352	0	5669	307	4.47	2	4	20
25Apr94	5	742	0	12306	325	4.34	0	3	20

Appendix 1.2. Exploratory data analysis for N_2O emission activity from July 1993 to April 1994 in the clay loam, fallow site.

Sampling date	Median	Mean	Min.	Max.	C.V.	Skewness	No. extreme outliers		No. of sampling points
							Shoulder	Footslope	
	<----- μg N_2O-N m^{-2} d^{-1} ----->				(%)				
7Jul93	46	227	8	4059	322	5.16	0	3	31
19Aug93	47	101	26	1263	218	5.03	1	2	32
21Oct93	21	27	5	77	70	1.38	0	0	20
25Nov93	2	4	0	12	116	0.78	0	0	20
17Mar94	66	8891	0	90862	262	3.01	0	4	20
24Mar94	0	2972	0	38294	300	3.71	0	3	20
29Mar94	126	1531	0	10623	196	2.28	0	3	20
5Apr94	0	209	0	1757	246	2.71	1	3	20
9Apr94	0	831	0	10307	310	3.29	0	3	20
18Apr94	0	34	0	459	309	3.86	1	2	20
25Apr94	0	8	0	93	300	3.13	0	2	20

Appendix 1.3. Exploratory data analysis for N_2O emission activity from May 1993 to April 1994 in the clay loam, pasture site.

Sampling date	Median	Mean	Min.	Max.	C.V.	Skewness	No. extreme outliers		No. of sampling points
	<----- μg N_2O-N m^{-2} d^{-1} ----->				(%)		Shoulder	Footslope	
28May93	0	2	0	42	404	5.10	2	6	87
26Jun93	50	53	10	146	47	1.34	0	1	44
27Jun93	15	18	6	60	57	1.95	0	1	44
6Jul93	40	56	16	238	79	2.60	0	3	44
21Oct93	0	9	0	90	273	3.25	1	2	20
25Nov93	0	0	0	0	0	0.00	0	0	20
17Mar94	0	6	0	55	266	2.55	2	1	20
24Mar94	0	30	0	276	117	1.14	0	0	20
29Mar94	0	35	0	883	187	2.44	1	1	20
5Apr94	5	77	0	500	286	2.91	3	1	20
9Apr94	0	67	0	770	285	3.26	3	1	20
18Apr94	108	953	0	12493	290	4.22	1	0	20
25Apr94	1	194	0	1840	260	2.88	0	3	20

Appendix 1.4. Exploratory data analysis for N_2O emission activity from May 1994 to May 1995 in the clay loam, fertilized wheat site.

Sampling date	Median	Mean	Min.	Max.	C.V.	Skewness	No. extreme outliers		No. of sampling points
							Shoulder	Footslope	
	<-----	$\mu g\ N_2O\text{-}N\ m^{-2}\ d^{-1}$			---->	(%)			
18May94 (after fertilization at seeding)	0	1123	0	10080	256	2.79	0	2	20
23May94 (seedling growth)	50	4506	0	53967	284	3.54	0	2	20
14Jun94 (after fertilization at seedling stage)	658	3628	0	33286	213	3.37	0	2	20
16jun94 (tillering)	2299	6137	0	38646	154	2.62	0	2	20
30Jun94 (tillering, stem elongation)	1375	2098	252	5861	81	0.96	0	0	20
8Jul94 (stem elongation)	1013	1384	194	4171	92	1.31	0	0	20
19Jul94 (inflorescence)	1358	2919	86	21994	167	3.47	0	1	20
30Jul94 (milk)	318	370	0	1455	90	1.86	0	0	20
8Aug94 (dough)	128	396	0	2560	174	2.38	0	3	20
18Aug94 (ripening)	110	213	0	783	121	0.99	0	0	20
29Aug94 (harvesting)	127	267	0	1676	151	2.46	0	1	20
20Sep94	0	49	0	324	183	2.26	0	2	20
4Oct94	0	0	0	0	0	0	0	0	20
8Nov94	0	1	0	29	448	4.47	0	1	20
14Mar95	37	39	0	108	82	0.49	0	0	20
21Mar95	35	33	0	119	97	0.98	0	0	20
13Apr95	0	286	0	3207	267	3.53	2	0	20
18Apr95	650	3686	0	31201	215	2.92	2	1	20
21Apr95	792	7555	11	109244	328	4.26	0	2	20
26Apr95	600	7713	0	104139	302	4.13	0	3	20
3May95	777	1908	0	14542	203	2.86	0	3	20
12May95	22	2948	0	53388	404	4.43	1	3	20
19May95	65	1766	0	19333	264	3.27	0	3	20

Appendix 1.5. Exploratory data analysis for N_2O emission activity from May 1994 to May 1995 in the clay loam, pasture site.

Sampling date	Median	Mean	Min.	Max.	C.V.	Skewness	No. extreme outliers		No. of sampling points
	<----- $\mu g\ N_2O\text{-}N\ m^{-2}\ d^{-1}$ ----->				(%)		Shoulder	Footslope	
18May94	52	168	0	612	132	1.13	0	0	20
23May94	18	45	0	425	215	3.58	1	1	20
14Jun94	21	37	0	248	156	2.93	0	1	20
16jun94	22	50	0	240	136	1.50	0	0	20
30Jun94	60	105	0	428	118	2.29		1	10
8Jul94	68	65	0	150	80	-0.02		0	10
19Jul94	17	112	0	1044	218	3.32	0	2	20
30Jul94	41	178	0	1277	219	3.07		1	10
8Aug94	36	31	0	77	89	0.21		0	10
18Aug94	6	22	0	82	132	1.19	0	0	20
29Aug94	15	15	0	25	52	-0.07		0	10
20Sep94	0	4	0	49	294	3.53	1	2	20
4Oct94	0	13	0	74	200	2.03		1	10
8Nov94	0	0	0	0	0	0		0	10
14Mar95	0	2	0	14	234	2.57	0	2	20
21Mar95	1	17	0	131	210	2.58	1	0	20
13Apr95	2	10	0	85	192	3.49	1	0	20
18Apr95	12	61	0	432	181	2.60	1	0	20
21Apr95	214	548	0	4649	200	3.46	1	0	20
26Apr95	51	107	0	358	122	0.99	0	0	20
3May95	13	118	0	935	200	2.81	0	1	20
12May95	0	8	0	62	246	2.59	2	1	20
19May95	52	168	0	612	132	1.14	0	0	20

Appendix 1.6. Exploratory data analysis for N_2O emission activity from May 1994 to May 1995 in the fine sandy loam, fertilized canola site.

Sampling date	Median	Mean	Min.	Max.	C.V.	Skewness	No. extreme outliers		No. of sampling points
							Shoulder	Footslope	
	<-----	$\mu g\ N_2O\text{-}N\ m^{-2}\ d^{-1}$			---->	(%)			
18May94	0	7263	0	112596	349	4.18	0	3	20
23May94	449	4773	0	45115	222	3.26	0	2	20
14Jun94	664	7160	0	82359	265	3.69	0	3	20
16jun94	487	6435	0	34779	173	1.81	0	2	20
30Jun94 (after fertilization at seeding)	2208	5633	56	29490	137	2.01	1	2	20
8Jul94 (rosetting)	504	3429	5	26833	208	2.78	0	2	20
19Jul94 (budding)	4496	13966	0	173717	86	4.31	0	1	20
30Jul94 (flowering))	789	3884	0	31230	202	2.84	0	3	20
8Aug94 (flowering)	483	1961	4	14887	183	2.93	0	2	20
18Aug94 (ripening)	151	348	0	2326	162	2.68	0	1	20
29Aug94 (ripening)	114	1052	0	18833	398	4.46	0	2	20
20Sep94 (after harvest)	0	38	0	679	398	4.42	0	3	20
4Oct94	0	399	0	5969	353	4.07	1	3	20
8Nov94	0	28	0	354	337	3.69	0	3	20
14Mar95	0	0	0	4	443	4.46	1	1	20
21Mar95	0	3	0	24	211	2.59	1	1	20
13Apr95	0	831	0	7428	238	2.75	4	0	20
18Apr95	799	2737	0	15797	172	2.10	1	2	20
21Apr95	482	8005	0	57749	207	2.15	0	4	20
26Apr95	229	11597	0	81671	192	2.16	0	4	20
3May95	100	13232	0	199641	106	4.26	0	4	20
12May95	0	2468	0	17148	209	2.00	0	4	20
19May95	54	1015	0	5941	162	1.86	0	2	20

Appendix 1.7. Exploratory data analysis for N_2O emission activity from June 1994 to May 1995 in the sandy, fertilized oat site.

Sampling date	Median	Mean	Min.	Max.	C.V.	Skewness	No. extreme outliers		No. of sampling points
	<----- $\mu g\ N_2O\text{-}N\ m^{-2}\ d^{-1}$ ----->				(%)		Shoulder	Footslope	
30Jun94 (after fertilization at seeding)	272	394	0	2731	155	3.20	1	0	20
8Jul94 (tillering)	36	82	0	274	113	0.82	0	0	20
19Jul94 (tillering, stem elongation)	29	145	0	733	153	1.79	0	0	20
30Jul94 (inflorescence)	1	55	0	410	226	2.36	2	2	20
8Aug94 (milk)	0	5	0	55	295	2.94	3	1	20
18Aug94 (dough)	0	5	0	55	295	2.94	3	1	20
29Aug94 (ripening)	18	24	0	80	103	1.32	0	0	20
20Sep94 (after harvest)	0	2	0	31	343	4.46	2	1	20
4Oct94	0	6	0	27	163	1.50	2	2	20
8Nov94	0	1	0	4	141	2.08	1	1	20
14Mar95	3	40	0	175	155	1.44	0	0	20
21Mar95	3	11	0	87	191	2.94	1	0	20
13Apr95	478	1499	0	12190	185	3.34	0	1	20
18Apr95	193	807	0	5889	180	2.63	0	2	20
21Apr95	185	322	0	1171	119	1.22	0	0	20
26Apr95	0	97	0	1171	272	3.89	0	2	20
3May95	0	5	0	108	481	4.47	1	0	20
12May95	0	17	0	230	317	3.72	2	2	20
19May95	0	2	0	39	433	4.47	0	1	20

Appendix 1.8. Exploratory data analysis for N_2O emission activity from June 1994 to May 1995 in the sandy, pasture site.

Sampling date	Median	Mean	Min.	Max.	C.V.	Skewness	No. extreme outliers		No. of sampling points
	<----- μg N_2O-N m^{-2} d^{-1} ----->				(%)		Shoulder	Footslope	
30Jun94	19	67	0	799	269	4.12	1	0	20
8Jul94	37	57	0	192	122	1.00		0	10
19Jul94	27	77	0	318	137	1.53		0	10
30Jul94	1	20	0	93	157	1.38	0	0	20
8Aug94	0	0	0	0	0	0		0	10
18Aug94	0	0	0	0	0	0		0	10
29Aug94	1	9	0	35	133	1.11	0	0	20
20Sep94	0	6	0	44	240	2.51		2	10
4Oct94	0	3	0	22	208	2.30	1	3	20
8Nov94	0	6	0	48	215	2.47	3	0	20
14Mar95	0	5	0	29	200	2.21	0	2	20
21Mar95	0	9	0	137	359	4.15	2	1	20
13Apr95	1	432	0	5446	298	3.90	0	2	20
18Apr95	84	813	0	9341	260	3.83	0	0	20
21Apr95	133	445	0	3620	189	3.15	0	1	20
26Apr95	4	137	0	731	177	1.90	1	2	20
3May95	0	41	0	581	315	4.24	0	1	20
12May95	0	74	0	414	167	1.86	0	1	20
19May95	0	8	0	70	240	2.53	1	3	20

Appendix 1.9. Exploratory data analysis for N_2O emission activity from June 1994 to May 1995 in the sandy, forest site.

Sampling date	Median	Mean	Min.	Max.	C.V.	Skewness	No. extreme outliers		No. of sampling points
	<----- $\mu g\ N_2O\text{-}N\ m^{-2}\ d^{-1}$ ----->				(%)		Shoulder	Footslope	
30Jun94	0	6	0	28	167	1.64		0	10
8Jul94	0	1	0	9	200	4.06	2	0	20
19Jul94	26	36	0	162	132	2.39		1	10
30Jul94	5	14	0	36	114	0.51		0	10
8Aug94	0	2	0	9	166	1.06	0	0	20
18Aug94	0	1	0	12	360	3.16		1	10
29Aug94	6	7	0	11	18	0.51		0	10
20Sep94	0	0	0	0	0	0		0	10
4Oct94	0	3	0	17	186	2.15		0	10
8Nov94	0	1	0	4	173	0.81		0	10
14Mar95	3	15	0	52	129	0.99	0	0	20
21Mar95	1	2	0	6	141	0.46	0	0	20
13Apr95	11	44	0	360	210	3.25	0	1	20
18Apr95	0	45	0	273	165	2.11	1	0	20
21Apr95	0	0	0	2	246	2.60	1	2	20
26Apr95	0	0	0	0	0	0	0	0	20
3May95	0	2	0	28	320	4.30	0	4	20
12May95	0	22	0	183	210	2.71	1	0	20
19May95	0	22	0	293	325	3.52	2	2	20